

INVESTIGATION OF FUEL VALUES AND COMBUSTION
CHARACTERISTICS OF RDF SAMPLES

A THESIS SUBMITTED TO
THE GRADUATE SCHOOL OF NATURAL AND APPLIED SCIENCES
OF
MIDDLE EAST TECHNICAL UNIVERSITY

BY
AYŞE SEVER AKDAĞ

IN PARTIAL FULFILLMENT OF THE REQUIREMENTS
FOR
THE DEGREE OF MASTER OF SCIENCE
IN
ENVIRONMENTAL ENGINEERING

AUGUST 2014

Approval of the thesis:

**INVESTIGATION OF FUEL VALUES AND COMBUSTION
CHARACTERISTICS OF RDF SAMPLES**

submitted by **AYŞE SEVER AKDAĞ** in the partial fulfillment of the requirements for the degree of **Master of Science in Environmental Engineering Department, Middle East Technical University** by,

Prof. Dr. Canan ÖZGEN
Dean, Graduate School of **Natural and Applied Sciences**

Prof. Dr. F.Dilek SANİN
Head of Department, **Environmental Engineering**

Prof. Dr. F. Dilek SANİN
Supervisor, **Environmental Engineering Dept., METU**

Prof. Dr. Aysel ATIMTAY
Co-Supervisor, **Environmental Engineering Dept., METU**

Examining Committee Members:

Prof. Dr. Gürdal Tuncel
Environmental Engineering Dept., METU

Prof. Dr. F. Dilek SANİN
Environmental Engineering Dept., METU

Prof. Dr. Aysel ATIMTAY
Environmental Engineering Dept., METU

Prof. Dr. Gülen Güllü
Environmental Engineering Dept., Hacettepe University

Assoc. Prof. Dr. Ayşegül AKSOY
Environmental Engineering Dept., METU

Date: 28 August 2014

I hereby declare that all the information in this document has been obtained and presented in accordance with academic rules and ethical conduct. I also declare that, as required by these rules and conduct, I have fully cited and referenced all materials and results that are not original to this work.

Name, Last Name: Ayşe SEVER AKDAĞ

Signature:

ABSTRACT

INVESTIGATION OF FUEL VALUES AND COMBUSTION CHARACTERISTICS OF RDF SAMPLES

Sever Akdağ, Ayşe

M.S., Department of Environmental Engineering

Supervisor: Prof. Dr. F. Dilek Sanin

December 2011, 131 pages

Municipal solid waste (MSW) is an unavoidable by-product of human activities. The generation of MSW tends to increase with the growing population and the economic development of the society.

Landfilling is one of the most common disposal methods for MSW in the world. However, there are numerous disadvantages of landfills including the potential to create air, soil and water pollution. Also, many valuable resources are wasted when waste is landfilled. Furthermore, many countries have established rules to limit the amount of organic fraction (biodegradable) of wastes sent to landfill, and encourage establishing environmentally sustainable waste management strategies. In this sense, waste to energy strategies have come prominence because the strategies increase resource efficiency and replace fossil fuels with renewable energy resources (material and energy recovery instead of landfill disposal). Producing Refuse Derived Fuel (RDF) is one of the waste to energy strategies. RDF is an alternative fuel produced from energy-rich MSW materials diverted from landfills.

This study aims to investigate the thermal characteristics and co-combustion efficiency of two RDF samples obtained from two municipal solid waste recovery

facilities in Turkey as alternative fuels. On these samples, proximate and ultimate analyses are conducted in order to articulate the thermal characteristics of both RDF. Thermogravimetric analyses (TGA) are conducted to observe the combustion behavior of RDF samples, coal and petroleum coke samples. Also, elemental compositions of RDF samples' ash are determined by XRF analysis. These samples are co-combusted in a lab-scale reactor in mixtures with coal and petroleum coke at certain percentages where co-combustion processes and efficiencies are investigated.

The all analysis indicated that calorific values of RDF samples on dry basis are close to that of coal and a little lower compared to petroleum coke used in this study. However, when the RDF fraction in the mixture is higher than 10%, the CO concentration in the flue gas increases and so the combustion efficiency decreases crucially; furthermore, the combustion characteristics of the fuel mixtures changes from char combustion to volatile combustion. However, RDF addition to the fuel mixtures decreases the SO₂ emission. No NO_x profile was obtained in this study showing the effect of RDF addition. Also, when the RDF is combusted alone the slagging and fouling indices of its ash was found as higher than the limit values.

Keywords: refuse derived fuel, thermal analysis, combustion

ÖZ

ATIKTAN TÜRETİLMİŞ YAKIT ÖRNEKLERİNİN YAKIT DEĞERLERİNİN VE YANMA KARAKTERLERİNİN İNCELENMESİ

Sever Akdağ, Ayşe

Yüksek Lisans, Çevre Mühendisliği Bölümü

Tez Yöneticisi: Prof. Dr. F. Dilek Sanin

Eylül 2013, 131 Sayfa

Evsel katı atık insan aktivitelerinin kaçınılmaz bir yan ürünüdür. Evsel katı atıkların üretimi, çoğalan nüfus ve toplumun ekonomik kalkınması ile artma eğilimindedir.

Düzenli depolama, evsel katı atıklar için dünyadaki en yaygın bertaraf yöntemidir. Fakat düzenli depolama alanlarının hava, toprak ve su kirliliği yaratma potansiyellerini içeren pek çok dezavantajları vardır. Ayrıca, atık gömüldüğü takdirde birçok değerli kaynak da harcanmış olmaktadır. Buna ek olarak, birçok ülke, düzenli depolama sahalarına gönderilecek atıkların organik (biyolojik ayrışabilir) içeriğini sınırlandırmak için kurallar koymakta ve sürdürülebilir çevresel atık yönetimlerinin oluşturulmasını teşvik etmektedir. Bu bağlamda, atıktan enerji stratejileri, kaynak verimliliğini arttırdıklarından ve yenilenebilir enerji kaynaklarının fosil yakıtların yerine kullanılmasını sağladıklarından önem kazanmaktadır (düzenli depolama yerine malzeme ve enerji geri kazanımı). Atıktan türetilmiş yakıt (ATY) atıktan enerji stratejilerinden bir tanesidir. ATY, düzenli depolamaya gönderimi engellenen enerji bakımından zengin olan evsel katı atıklardan üretilen alternatif bir yakıttır.

Bu çalışmanın hedefi Türkiye deki iki adet evsel katı atık geri kazanım tesisinden alınmış iki adet atıktan türetilmiş yakıtın termal karakterizasyonlarını ve yanma verimliliklerini alternatif yakıt olarak araştırmaktır. Alınan örneklerin karakteristik özelliklerinin belirlenmesi amacıyla yaklaşıp ve elemental analizleri yapılmıştır. ATY, kömür ve petrokok örneklerinin yanma sırasındaki davranışlarının gözlenmesi için termogravimetrik analizler (TGA) yapılmıştır. Ayrıca, atıktan türetilmiş yakıtların küllerinin elemental kompozisyonu X-Ray Fluorescence analizi (XRF) ile belirlenmiştir. Bu örnekler, kömür ve petrokok ile birlikte belli oranlarda karıştırılarak yanma süreçleri ve verimliliklerinin araştırıldığı laboratuvar ölçekli reaktörde yakılmıştır..

Tüm bu analizlerin sonucunda, kuru bazda ATY örneklerinin kalorifik değerinin, bu çalışmada kullanılan kömür örneğine çok yakın ve petrokok örneğinden çok az düşük olduğu gösterilmiştir. Fakat ATY karışım oranı %10'dan yüksek olduğunda, baca gazındaki CO miktarı artmış buna bağlı olarak da yanma verimliliği önemli ölçüde düşmüştür; ayrıca, yakıt karışımlarının yanma karakteristiği kül yanmasından uçucu madde yanmasına doğru değişmiştir. Fakat yakıt karışımına ATY eklenmesi SO₂ emisyonunu düşürmüştür. ATY eklenmesinin etkisini gösteren herhangi bir NO_x profili elde edilememiştir. Ayrıca, ATY tek başına yakıldığında, külünün curuf ve deposit oluşturma indeksleri, sınır değerlerden yüksek bulunmuştur.

Anahtar sözcükler: atıktan türetilmiş yakıt, termal analiz, yakma

To my husband and family...

ACKNOWLEDGEMENTS

First and foremost, I am heartily thankful to my supervisor Prof. Dr. F. Dilek Sanin for her precious guidance, advice and support throughout this study. Her willingness to motivate me contributed greatly to this research. Also, I would like to express my deepest gratitude to my co-supervisor Prof. Dr. Aysel Atımtay for her support. I feel very lucky for having chance to work with them.

I am thankful to my examining committee members Prof. Dr. Gürdal Tuncel, Prof. Dr. Gülen Güllü and Assoc. Prof. Dr. Ayşegül Aksoy for their valuable suggestions and comments.

I am also thankful to my friend Onur Atak for her most noteworthy support.

I would also like to thank to all faculty members, my friends, and colleagues in Hacettepe University Environmental Engineering Department for their support, patience and valuable comments.

I would like to express my gratitude to my family for their unconditional love. Awareness of being loved no matter what you do must be the most comforting feeling in the world.

Lastly, I want to express my deepest gratitude to my husband, Osman Akdağ, for his love, assistance and understanding. Through every stage of this study, whenever I become desperate, his existence has comforted me and made me go on. I could have never completed this thesis without him.

TABLE OF CONTENTS

ABSTRACT.....	v
ÖZ	vii
ACKNOWLEDGEMENTS.....	x
TABLE OF CONTENTS	xi
LIST OF TABLES	xiv
LIST OF FIGURES	xvi
LIST OF ABBREVIATIONS	xix
CHAPTERS	
1. INTRODUCTION	1
2. LITERATURE REVIEW.....	3
2.1. Municipal Solid Waste (MSW).....	3
2.1.1. Definitions of MSW.....	3
2.1.2. Municipal Solid Waste Generation Rates.....	4
2.1.3. Municipal Solid Waste Characteristics.....	7
2.1.4. Municipal Solid Waste Management and Hierarchy	9
2.1.5. Handling of Municipal Solid Waste	11
2.1.6. Situation of Municipal Solid Waste Management in Turkey	15
2.2. Refuse Derived Fuel (RDF)	16
2.2.1. Refuse Derived Fuel Production.....	18
2.2.2. Current Perspectives of Refuse Derived Fuel.....	22
2.3. Studies on Thermal Processing of RDF	25
2.3.1. Pyrolysis/Gasification of RDF.....	26
2.3.2. Co-Combustion of RDF.....	27
2.3.3. Characteristics of Bottom Ash Produced by Combustion RDF	39

2.4. Studies on Thermal Analysis of RDF	44
3. MATERIALS AND METHODS	49
3.1. The Material Recovery Facilities Investigated	49
3.2. Thermal Characterization of RDF Samples.....	52
3.2.1. Proximate Analysis	52
3.2.2. Ultimate Analysis.....	52
3.2.3. Calorific Values	55
3.2.4. Micro X-Ray Fluorescence (XRF) Analysis.....	56
3.3. Thermogravimetric Analysis (TGA) of RDF Samples.....	57
3.4. Laboratory Scale Combustion Experiments of RDF Samples-Coal Mixtures and RDF Samples-Petroleum coke Mixtures	58
3.4.1. Flue Gas Analyzer.....	60
3.4.2. Sample Preparation for Combustion Experiments.....	62
3.4.3. Combustion Experiments.....	65
4. RESULTS AND DISCUSSION	69
4.1. Thermal Characterization of RDF, Coal and Petroleum coke Samples	69
4.1.1. Proximate/Ultime Analysis of RDF, Coal and Petroleum coke Samples	69
4.1.2. Determination of Ash Composition of RDF Samples by XRF Analysis..	78
4.2. Co-combustion of RDF-Coal and RDF Petroleum coke Mixtures.....	82
4.3. Thermogravimetric Analysis (TGA) of RDF, Coal and Petroleum coke Samples.....	101
5. CONCLUSIONS	107
6. FUTURE STUDIES AND RECOMMENDATIONS	109

REFERENCES..... 111

APPENDICES

A. EMISSIONS OBTAINED IN CO-COMBUSTION EXPERIMENTS 121

LIST OF TABLES

Table 2.1 Materials generated (in percent of total generation) in the MSW stream in U.S. in 1960 to 2005.....	8
Table 2.2 The amounts of RDF combusted in cement factories in Turkey	16
Table 2.3 Types of RDF.....	18
Table 2.4 Quality parameters for RDF used in coal-fired power plants	23
Table 2.5 Conversion rate for RDF production according to treatment process and country.....	24
Table 2.6 Comparison of fuel characteristics of various materials	28
Table 2.7 Comparison of emission from WTE facilities with those from fossil fuels	38
Table 2.8 Empirical relations for slagging and fouling tendency of ash composition	41
Table 3.1 Experimental Setup of TGA.....	58
Table 3.2 Percentages of RDF in mixtures	62
Table 3.3 Calorific value of RDF samples and coal and petroleum coke	64
Table 3.4 Mass of RDF samples, coal and petroleum coke used to obtain different fuel mixtures (each pellet has 1000 calories).....	64
Table 4.1 Proximate analysis of RDF samples, coal and petroleum coke	70
Table 4.2 Comparison of proximate analysis with literature data.....	71
Table 4.3 Ultimate analysis of RDF samples, coal and petroleum coke	72
Table 4.4 Comparison of ultimate analysis with literature data.....	73
Table 4.5 SRF classification according to CEN standardization	77
Table 4.6 Inorganic element contents of RDF samples (% by wt.)	79

Table 4.7 Slagging and fouling indices of RDF samples.....	81
Table 4.8 Amount of carbon(g) introduced into the reactor by different mixtures....	86
Table 4.9 Amount of carbon released as CO and CO ₂ by combustion experiments .	88
Table 4.10 Percentage of carbon captured as CO and CO ₂ in combustion experiments (%).....	89
Table 4.11 Multiple range test for RDF _A -Coal co-combustion experiments' efficiency results	94
Table 4.12 Multiple range test for RDF _A -Petroleum coke co-combustion experiments' efficiency results	95
Table 4.13 Multiple range test for RDF _B -Coal co-combustion experiments' efficiency results	95
Table 4.14 Multiple range test for RDF _B -Petroleum coke co-combustion experiments' efficiency results	95
Table 4.15 Percentage of nitrogen converted to NO _x in combustion experiments (%)	99
Table 4.16 Percentage of sulfur converted to SO ₂ in combustion experiments (%)..	99

LIST OF FIGURES

Figure 2.1 Waste generation by region in the World	4
Figure 2.2 MSW Generation Rates, 1960-2012 in the USA	6
Figure 2.3 MSW Generation Rates, 1994-2012 in Turkey	7
Figure 2.4 Waste hierarchy	10
Figure 2.5 Total MSW Disposed of Worldwide	11
Figure 2.6 Development of Municipal Waste Management in 32 European Countries, 2001-2010.....	13
Figure 2.7 Composition of municipal solid waste stream in Turkey	16
Figure 2.8 Process flow a typical RDF producing plant	20
Figure 2.9 Principles for distinguishing SRF from RDF	21
Figure 2.10 Growth of RDF in Europe	23
Figure 2.11 Development of the amounts of SRF used in Germany	25
Figure 2.12 Chlorine content and molarity ratios of sulphur to chlorine for chosen fossil fuels, biomass fuels and RDF	43
Figure 3.1 Flow diagram of the Material Recovery Facilities	51
Figure 3.2 RDF Samples	52
Figure 3.3 Truspec Leco CHN-S elemental analyzer	54
Figure 3.4 Leco AC 500 calorimeter.....	55
Figure 3.5 Perkin Elmer Pyris STA 6000 TG analyzer.....	57
Figure 3.6 Lab scale combustion setup	59
Figure 3.7 The picture of reactor used in the study.....	59
Figure 3.8 Madur photon flue gas analyzer.....	61
Figure 3.9 Example of a pellet	65

Figure 3.10 Emissions measured in a combustion experiments	66
Figure 4.1 Comparison of calorific values of different fuel types	74
Figure 4.2 Comparison of volatile matter and C-content of the fuel of different coals and different SRF	75
Figure 4.3 C/H and C/O – ratio of different biomass fuels and of SRF.....	76
Figure 4.4 Results of co-combustion of coal with 3% RDF-B	84
Figure 4.5 Combustion Efficiency of RDF-A.....	90
Figure 4.6 Combustion Efficiency of RDF-B	91
Figure 4.7 Box and whisker plot for RDF _A -Coal co-combustion experiments' efficiency results	92
Figure 4.8 Box and whisker plot for RDF _A -Petroleum coke co-combustion experiments' efficiency results	93
Figure 4.9 Box and whisker plot for RDF _B -Coal co-combustion experiments' efficiency results	93
Figure 4.10 Box and whisker plot for RDF _B -Petroleum coke co-combustion experiments' efficiency results	94
Figure 4.11 TGA and DTG profiles of RDF-A.....	101
Figure 4.12 TGA and DTG profiles of RDF-B.....	102
Figure 4.13 TGA and DTG profiles of coal.....	104
Figure 4.14 TGA and DTG profiles of petroleum coke	105
Figure A-1 Results of combustion of RDF-A.....	121
Figure A-2 Results of co-combustion of coal with 3% RDF-A.....	121
Figure A-3 Results of co-combustion of coal with 5% RDF-A.....	122
Figure A-4 Results of co-combustion of coal with 10% RDF-A.....	122
Figure A-5 Results of co-combustion of coal with 20% RDF-A.....	123
Figure A-6 Results of co-combustion of coal with 30% RDF-A.....	123
Figure A-7 Results of co-combustion of petroleum coke with 3% RDF-A.....	124

Figure A-8 Results of co-combustion of petroleum coke with 5% RDF-A.....	124
Figure A-9 Results of co-combustion of petroleum coke with 10% RDF-A.....	125
Figure A-10 Results of co-combustion of petroleum coke with 20% RDF-A.....	125
Figure A-11 Results of co-combustion of petroleum coke with 30% RDF-A.....	126
Figure A-12 Results of co-combustion of RDF-B	126
Figure A-13 Results of co-combustion of coal with 3% RDF-B	127
Figure A-14 Results of co-combustion of coal with 5% RDF-B	127
Figure A-15 Results of co-combustion of coal with 10% RDF-B	128
Figure A-16 Results of co-combustion of coal with 20% RDF-B	128
Figure A-17 Results of co-combustion of coal with 30% RDF-B	129
Figure A-18 Results of co-combustion of petroleum coke with 3% RDF-B	129
Figure A-19 Results of co-combustion of petroleum coke with 5% RDF-B	130
Figure A-20 Results of co-combustion of petroleum coke with 10% RDF-B	130
Figure A-21 Results of co-combustion of petroleum coke 20% RDF-B	131
Figure A-22 Results of co-combustion of petroleum coke 30% RDF-B	131

LIST OF ABBREVIATIONS

ASTM:	the American Society for Testing and Measurement
CFB:	Circulating Fluidized Bed
DTG:	Differential Thermal Gravimetric Analysis
HDPE:	High-Density Polyethylene
IPCC:	Intergovernmental Panel on Climate Change
LDPE:	Low-Density Polyethylene
MFR:	Material Recovery Facility
MSW:	Municipal Solid Waste
MSWM:	Municipal Solid Waste Management
OECD:	Organization for Economic Co-operation and Development
PCBs:	Polychlorinated Biphenyls
PCDD/F:	Polychlorinated dibenzodioxin and Furan
PVC:	Polyvinyl Chloride
RDF:	Refuse Derived Fuel
SRF:	Solid Recovery Fuel
TGA:	Thermogravimetric Analysis
VM:	Volatile Matter
VOCs:	Volatile Organic Compounds
WTE:	Waste to Energy
XRD:	X-Ray Diffraction
XRF:	X-Ray Fluorescence

CHAPTER 1

INTRODUCTION

Municipal Solid Waste (MSW) is an unavoidable by-product of human activities. MSW generation increases with population growths and economic development as well as changes in lifestyles and in consumption patterns. Establishment of affordable, effective and precisely sustainable Municipal Solid Waste Management (MSWM) is crucial for sustainable development and promoting public health.

Current global MSW generation levels are approximately 1.3 billion tonnes per year, and are expected to increase to approximately 2.2 billion tonnes per year by 2025. In other words, in next ten years, waste generation rate will increase from 1.2 to 1.42 kg per person per day (Hoorweg and Bhada, 2012).

Many methods have been used to dispose of solid waste. Landfilling of MSW is one of the most common disposal methods in the world. However, there are numerous disadvantages of landfills including the potential to create air, soil and water pollution. In addition, the landfill areas are diminishing in many countries and many valuable resources are buried in the ground when waste is landfilled. Furthermore, the European Union established Landfill Directive (1999/31/EC) to limit the amount of biodegradable fraction of wastes sent to landfills. As a result of all of these limitations, *waste to energy strategies* is gaining more and more attention.

Refuse derived fuel (RDF) approach which is one of the *waste to energy strategies* that has been utilized recently to solve both waste and energy problems simultaneously. RDF is an alternative fuel produced from energy-rich MSW materials diverted from landfills. In other words, RDF refers to the segregated high calorific fraction of processed MSW. The use of RDF in the thermal processes became a hot topic and starts to receive wide attention in the world as RDF approach provides a dramatic decrease in space requirement and effectively utilizes the

reusable energy of the solid waste. Also, simpler handling and storing of RDF make this option more attractive than the incineration of low-quality waste (Ferrer et al., 2005). In these studies, it is stated that its high energy content and homogeneity make RDF compatible with conventional fossil fuel.

However, the amounts of research works about the subject are limited. Therefore, more research activities are necessary for the better understanding of fuel values and combustion characteristics of RDF by burning it as alternative fuel in the incineration systems.

In this context, this study aims to investigate the thermal characteristics and combustion efficiency of two RDF samples obtained from two metropolitan municipalities' solid waste recovery facilities in Turkey. On these samples, proximate and ultimate analyses are conducted in order to articulate the thermal characteristics of RDF samples. Thermogravimetric analyses (TGA) are conducted to reveal the combustion kinetics. Also, elemental compositions of RDF samples' ash are determined by XRF analysis. These samples are co-combusted in a lab-scale reactor in blends with coal and petroleum coke at certain percentages, where combustion processes and efficiencies are investigated.

The structure of the thesis is as follows. The following section, Chapter 2, provides a brief literature survey on the subject. Then the materials and methods used to carry out the planned study are described in Chapter 3. Chapter 4 summarizes and discusses the results obtained and a brief conclusion is given in Chapter 5. Finally in Chapter 6 suggestions for future work are provided.

CHAPTER 2

LITERATURE REVIEW

This chapter consists of three major topics. First, general information regarding MSW are reviewed. Second, RDF production process and its current perspective are stated. Finally, studies in literature regarding thermal processing and thermal analysis of RDF are also discussed.

2.1. Municipal Solid Waste (MSW)

2.1.1. Definitions of MSW

The waste such as product packaging, grass clippings, furniture, clothing, bottles, food scraps, newspapers, appliances, paint, and batteries which are the result of the daily life activities of people in houses, schools, hospitals, and businesses are categorized as Municipal Solid Waste (MSW). However, construction waste, industrial waste, and hazardous waste are not included in MSW category (URL 1).

OECD defines MSW as the waste that is collected and treated by/for municipalities. In this definition, the waste from households, including bulky waste, similar waste from commerce and trade, office buildings, institutions and small businesses, yards and gardens, street sweepings, contents of litter containers, and market cleansing are included in MSW. However, the waste from municipal construction and demolition, and municipal sewage network and treatment are not included in MSW category.

The *IPCC* definition for MSW includes the food waste, garden and park waste, paper and cardboard, wood, textiles, nappies (disposable diapers), rubber and leather, plastics, metal, glass (and pottery and china), and other (e.g., ash, dirt, dust, soil, electronic waste) (Hoorweg and Bhada, 2012).

The content of MSW varies between developing and developed countries, as well as between regions and cities in countries. For instance, MSW composition in developing countries includes a much larger proportion of organic waste than in developed countries (Hoornweg and Bhada, 2012).

2.1.2. Municipal Solid Waste Generation Rates

The economic development, industrialization level, population growth, public habits, and local climate affect the MSW generation rate. Generally, the amount of solid waste produced is greater for higher levels of economic development and rate of urbanization. This can also be understood when the solid waste generation rates per region are investigated. As it is presented in Figure 2.1, almost half of the solid waste in the world is produced by OECD countries while the solid waste produced in Africa and South Asia is the least (Hoornweg and Bhada, 2012).

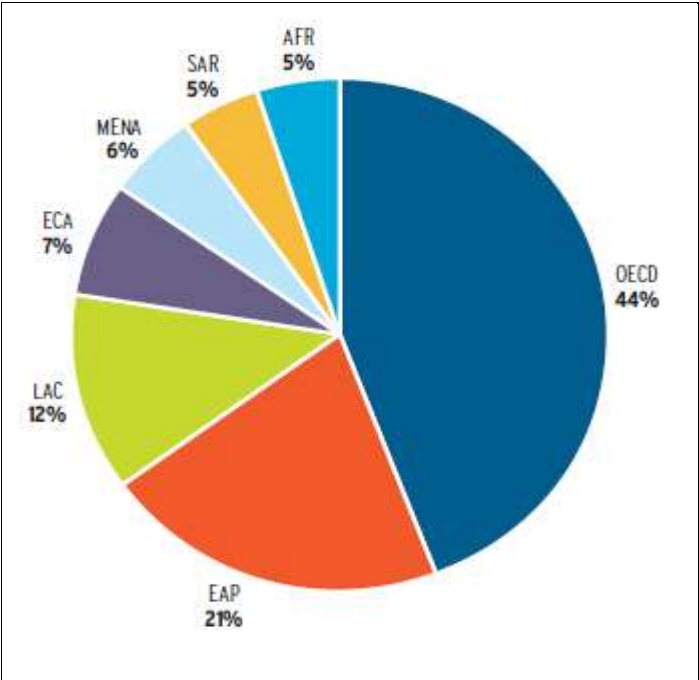


Figure 2.1 Waste generation by region in the World (Hoornweg and Bhada, 2012)

Abbreviations in the graph are given below.

AFR: Africa Region

EAP: East Asia and Pacific Region

ECA: Europe and Central Asia Region

LAC: Latin America and the Caribbean Region

MENA: Middle East and North Africa Region

OECD: Organization for Economic Co-operation and Development

SAR: South Asia Region

Currently, approximately 1.3 billion tonnes MSW per year is generated, and this rate is expected to increase to about 2.2 billion tonnes per year by 2025. In other words, in the next ten years, per capita waste generation will increase from 1.2 to 1.42 kg per person per day (Hoornweg and Bhada, 2012).

In 2012, in the USA, 715 kg MSW per person (1.96 kg per person per day) is generated, which means 251 million tons of MSW was generated totally in USA in this year (U.S. EPA, 2012). The MSW generation rates in USA from 1960 to 2012 are presented in Figure 2.2. The increasing trend of MSW generation is seen from this figure; for instance, the generation of MSW in USA increased at a rate of 2.5% from year 2002 to year 2004.

In EU-27 countries (Austria, Belgium, Bulgaria, Cyprus, Czech Republic, Denmark, Estonia, Finland, France, Germany, Greece, Hungary, Ireland, Italy, Latvia, Lithuania, Luxembourg, Malta, Netherlands, Poland, Portugal, Romania, Slovakia, Slovenia, Spain, Sweden, United Kingdom) 246 million tons of MSW was generated in 2012, which corresponded to 524 kg MSW per capita (1.43 kg per person per day) (Blumenthal, 2012).

Annually, more than 25 million tons of MSW, which is equivalent to approximately 1.12 kg per capita per day, is generated in Turkey (URL 2). The graph showing the MSW generation amounts in Turkey by year is given in Figure 2.3. The years in the graph is starting from 1994 because TUIK has initiated collecting the data from municipalities in this year. Thus, before this year there is no data access about the MSW amount generated in Turkey. As seen from the graph, the MSW generation increases between the years 1994 and 2003. However, after 2003, the increase rate in the MSW generation decreases.

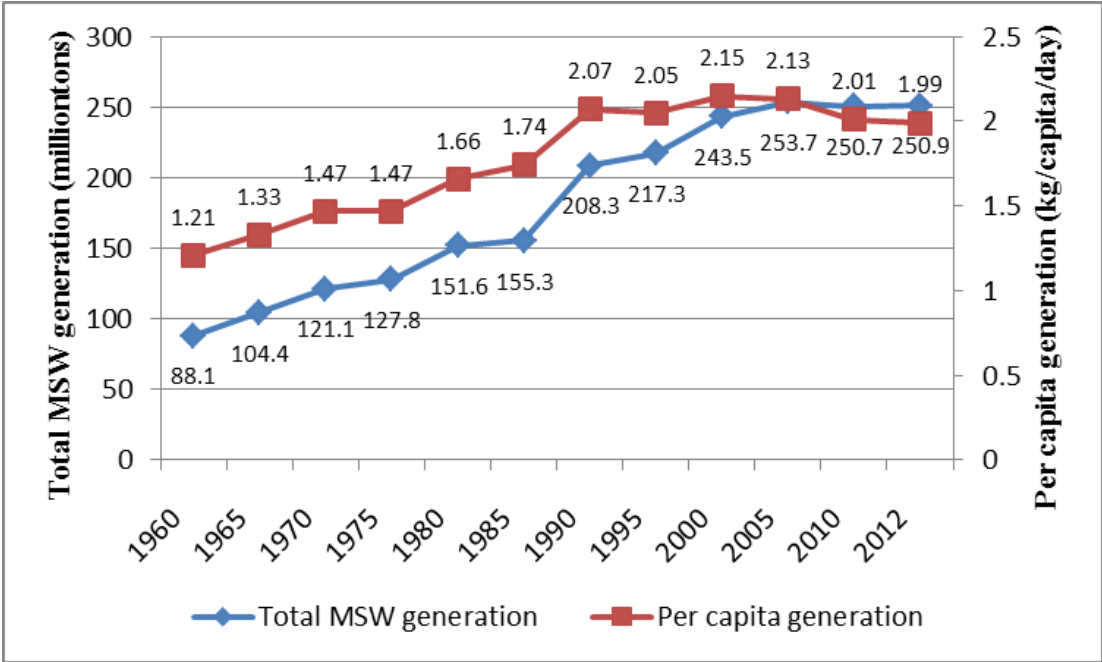


Figure 2.2 MSW Generation Rates, 1960-2012 in the USA (URL 1)

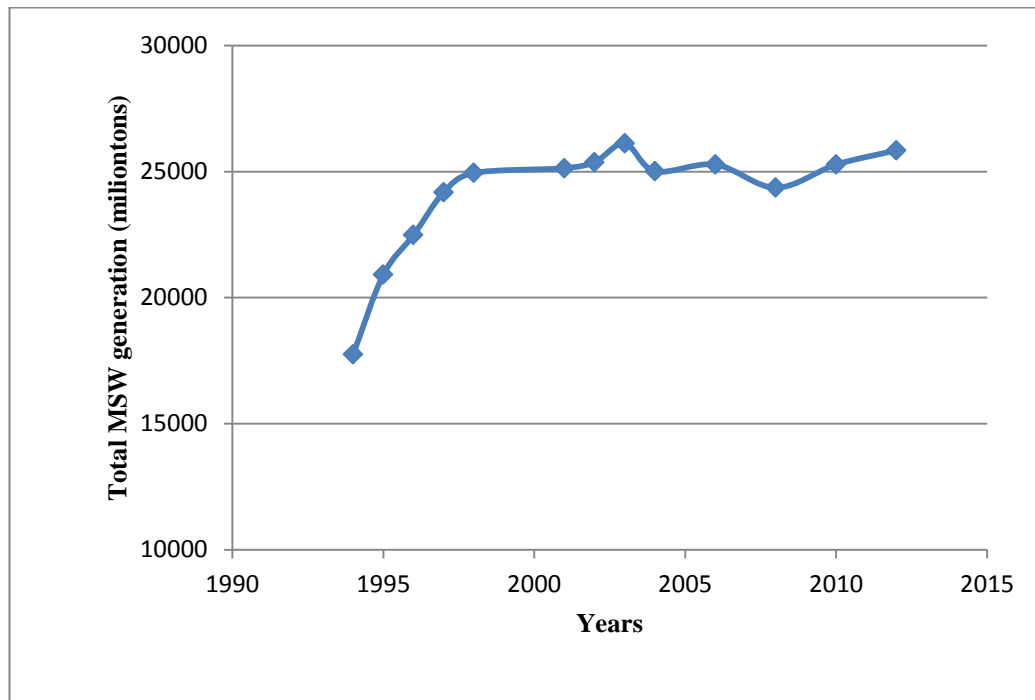


Figure 2.3 MSW Generation Rates, 1994-2012 in Turkey (URL 2)

2.1.3. Municipal Solid Waste Characteristics

Characteristics of the MSW should be understood in order to detect and make good planning about the long-term trends in waste stream. In this way, the oversizing or undersizing of waste treatment facilities can be prevented and these facilities can be built in a more cost-effective way.

Two basic methods, which are sampling and material flow methodology, are used for characterization of MSW. Material flow analysis is a systematic assessment of the flows and stocks of wastes within a system defined in space and time. Sampling method is applied for collecting the representative municipal solid waste in waste stream. First, the garbage bag from arrival waste loads is picked up randomly then the wastes are separated according to the selected classification such as wood, paper, class and green waste; each category is weighted by using a weight balance.

Data on the most notable materials get by sampling method, in MSW stream according to years in the U.S.A is shown in the Table 2.1.

Table 2.1 Materials generated (in percent of total generation) in the MSW stream in U.S. in 1960 to 2005 (Tchobanoglous et al., 1993).

Materials	1960	1965	1970	1975	1980	1985	1990	1995	1998	2005
Paper and paperboard	34.0	36.5	36.6	33.8	36.4	37.8	35.4	38.6	38.2	39.6
Glass	7.6	8.3	10.5	10.6	10.0	7.9	6.4	6.1	5.7	4.7
Metals:										
Ferrous	11.7	10.6	10.2	9.6	8.3	6.8	6.2	5.5	5.6	5.7
Aluminum	0.4	0.5	0.7	0.9	1.1	1.3	1.4	1.4	1.4	1.6
Nonferrous metals	0.2	0.5	0.6	0.7	0.8	0.6	0.5	0.6	0.6	0.6
Plastics	0.5	1.4	2.4	3.4	4.5	6.7	8.3	8.9	10.2	11.2
Rubber and leather	2.1	2.3	2.5	3.0	2.8	2.8	2.8	2.9	3.1	3.2
Textiles	2.0	1.8	1.7	1.7	1.7	1.7	2.8	3.5	3.9	4.3
Wood	3.4	3.2	3.1	3.3	4.6	5.0	5.9	4.9	5.4	6.6
Other	0.1	0.4	0.7	1.3	1.7	1.8	1.5	1.7	1.8	1.8
Others:										
Food wastes	13.9	12.2	10.6	10.5	8.6	7.9	10.1	10.3	10.0	9.8
Yard trimmings	22.7	20.7	19.2	19.7	18.1	18.0	17.1	14.0	12.6	9.6
Misc Inorganic waste	1.5	1.5	1.5	1.6	1.5	1.5	1.4	1.5	1.5	1.5
Total MSW generated	100	100	100	100	100	100	100	100	100	100

2.1.4. Municipal Solid Waste Management and Hierarchy

MSW has many negative effects on the environment; however, the level of this environmental damage depends on the waste management strategy. The U.S Environmental Management Agency (EPA) has identified four basic management strategies for MSWM. These are: source reduction, recycling and composting, waste-to-energy facilities, and landfills.

Source reduction aims to reduce the amount and volume of waste at the generation points. This can be achieved by different ways. For instance, the items can be reused or donated, or can be bought in bulk, packages of the products can be reduced; products can be redesigned considering the waste generated when they are used, and the toxicity can be reduced (URL 1).

Recycling provides reduction of the amount of raw materials needed to market by separating reusable products from the municipal waste stream. For this purpose, useful materials in trash, such as paper, plastic, glass, and metals are taken and reused in making new products (URL 1).

Composting is the biological decomposition of the biodegradable organic fraction of MSW under aerobic or anaerobic conditions to a circumstance adequately stable for non-nuisance storage and handling and for safe use in land applications (Tchobanoglous et al., 1993).

Energy recovery from waste can be applied when the waste is non-recyclable. This type of waste is converted into useable heat, electricity, or fuel by the *waste-to-energy (WTE)* technologies combining waste processing and energy generation. WTE reduces the amount of MSW intended for landfilling and decreases the consumption of fossil fuels (URL 1; Nemet et al., 2011).

Landfills are the engineered areas used for placing the waste into the land. They are commonly used as final waste disposal site (URL 1).

The management strategies can also be considered in a hierarchical order. (See Fig. 2.4) The hierarchy concept classifying the management strategies is proposed to reduce the environmental damage caused by the waste. This concept suggests reducing the negative effects of the waste on environment by making more sustainable use of it.



Figure 2.4 Waste hierarchy (URL 3)

According to the waste management hierarchy, *source reduction and reuse* is the most desirable alternative to reduce the negative impacts of waste on the environment; while, *disposal* of the waste (mainly landfilling) is the least desirable method and should be minimized. Energy recovery from waste is considered after the maximum amount of recycling has been achieved.

2.1.5. Handling of Municipal Solid Waste

Although environment friendly strategies such as reuse and recycling are applied, the generation rate of MSW is increasing continuously and a great amount of MSW should be managed and disposed of.

In high income countries, generally landfilling is used for disposal of MSW using engineered landfills; while, for most of the low and lower middle income countries using open dumps for MSW is a more common method. Also, there are poorly operated landfills, which can also be classified as controlled dumping, in some middle-income countries (Hoornweg and Bhada, 2012).

The current worldwide distribution of MSW handling and disposal methods used is shown in Figure 2.5. The values shown in the figure are approximated using the data collected from different years.

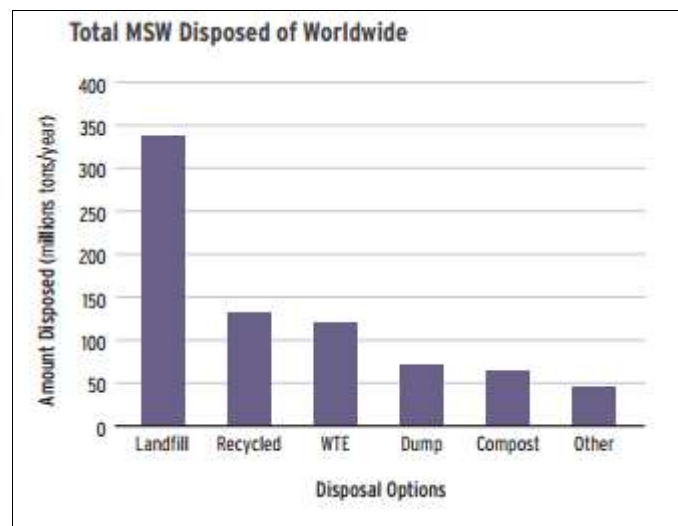


Figure 2.5 Total MSW Disposed of Worldwide (Hoornweg and Bhada, 2012)

Despite landfilling is a common disposal method, this method has many drawbacks. Landfilling causes leachate problems and air pollution. Besides, there is scarcity of

available space for landfilling. When all these disadvantages are considered, it is obvious that landfilling is not a sustainable MSW management strategy. In addition, European Union (EU) imposed a restriction about landfilling with the Landfill Directive (1999/31/EC). According to this directive, by 2013, EU Member States have to reduce the amount of landfilled biodegradable waste to 50% of the amount in 1995, and by 2016 (for some countries 2020), they have to reduce this amount to 35% of the one in 1995.

There are also other treatment and disposal methods such as composting, dumping into ocean, incineration without energy recovery and incineration with energy recovery. In composting, the waste is decomposed; therefore, it is only applicable for biodegradable waste. The other method, dumping into ocean, is one of the cheapest options; however, it is the most harmful one to the marine environment (Dong and Lee, 2009). This option is strictly prohibited and no longer practiced in the developed countries. Incineration without energy recovery method involves non-autogenic combustion. This method is an expensive option due to the need for continuous fuel supply and not environmentally friendly since the combustion processes at low temperature in open-burning cause drastic air pollution. Therefore, this method is also discouraged (Hoornweg and Bhada, 2012).

For the non-recyclable and non-reusable wastes, incineration with energy recovery is the most favorable method among the others mentioned before. It provides reduction of space requirement and thermal energy recovery (Chyang et al., 2010). The cost of landfilling is lower than the cost of incineration, but over the years, environmental specialists have proven that landfills generated more net CO₂ emissions; while, incineration of the waste coupled with recycling and recovery of energy reduces the emission by saving cost of energy production through fossil fuel (Abd Kadir et al., 2013). Consequently, for disposal of MSW, landfilling method has been gradually replaced with incineration with energy recovery method. In 2012, over 29 million tons of waste in US, which corresponds to 11.7 percent, is disposed of by incineration with energy recovery (U.S EPA, 2012).

In Figure 2.6, the distribution of MSW disposal methods used in 32 European countries (EU-27 Member States, Croatia, Iceland, Norway, Switzerland and Turkey) between years 2001 and 2010 is presented. From 2001 to 2010 the amount of landfilling of MSW is reduced by almost 40 million tonnes and the amount of incineration of MSW is increased by almost 15 million tonnes (EEA Report, 2013).

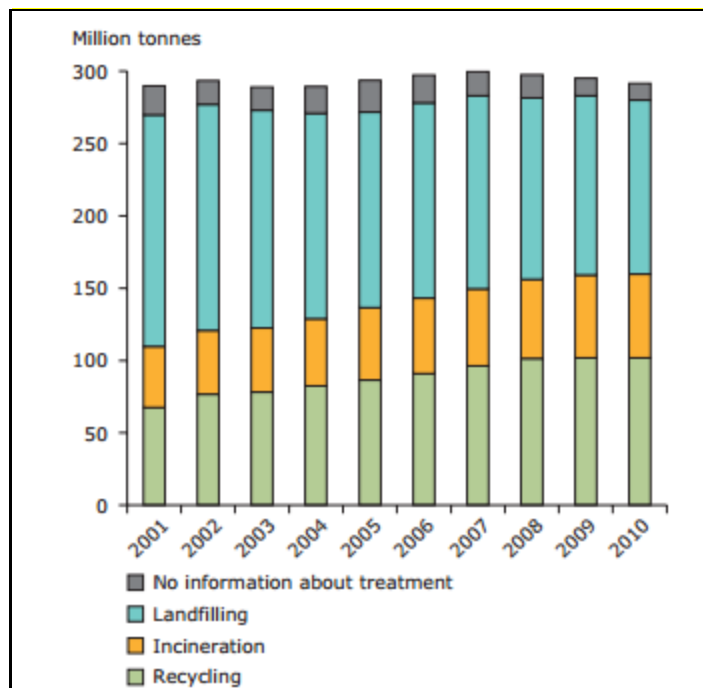


Figure 2.6 Development of Municipal Waste Management in 32 European Countries, 2001-2010 (EEA Report, 2013)

When incineration with energy recovery is applied to MSW, the volume of the waste decreases to about 10% of the original volume (90% volume reduction) and the mass of the waste decreases to 25% of the original mass (75% mass reduction). Besides, the energy that the waste contains is recovered. That is why, incineration with energy recovery is a favorable method, providing that the required pollution control mechanisms and costs are addressed properly (Hoorweg and Bhada, 2012).

Incineration was only used for reducing the volume of waste and destroying the harmful substances it contained in the past. However, nowadays, incineration process is combined with energy recovery since MSW contains a great amount of energy to be recovered. This recovered energy can be used in the form of heat and/or electricity. To conceive the effect of energy recovered from the waste, the implementation in Denmark can be given as an example; in 2005, 4.8% of electricity used and 13.7% of total heat consumption is produced by waste incineration (Bosmans et al., 2013). The countries which use this *waste fuel* as an energy source take the advantage of extending their national resources and reducing the need for imported fuels. It is estimated that the 14% of total world energy consumption is provided by biomass. This method is a reliable and economically feasible method for producing energy (Ekmann et al., 1998).

Using MSW in *Waste-to-Energy* systems is not straightforward. The materials contained in MSW widely vary in size, shape and composition. Using MSW as a direct input for the waste-to-energy system leads to instability in operating conditions of the system which results in quality fluctuations in the end products. Besides, in order to maximize the process efficiencies, advanced thermochemical treatment methods, which require feeding the system with an input which has sufficiently high calorific value, should be applied. Because of these reasons, MSW is not used “as received” in waste-to-energy systems; instead, a processed form of MSW, refuse derived fuel (RDF), is used as input (Bosmans et al., 2013).

The main benefits of converting MSW to RDF are a higher calorific value, more homogeneous physical and chemical compositions, lower pollutant emissions, lower ash content, reduced excess air requirement during combustion and finally, easier storage, handling and transportation (Bosmans et al., 2013).

Since the focus in this study is the investigation of the thermal characteristics and combustion efficiency of RDF. The more detailed information about RDF is given in section 2.2.

2.1.6. Situation of Municipal Solid Waste Management in Turkey

Turkey is an economically developing country therefore the industrialization and the living standards are increasing each day. This causes the amount of solid waste to increase and the disposal problems of the waste arises consequently. The traditional method of solid waste disposal in Turkey was to dump the waste at open sites. The number of open sites of solid waste disposal in Turkey was over 2000 in 2008 (Turan et al., 2009).

In 2010, 25 million tonnes MSW (1.12 kg per capita per day), which is 84% of total MSW generated, is collected in Turkey. The amount of MSW which is landfilled is increased by 5% from 2001 to 2010. From years 2003 to 2012, the number of sanitary (engineered) landfill sites has increased from 15 to 68. In year 2012, according to TurkStat data, the share of MSW sent to sanitary landfills is 59.9%, and the share of MSW dumped into municipality dumpsites is 37.8%. The amount of MSW composted or disposed by other methods is 2% of total MSW collected. That is to say, in 2012, the share of MSW landfilled in Turkey is 97.7%, which is a great amount. This shows the need for other MSW management strategies in Turkey. Also, the municipal solid waste composition data taken from the Ministry of Environment and Urbanization is given Fig 2.7. Unfortunately, the last available information in the ministry is for the year 2006 (MoEU, 2014). As seen from the figure, the organic content of the waste stream is highest. The paper and cardboard fraction is higher than the metal, glass and plastic fraction.

The amount of landfilled biodegradable MSW is aimed to be decreased by the By-law on Landfill of waste (No: 27533 2012/03) in scheduled period. As it is stated by the Turkish Ministry of Environment and Urbanization, strategies are being prepared to decrease the amount of MSW landfilled (Milios, 2013). One strategy is RDF production and combustion in cement factories. The amounts of combusted RDF in cement factories according to years is given in Table 2.2. As seen from the table, RDF generation rate is increasing by the years (MoEU2, 2014)

Table 2.2 The amounts of combusted RDF in cement factories in Turkey (data provided by MoEU),

Years	Amounts of RDF (tones)
2010	25.414
2011	78.177
2012	157.557
2013	179.935

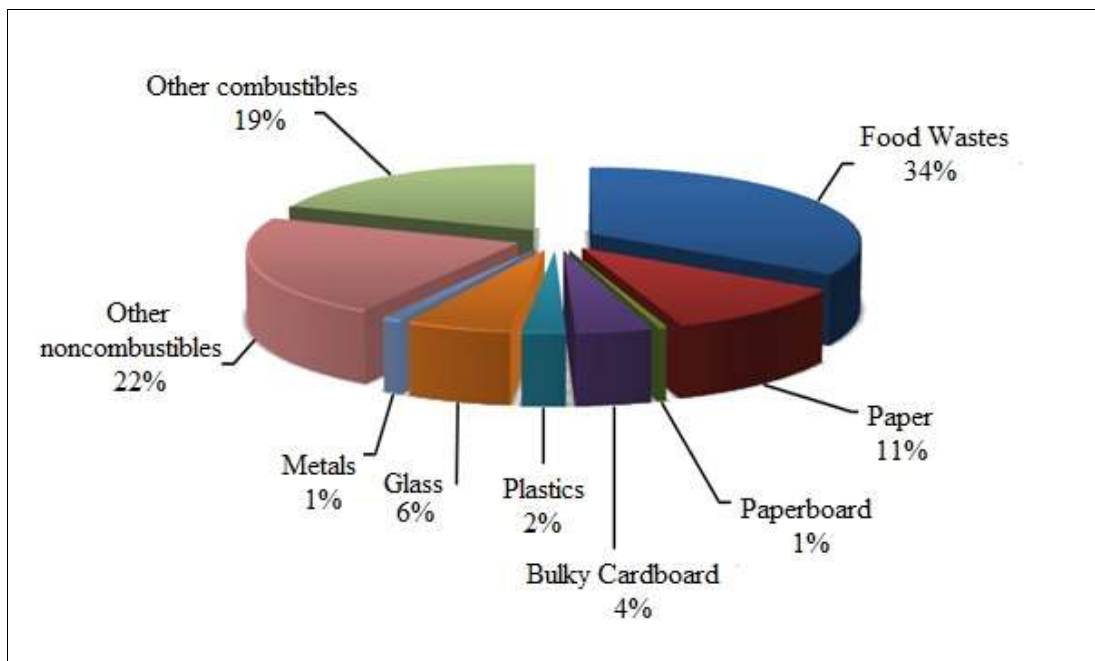


Figure 2.7 Composition of Municipal Solid Waste Stream in Turkey in 2006 (MoEU, 2014)

2.2. Refuse Derived Fuel (RDF)

Producing secondary fuels from the waste saves the primary fuels and reduces the amount of waste landfilled. Therefore, especially in energy intensive industries, use of secondary fuel is essential in order to save the primary fuels and to meet the

requirements of waste management policies which limits the amount of waste landfilled (Pretz et al., 2003).

Using MSW directly as secondary fuel is not an efficient way as mentioned before; therefore, it is processed and then used in the waste-to-energy systems. The purpose of this treatment process is to convert the waste into a homogeneous, highly calorific, chemically and biologically stable secondary fuel and to reduce the pollutant emissions, the ash content, and the excess air requirement during combustion. In addition, this treatment makes the secondary fuel easier to store, handle and transport. In this content, RDF is one of the promising methods for utilizing the MSW to be used in waste-to-energy systems (Cesi Ricerca Report, 2007). The RDF method can be the crucial part of an integrated waste management system in which recycling targets and the requirements for the amount of biodegradable material landfilled specified in 1999 Landfill directive are met. Sorting the biodegradable materials in MSW and using them in RDF production reduces the amount of biodegradable materials landfilled (Gendebien et al., 2003).

MSW is treated with several processes such as sorting the recyclable and noncombustible materials, shredding, screening, drying, and pelletization (Bosmans et al., 2013) in production of RDF. Further description about these processes is given in the following part. These processes are applied to sort the high calorific materials in MSW and to improve the combustion performance of the waste; therefore, RDF, indeed, is the segregated high calorific fraction of MSW (Gendebien et al., 2003).

After crushing, drying and solidifying processes, RDF becomes a promising secondary fuel, having the almost same energy potential as coal. The heating value of RDF can be over 3500 kcal/kg (Piao et al., 2000). This demonstrates the potential of RDF in becoming a common secondary fuel.

Also, the form of RDF has been mentioned by Alter, 1983. The types of RDF are given in table 2.3. According to this table, the RDF samples used in this study constitute RDF-3 or RDF-5 prepared by densifying.

Table 2.3 Types of RDF (Alter, 1983)

RDF-1	Wastes used as fuel in as discarded form
RDF-2	Wastes processed to coarse particle size with or without ferrous metal separation
RDF-3	Shredded fuel derived from MSW that has been processed to remove metal, glass and other inorganic materials (this material as a particle size such that 95 wt% passes through 50-mm square mash screen)
RDF-4	Combustible waste processed into powder form, 95 wt% passes 10 mash (2mm)
RDF-5	Combustible waste densified into form of pellets
RDF-6	Combustible waste processed into liquid fuel
RDF-7	Combustible waste processed into gaseous fuel

2.2.1. Refuse Derived Fuel Production

The unwanted materials are separated and the combustion characteristic of the waste is improved by several operation units placed in Material Recovery Facilities (MRFs). As mentioned before, these unit operations generally include screening, size reduction, classification (separation of recyclables and wet organic materials), drying and densification. The unit operations to be applied are decided considering the composition of MSW and the desired quality of RDF, and these operations are arranged accordingly (Caputo and Pelagagge, 2002). Besides, typical process flow diagram of RDF producing is given Fig 2.8.

The brief explanations of the unit operations of MRFs to produce RDF are given below.

Manual Separation: In many facilities workers may manually separate the bulk items such as appliances, furniture, etc. before mechanical processing.

Screening: The materials in MSW stream is divided by screens. The materials retained on the screen are called as oversize and the materials passed through the screen are called as undersize. In mixed MSW processes Trommel screen is the commonly used screen type.

Size Reduction: Uniformity in size is achieved by *shredding* the mixed waste. Hammermills and shear shredder are used commonly in this operation.

Air Classification: This is a separation operation in which the materials are separated by means of their different aerodynamic characteristics, such as size, density and geometry etc.

Magnetic Separation: This is another separation operation in which the ferrous metals are sorted out from the mixed MSW.

Drying and Densification: By unit operations such as *briquetting, pelletizing* etc. the quality of the RDF is improved.

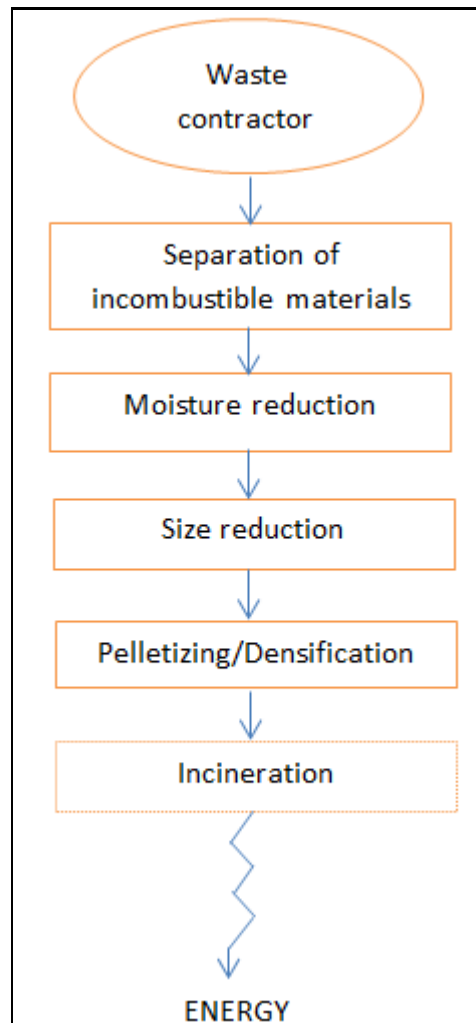


Fig 2.8 Process flow a typical RDF producing plant

At this point, as a last note about the RDF production, the Solid Recovered Fuel (SRF) concept should be mentioned. When the specific standard EN15359, which is developed by CEN/TC343 established on 13 March 2002 according to a mandate of European Commission, is applied on the production of RDF, the resulting fuel is called as SRF.

The main difference between SRF and RDF is that in the production of SRF the quality criteria is applied and the quality of the fuel is ensured; while RDF is generally a natural outcome of the waste treatment operations mentioned before.

That means SRF has a standard and controllable quality. The free trade of SRF on internal market will be supported by the European Standards for SRF. The flow chart that presents the difference between SRF and RDF is given in Figure 2.9.

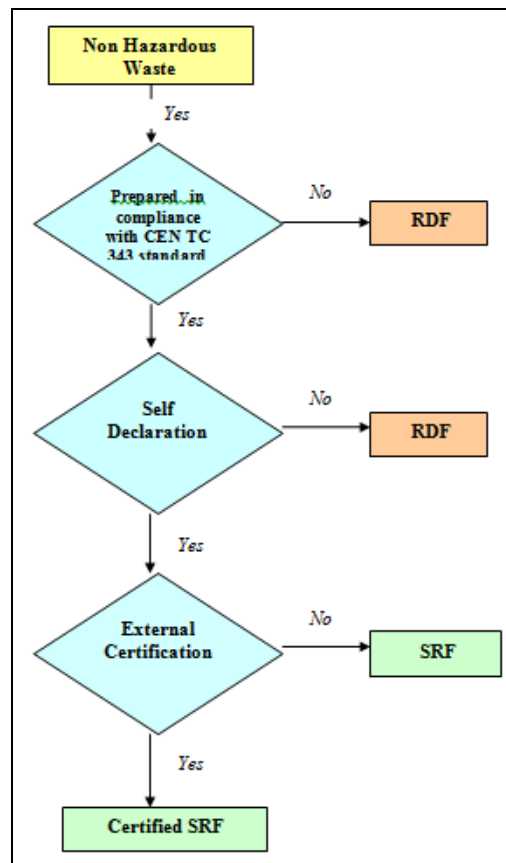


Figure 2.9 Principles for distinguishing SRF from RDF (URL 4)

The criteria and fuel parameter used for defining the characteristics of SRF are given in section 4.1.1 Table 4.5. EN15359 lays down the classification and specification requirements of SRF. It is worth to note that the lower class numbers in the definition mean a “cleaner fuel”, which is more desirable (URL 4).

The current perspectives and use of RDF are presented in Section 2.2.2.

2.2.2. Current Perspectives of RDF

RDF is a promising secondary fuel especially in energy intensive industries such as cement, and power generation. Cement kilns, lime kilns, power plants, and industrial boilers are the examples of potential application areas of RDF. Moreover, RDF is used as substitute of carbon in steel mills. RDF is used for energy generation in UK, for multi-fuel district heating and in paper mill boilers in Finland, in cement kilns in Austria, Denmark, Netherlands, Belgium, and Italy (Gendebien et al., 2003). In these applications, fluidized bed, which has certain advantages in combustion, is commonly used in incineration process.

It is reasonable to use RDF in cement kilns since the flame temperatures at which the combustion occurs in cement kilns is very high, about 1450°C, and the solid residence time is relatively high about more than 15 seconds at main burner. Therefore, to use RDF in cement kilns, a special firing technology is not needed; only RDF handling system is required. However, to control the air pollutant emission there is an upper limit in addition to the total fuel (maximum 30% by weight) (Lockwood and Ou, 1993).

Using RDF in coal-fired power plants and district heating plants is another common application. The main disadvantage using RDF is that the acidic gases, such as HCl, cause the surface corrosion in heat exchanger. Furthermore, these gases may also stimulate the formation of dioxin (Liu et al., 2001).

The quality of RDF to be used in these plants depends on the type of the plants. The quality parameters for hard coal fired power plant and lignite power plant are given in Table 2.4.

Table 2.4 Quality parameters for RDF used in coal-fired power plants (Ibbetson and Wengenroth, 2007)

Quality parameter	Hard coal power plant	Lignite power plant
Calorific value (MJ/kg)	Min. 20	Min. 11
Particle size (mm)	< 20	< 25 as soft pellet
Ash content (%)	Low	Can be high
Chlorine (%)	Depends on S content, in general < 1%	Depends on S content, in general < 1%

The RDF production in Europe is highly affected from the landfill directive 1999/31/EC. Encouraging separation and recycling operations indirectly increases the RDF production since the residue of these operations is the high calorie materials which are convenient for being used as RDF. The impact of this directive is illustrated in Figure 2.10. The production of RDF is increased from 1.4 Mt to 12.4 Mt in 5 years in Europe (Gendebien et al., 2003).

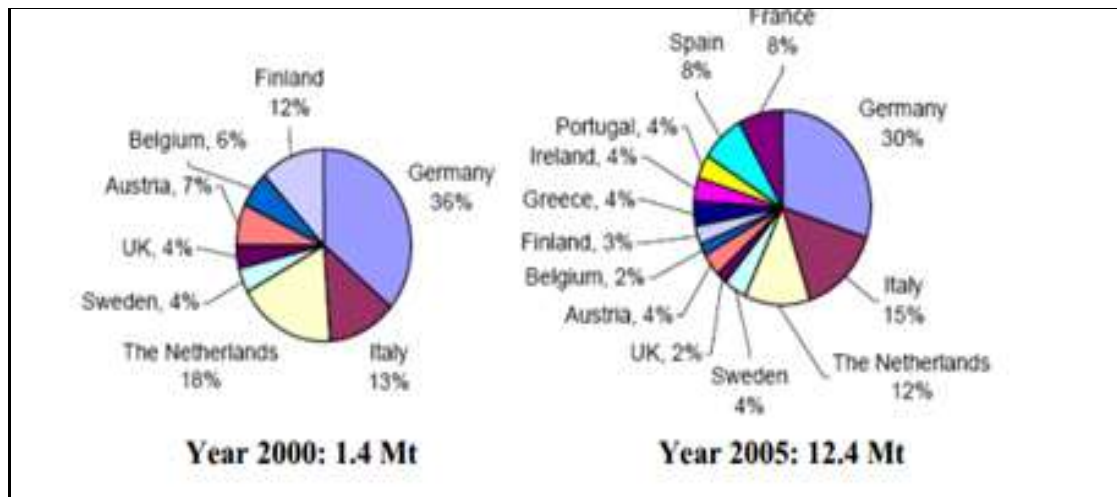


Figure 2.10 Growth of RDF in Europe

The type of collection of MSW, waste treatment processes and quality requirements affect the quantity of RDF produced per ton of MSW. The quantity of RDF produced varies between 23% and 50% of the amount of MSW. Table 2.5 presents the rate of RDF production in different countries (Gendebien et al., 2003).

Table 2.5 Conversion rate for RDF production according to treatment process and country

Country	Rate (%)
Austria	23
Belgium	40-50
Finland	Variable
Netherlands	35
United Kingdom	22-50

The production and the use of RDF increases every passing day and it is expected to increase in the future too. Figure 2.11 presents the amounts of SRF use in different sectors in Germany.

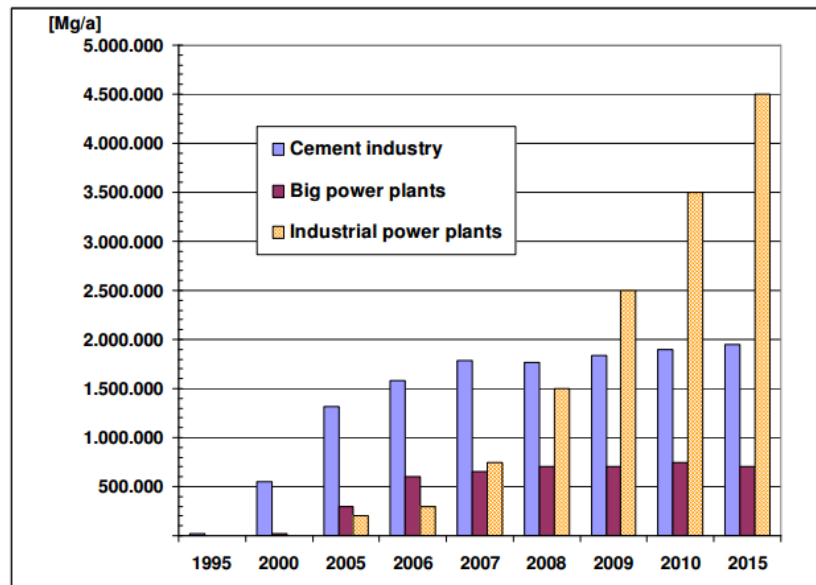


Figure 2.11 Development of the amounts of SRF used in Germany (Abfallwirtschafts et al., 2012)

As RDF is extensively produced and used, the researches about the use of RDF in combustion processes increases. Following section gives a brief summary of these studies.

2.3. Studies on Thermal Processing of RDF

RDF has a heterogeneous composition (e.g. size, higher inert material composition, volatile matter, chlorine, alkali and heavy metal content), lower calorific value, lower bulk density, and lower energy conversion density when compared with the fossil fuels. These differences affect the ignition, combustion characteristics, formation of slag, corrosion possibility, and efficiency (Beckmann and Ncube, 2007).

Many researches are made to investigate the technical and environmental feasibility of pyrolysis, gasification and combustion of RDF in various sectors.

Fluidized bed reactors and drop tube furnaces are the most commonly used combustion reactor types in the pilot scale studies; and cement factories, coal-fired power plants, MSW incinerators are common examples selected for investigation of use of RDF in thermal processes.

2.3.1. Pyrolysis & Gasification of RDF

Pyrolysis and gasification are the advanced thermal waste treatment technologies.

Pyrolysis is decomposing the organic material at high temperatures, around 350-400°C, in an oxygen-free environment. The main product of this process is syngas, which can be used as a secondary fuel in power plants or as a feedstock in chemical industries (URL 5). Temperature and residence time are two important process variables. Moderate process temperatures and short vapor residence time is the optimum conditions for this process for producing liquids; lower temperature and longer residence time causes the charcoal production; higher temperature and lower residence time increases the conversion of biomass to gas (Wilson et al., 2013).

In gasification process organic materials are dissociated at very high temperatures in the oxygen-starved thermal reactor. Synthesis gas and char are produced at the end of the process. The synthesis gas mainly includes CO₂ and H₂O. Using charcoal, CO₂ and H₂O are reduced to CO and H₂ (Wilson et al., 2013). Reactor design and operational parameters affect the products of the process. Some methane and other higher hydrocarbons (HC) may be produced by the process. The gasification agent causes various heterogeneous reaction to occur which converts the feedstock to gas. This gas includes CO, CO₂, CH₄, H₂, H₂O, inert gases (included in gasification agent), trace amounts of higher HCs. In addition, various contaminants such as char particles, tars, ash are produced (Kalyani and Pandey, 2014).

Wang et al., 2002 investigated pyrolysis and combustion in a two-part reactor. The reactor consists of a spouting-moving bed pyrolyzer and a gas combustor. In this study, a wide range of operating conditions is applied and the reactor performed well

under all these conditions. As an outcome of the study, it is stated that increasing the excess air ratio from 1.25 to 1.82 decreases the CO emissions from 298 ppm to 72 ppm; moreover, increasing the excess air ratio from 1.25 to 1.92 decreases the NOx emissions from 75 ppm to 43 ppm. This shows the significant effect of excess air on the emissions. This study is an example for the argument mentioned before; the operation conditions in processes such as pyrolysis and gasification considerably affects the products.

Incineration is used for recovering the energetic value of the waste while both pyrolysis and gasification may also be used for recovering the chemical value. The products of pyrolysis and gasification processes may be used as feedstock for other process or may be a secondary fuel (Bosmans et al., 2013).

However, the pyrolysis and gasification processes have some drawbacks; the technologies of these processes are complex and difficult, and relatively unproven at commercial scale. Also some amount of energy produced is used by the process itself, which reduces the total benefits (Arena, 2012).

2.3.2. Co-combustion of RDF

The combustible materials in the solid waste are thermally oxidized with combustion process to produce the heat energy. This thermal energy can be used in power plants, industrial process, and district heating. The products of the combustion include flue gas, fly and bottom ashes.

For decades, the wastes have been co-combusted with the coal in coal-fired plants in order to reduce the volume of the waste, recover the energy of the waste, and replace the fossil fuels with a secondary fuel (Ekman et al., 1998). However, the studies about the co-combustion of RDF were started later, in mid-1990s (Kobyashi et al., 2005).

As it is presented in Table 2.6, the calorific value of RDF is much higher when compared with the basic MSW.

Table 2.6 Comparison of fuel characteristics of various materials (Tchobanoglous and Kreith, 2002).

Fuel type	Energy Content (Btu/lb)
Coal (anthracite)	12,000-14,000
Coal (bituminous)	11,000-13,000
Tires	12,000-16,000
Mixed MSW	3,500-5,500
Typical RDF	5,200-7,300

The effect of mixing the waste with the coal on the SO_x and NO_x emissions and on ash is investigated in the study done by Norton and Levine (1989). To understand the effects, the sulfur, nitrogen, ash and moisture content of coal and MSW should be compared. 1-4% of coal and 0.1-0.4% of MSW is constituted by sulfur, and 1-2% of coal and 0.6% or less of MSW is constituted by nitrogen. The ash contents of both coal and MSW are variable. The MSW has a higher content of moisture. The emissions are affected by the content of these fuels as well as the mixture fractions. Mixing MSW with coal mainly decreases the sulfur percentage and increases the ash and moisture content. The nitrogen percentage decreases but the change is relatively small. The SO_x emission is directly affected by the sulfur content of the fuel, while the NO_x emission mainly depends on the combustion temperature. The particulate emissions highly depend on the ash content of the fuel. Based on the fuel analyses done by considering these, the sulfur emissions are expected to decrease and particulate emissions are expected to increase when coal and MSW are co-combusted. The nitrogen emissions are difficult to predict since it mainly depends on the combustion temperature.

Chang et al. (1998) conducted an analysis to compare the combustion performance of MSW and RDF by burning them in the same incinerator. The heat balance, ash property, and the quality of flue gas are investigated and compared. This study states

that MSW has lower average heating value, higher toxic substance emissions caused by incomplete combustion, and lower energy recovery potential. When RDF is used as a fuel instead of MSW, the heavy metals in the fly ash is reduced and the flue gas quality is improved. As a result of this study, RDF has a higher heating value which provides higher energy recovery efficiency.

As it is stated by Pretz et al. (2003), formation of the flue gases of CO, HCl, HF, HBr, HI, NO_x, SO₂, VOCs, PCDD/F, PCBs and heavy metal compounds is affected by the composition of material and the operating conditions. The high combustion temperatures makes volatile heavy metals and inorganic compounds to evaporate (partly or totally, depending on the temperature), then these materials are transferred to flue gas and ash (both bottom and flying).

The nitrogen in the waste and combustion air causes nitrogen oxides to form as a product of the combustion process. Nitric oxide (NO), nitrogen dioxide (NO₂) and nitrous oxide (N₂O) are the compounds combination of which is referred as NO_x. The primary component of NO_x is NO, but small amounts of NO₂ and N₂O are also formed as a result of incineration process. Low temperatures (less than 1090°C) in combustion process leads to production of nitrogen oxides. Since MSW combustion temperature is relatively low, the 70 to 80 percent of NO_x formation in MSW incineration is caused by the nitrogen included in the waste. In MSW the main source of nitrogen is the acrylic plastics (Tchobanoglous and Kreith, 2002).

The incomplete oxidation of carbon leads to carbon monoxide (CO) emission in the combustion process. CO is converted to carbon dioxide (CO₂) if the temperature is sufficiently high and there is sufficient amount of oxygen (O₂), and a good mixing of gases is achieved for a long enough time. In the first stages of combustion in an incineration unit CO, hydrogen (H₂), and unburned hydrocarbons are released. These gases converted to CO₂ and H₂O by providing more air to the system. However, if excess amount of air is added the temperature gets very low and the oxidation reactions are retarded; conversely, if less than enough air is added, mixing cannot be

achieved and again this results in incomplete oxidation which causes CO emission to increase (Tchobanoglous and Kreith, 2002).

The level of CO concentration directly indicates the effectiveness and efficiency of combustion and the level of instabilities and non-uniformities in the process. More carbonaceous material is available when the condition in combustion process is unstable, which is resulted in formation of chlorinated dibenzo-dioxins (PCDD or CDD), chlorinated dibenzofurans (PCDF or CDF), and organic hazardous air pollutant materials. High levels of CO emission (several hundred ppmv) is generally correlated with high CDD/CDF emissions, which is caused by incomplete combustion; however, there is not such a correlation when the CO level is low since CDD/CDF formation is caused by many different mechanisms (Tchobanoglous and Kreith, 2002).

Hydrogen chloride (HCl) and sulfur dioxide (SO₂) are produced in waste incineration; hydrogen fluoride (HF), hydrogen bromide (HBr), and sulfur trioxide (SO₃) are also produced but in much lower amounts. The formation of HCl and SO₂ is directly related to the chlorine and sulfur present in the waste. The amounts of these materials depend on the local and seasonal conditions. Paper, food, and plastics are the main sources of chlorine, where asphalt shingles, gypsum wallboard, and tires are the main sources of sulfur in the waste. Relatively high amount of HCl is produced when PVC plastics are present in the waste (Tchobanoglous and Kreith, 2002).

Many RDF co-combustion studies have been conducted to monitor these emissions and its production processes.

Combustion behaviors of two different RDF samples, named as RDF-A and RDF-B, are investigated in the study done by Piao et al. (2000). RDF-A has lower density and strength than the RDF-B has. The samples are incinerated in fluidized bed with 0.3x0.3 m² area and 2.73 m length. The flue gas CO, NO_x and HCl concentrations are measured continuously. They have found that the CO concentration is higher for

RDF-A. The secondary air injection reduces the CO concentrations for both samples; however, the air ratio slightly affects the CO concentration for RDF-B while the CO concentration highly depends on the air ratio for RDF-A. The lower density and strength of RDF-A makes it easily breakable into small fragments which are burnt in the free board. When only primary air is injected at a bed temperature of 1073 K, the increase of air ratio causes the increase of NO_x concentration in the flue gas. However for both samples NO_x concentrations are reduced by injecting the secondary air. The lowest level of HCl concentration, which is 60 ppm, is achieved at 800 °C temperature. The HCl concentration is effectively controlled by the calcium compound addition; higher than 70% of HCl is removed even for temperatures higher than 1173K.

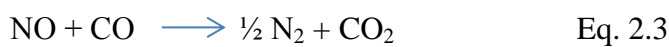
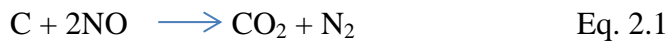
HCl concentration control is investigated in the research conducted by Liu et al. (2001). A single RDF pellet is incinerated in the fluidized bed. A Cl capture fraction of 70% is achieved when the molar ratio of Ca/Cl adjusted as 13. In addition, it is found that increasing the oxygen concentration in injected air decreases the fraction of Cl captured.

In continuous feed incineration systems, the success of combustion behavior and emission control experiments depends on the uniformity of fuel feed. For example, in the study done by Patumsawad and Cliffe (2002), the co-combustion of waste with coal is investigated. The waste fractions are 0%, 10%, 15% and 20% by weight in the study. When the results of the study is investigated, it is obvious that the fuel feed rate is not uniform. Therefore, the effect of excess air cannot be designated in this study. For example, for 15% MSW fraction excess air is increased from 40% to 55% but the combustion efficiency is not affected significantly (between 76% and 83% for both cases). This shows the importance of constant fuel feed rate in continuous feed incineration systems.

NO_x mechanisms are studied in the research conducted by Liu et al. (2002). When the coal proportion to RDF, volatile material content of which is very high, is increased, the amount of carbon or char above the bed increases. This results in the

destruction reaction of NO_x in the freeboard, according to the equations given below. Inversely, when the RDF to coal ratio is increased, NO reduction reaction decreases; therefore, the NO emission increases.

The NO destruction mechanism by char is given below (Liu et al., 2002):



Another study about the NO_x destruction is conducted by Tarelho et al. (2004). In this study, the CO concentration in combustion is very high; therefore, unburnt products such as C, CO, CH₂, CH, CH_i, etc., are entrained in the freeboard. This results in destruction of NO and the NO_x and concentrations decrease in the freeboard.

Composition of flue gas from RDF incinerators is investigated in the study done by Kobayashi et al. (2005). It is stated that the flue gas composition strongly depends on the composition of fuel (RDF) and the air ratio. The fuel ratio (fixed carbon/volatile matter) of RDF used in this study is very high; therefore, the samples are burnt immediately at the freeboard. This provides effective reduction of carbon dioxide concentration in the flue gas by secondary air injection. They investigated the effect of calcium component ratio of RDF on the NO_x and HCl emissions. The NO_x concentration increases with increasing calcium amount. In the study, this effect is associated with the increasing NO production through calcium oxide catalysis. The NO_x concentration increases when the Ca/(S+0.5Cl) molar ratio is increased. On the other hand, HCl concentration decreases with increasing calcium content of RDF. Calcium components react with HCl even at high temperatures.

Engblom et al. (2005) and Gani and Naruse (2005) conducted a research about NO_x emissions associated with the RDF fraction in co-combustion with coal. The NO_x emission change can be large when the RDF ratio is changed since the nitrogen

content and forms of nitrogen contained in RDF and coal are different. It is found that increasing RDF fraction of the fuel increases the NO and NO₂ concentrations in flue gas. This can be associated with the common form of N, which is NH₃, contained in RDF. As it is stated in Hämäläinen et al. (1994), NO is formed in the presence of NH₃ at typical fluidized bed combustion temperatures.

Hernandez-Atonal et al. (2007) conducted a series of combustion experiments with three different RDF samples in two atmospheric fluidized bed combustors. For various operating conditions, the temperature profiles, gas composition and fly ash characteristics are investigated.

The main conclusions of this experimental work are listed below and this results are in agreement with the ones presented in the other studies (Piao et al., 1999; Wang et al., 2002).

- As stoichiometric air ratio is reached, the CO concentration increases exponentially. The secondary air injection has a significant effect on reducing the CO concentration. Secondary air injection becomes more important when the fuel feed rates are high.
- A small amount of nitrogen contained in the fuel (between 2.3% and 4.3%) is converted to NO_x. The secondary air injection slightly decreases the NO_x concentration.
- The Ca/(S+0.5Cl) ratio should be between 1.6 and 2.2 to capture Cl efficiently in the fly ash.
- The temperatures are high and the particle removal efficiency of cyclone used in the test is low, which results in releasing the Pb, Sb, and other volatile metals in flue gas. Heavy metals which have low volatility are captured in the fly ash efficiently.

Wan et al. (2008) investigated the pollutant emissions from co-firing the RDF and coal. In this study the co-firing ratio is increased to 30% in total heat input and it is

shown that the NO_x emissions increase when the fraction of RDF in the mixture is increased.

In the study conducted by Wei et al. (2009), the RDF and coal are co-fired in an internally circulating fluidized bed and the chlorine and sulfur behaviors are investigated. During the RDF incineration a large amount of volatiles are released, which results in unburned gases materials. This is caused by the large amount of volatiles contained in RDF (more than 70%). In this study pulverized CaO is added during the RDF combustion and its effects on sulfur and chlorine absorption are investigated. It is shown that when CaO is added, the ratio of desulfuration is greater than the ratio of dechlorination. When CaO is added CO emission decreases significantly but NO emission decreases slightly. In addition to these, it is stated that increasing the fraction of RDF increases the HCl concentration in the flue gas.

Chyang et al. (2010) investigated the pollutant emissions from co-firing of RDF and coal. PCDD/Fs and HCl emissions are very important when the pollutant emission of RDF combustion is considered. PCDD/Fs and HCl emissions are caused by the chlorine contained in RDF. In this study it is shown that when the fraction of RDF is increased, NO_x and HCl emissions increase also. Because of NH₃ content of RDF, NO emission increases when the amount of RDF in feedstock is increased. Also the concentration of HCl at the bottom of the combustor is lower than the concentration at the top because of the secondary air injection. The scrubber has a significant effect on reducing the pollutant emissions. The results of this study which shows the increase of HCl concentration with increasing RDF fraction are in agreement with the results obtained in Hatanaka et al. (2005).

Abdul et al. (2011) conducted RDF combustion experiments in pilot-scale fluidized bed incinerator for determining the optimal conditions. The optimal condition mentioned is in terms of efficiency and emissions. In this study, it is stated that, high fluidization velocities decreases the temperature too much and causes non-sustainable temperature profiles. In addition, stoichiometric air ratio is not the optimal air ratio when the minimum flue gas emissions are desired.

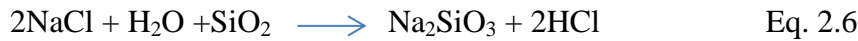
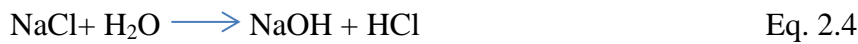
There are many waste and coal combustion studies which shows that sorbents provides a significant retention of sulfur when added to reactor. Also in some studies, it is shown that some materials such as calcium, potassium or sodium are contained in large amounts in biomass fuel and they have the same effect with sorbents and can be used for reducing the acid gas emissions (Dong et al., 2002).

In literature, there are also studies about the influence of RDF combustion on the CO₂ emission. In the study done in Prognos Report (2008), it is calculated that for a cement plant there is potential reduction of 1.04 tCO₂/t RDF and for an optimized waste combustion plant there is a potential reduction of 0.45 tCO₂/t RDF, compared to combustion of coal. In 2006, European cement industry achieved a savings of approximately 5Mt of coal (18 percent of coal use) and an about 8Mt of CO₂ emissions reduction in waste co-processing (CEMBUREAU, 2009). Also, when the reduction in landfill methane emissions, which consist of 60% methane, a gas with a global warming potential 21 times of CO₂, is considered the co-processing of RDF is better than incineration and landfilling of waste.

In the study done by Wang et al. (2014), it is shown that the co-firing RDF in coal fired power plants and cement kilns has important environmental effects; it can reduce global warming and acidification potential significantly.

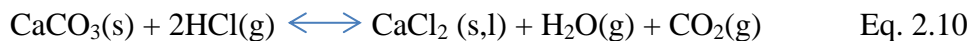
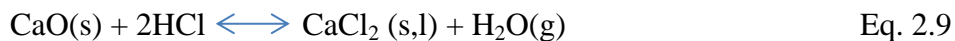
Chyang et al. (2010) investigated the pollutant emissions from co-firing RDF and coal. In the study, a vortexing fluidized bed incinerator is used. For HCl absorption, CaCO₃ at 850 °C is injected in the combustor. It is shown that the higher RDF co-firing ratio results in higher NO_x and HCl emissions. The NO_x concentration at the bottom of the combustor is greater than at the top. Adding CaCO₃ decreases the HCl concentration significantly; however, when the molar ratio of Ca/Cl is greater than 5, the HCl concentration decreases slightly. Adding CaCO₃ increases the chlorine content of fly ash. The CaCO₃ addition slightly decreases the PCDD/Fs emissions. As the conclusion of this study, it is stated that the main cause of PCDD/Fs formation is the incomplete combustion.

In the studies mentioned before, it is shown that the HCl emissions increase with the chlorine concentration. The mechanisms for HCl formation are presented in the study conducted by Dong et al. (2002). In this study, it is stated that NaCl and PVC may be the source of chlorine during the RDF combustion. The reactions for HCl formation mechanism given in the study are shown below.



where L is condensable organic matter, R is solid char and HC is volatile organic matter. From the reaction equations; it is obvious that when Cl, S, H₂O and O₂ are present at the same time, the HCl formation is promoted. High ratio of R is evidence of the high HCl emission. The increasing of H₂O and Cl contents in the fuel mixture also causes the high amount of R. The influence of temperature on the HCl is not obvious. However, HCl may be formed at lower temperatures.

Degradation mechanism of HCl is presented by Ferrer et al. (2005). In this study, it is stated that the degradation of HCl is higher for Ca rich mixtures. Limestone can be used for HCl capture. The reactions corresponding to the capturing process are given below:



Limestone also reacts with SO₂. It is shown in experimental studies that, when HCl is present with no SO₂, the conversion of CaO to CaCl₂ may be high; however, the conversion is almost zero when SO₂ is present. It is found that the capture of HCl is

dominated by the capture of SO_2 by limestone; the HCl concentration decreases slightly when limestone is added if SO_2 is present (Ferrer et al., 2005).

Ferrer et al. (2005) also conducted the study to determine Cl deposition problems. Also the solution of this problem with feedstock composition and coal quality optimization is investigated. The study is done by burning RDF and two coals in a circulating fluidized bed (CFB) reactor. RDF contains more chlorine, alkali and toxic elements when compared with the coal. During the combustion, the inorganic materials partially vaporize and chemical reactions of this vapor and other elements may occur. These materials finally condense in ash. Chlorine is volatilized as HCl and as alkali chlorides. HCl does not form deposits; however, alkali chlorides may be deposited to superheaters and causes corrosion, which occurs even when the temperature is lower than the melting points of pure salt components.

To have an idea about the alkali compounds in deposits, the molar ratio $\text{Cl}/(\text{K}+\text{Na})$ should be investigated. If $\text{Cl}/(\text{K}+\text{Na}) < 1$, that means not only chlorides but other alkali compounds are present too; if $\text{Cl}/(\text{K}+\text{Na}) = 1$, that means all alkalis are deposited as chlorides; and if $\text{Cl}/(\text{K}+\text{Na}) > 1$, this shows that Cl is bound not only to alkalis but also to other metals too (Ferrer et al., 2005).

There are also studies about the metal emissions from RDF combustion. These studies are mentioned in the following paragraphs.

Emissions of heavy metals in RDF combustion are investigated in the study done by Crujeira et al. (2010). A pilot fluidized bed is used for firing coal alone, co-firing RDF and coal, and firing RDF alone. The results are then compared. It is shown that in co-firing, when the amount of RDF is increased, the heavy metal emissions increases but still stay below the regulated limits, except chromium (Cr) and nickel (Ni) emissions. On the other hand, the mono-combustion of RDF leads to more severe heavy metal emissions, especially emissions of cadmium (Cd), lead (Pb), and copper (Cu). This is caused by both large amounts of input, high chlorine and low sulfur contents in RDF, which causes high volatility. Moreover, increasing the

combustion temperature from 850 to 900°C increases the emissions of most heavy metals. Therefore, in this study, it is concluded that, in an environmental point of view, mono-firing RDF is not a preferable way while co-firing RDF with coal is a more environmentally friendly way when heavy metals emissions are considered.

The emissions from waste-to-energy plant is shown together with the emissions from fossil fuel combustion in Table 2.7.

Table 2.7 Comparison of emission from WTE facilities with those from fossil fuels.
(Tchobanoglous and Kreith, 2002).

	Residual Oil	Bituminous coal (pulverized)	Lignite coal (pulverized)	Waste-to-energy (mass burn/refuse derived fuel)
Arsenic (As)	0.22	0.46	0.91	<0.033
Beryllium (Be)	0.06	0.03	0.06	<0.017
Cadmium (Cd)	0.18	0.10	0.11	0.063
Chromium (Cr)	0.24	4.56	570	<0.19
Copper (Cu)	3.19	2.28	3.42	0.43
Mercury (Hg)	0.04	0.23	0.23	0.17
Nickel (Ni)	1436	3.42	3.42	0.84
Lead (Pb)	0.34	0.87	0.11	0.44
Selenium (Se)	-	0.29	0.29	<0.022
Vanadium (V)	3.4	4.0	4.0	0.025
Zinc (Zn)	0.47	8.0	8.0	1.23
Particulate	1,030	440	440	150

Wagland et al. (2011) investigated the metal emissions from co-firing the SRF and RDF in a 50 kW fluidized bed incinerator. In this study, the elements of principal concern are As, Cd, Hg and Pb. As it is stated in Miller et al. (2002), at the temperatures between 800 and 900 °C, the volatility of these metals is the highest. In the study done by Wagland et al. (2011), it is shown that the fly ash contains the major fraction of metals of principle concern. When the SRF is co-fired the amounts of Cd and Pb in fly and bottom ash is found to be smaller. The co-firing of RDF increases the amount of heavy metals (except Zn, Mn and Hg) in bottom ash. The metal release of co-firing RDF is expected to be higher because of high metal content; but, it is observed that the difference of metal content of fly ash samples is not significant in the combustion studies and comparisons done. The amount of metals in flue gas and fly ash samples taken from SRF co-firing is within the acceptable range and it is lower than the one taken from RDF co-firing. A large fraction (up to 98%) of metals is found to be in fly ash except Hg and As. A large portion of Hg is found in flue gas while other metals are generally retained in fly ash. The volatility and mass of the metals determines if the metal is retained in fly ash or bottom ash. Cu, Zn, Cd, Pb, Cr and As are generally retained in the fly ash while Mn is retained in the bottom ash.

2.3.3. Characteristics of Bottom Ash Produced by Combustion of RDF

The characteristics of bottom ash should be investigated since there are some problems related to ash which cause some important operational problems such as corrosion, slagging and fouling. The ash related problems are briefly explained below.

Slagging is the formation of deposit on the surfaces at which heat transfer occurs. In slagging, the sticky particles which are close to flame adhere on these surfaces (Teixeira et al., 2012).

Fouling is the formation of deposit on the cooler surfaces. In fouling either sticky particles may adhere on the surface or the particles transported from hot zones by combustion gases may condensate on these cooler surfaces (Teixeira et al., 2012).

In the study conducted by Pettersson et al. (2008), the contents of ash and RDF are investigated. The RDF used in this study has about 11% ash content. Si, Ca, Na, K and Cl are the important components of this ash. The RDF contains materials such as paper, plastics, wood, rubber, and textiles. Because of improper manufacturing of RDF, different metals are also found. RDF has high chloride content when compared to other fuels. Many plastics such as PVC contain chlorine and this chlorine is released during the combustion. In this study the sodium and chloride in RDF is associated with the food packages with remaining salt.

In the study done by Pettersson et al. (2008), the aluminum content of RDF and its effect is investigated. Aluminum is found in non-soluble and only acid soluble forms in this RDF sample. In general, aluminum contained in RDF travels through the combustor unit and is not fully oxidized. Since this metal is soluble at low pH values it can be included in HCl extraction process. Presence of aluminum is not a reason for ash fouling generally. However it may cause ash handling problems because it is hydrolyzed when the ash is mixed with water and hydrogen gas is evolved.

Some indices are used for quantifying the relation between the composition of materials in ash and their potential of causing slagging/fouling. These indices are shown in Table 2.8. These indices are generally determined by the ratio of the alkalis and sulfur content of the ash.

Table 2.8 Empirical relations for slagging and fouling tendency of ash composition (Park and Jang, 2011)

Classification	Index	Formula		
Slagging	Base-to-Acid Ratio (B/A)	$\frac{Fe_2O_3 + CaO + MgO + K_2O + Na_2O}{SiO_2 + TiO_2 + Al_2O_3}$		
	Sulfur Ratio (Rs)	$\left(\frac{B}{A}\right) x S(\text{in dry fuel})$		
Fouling	Total Alkalis (TA)	$Na_2O + K_2O$		
	Na ₂ O Ratio (Rf)	$\left(\frac{B}{A}\right) x Na_2O$		
	Fouling Ratio (Fu)	$\left(\frac{B}{A}\right) x Na_2O + K_2O$		
Classification	Index	Tendency		
		Low	Medium	High
Slagging	Base-to-Acid Ratio (B/A)	<0.5	0.5<B/A<1	>1
	Sulfur Ratio (Rs)	<0.6	0.6<Rs<2	>2
Fouling	Total Alkalis (TA)	<0.3	0.3<TA<0.4	>0.4
	Na ₂ O Ratio (Rf)	<0.2	0.2<Rf<0.5	<0.5
	Fouling Ratio (Fu)	≤0.6	-	0.6<Fu≤4 0

In the study done by Jenkins et al. (1998), it is stated that the base-to-acid ratio is generally used for determining the slagging tendency of ash. In the equation of this ratio given below, the weight concentration of compounds is shown with labels of each compound.

$$\frac{B}{A} = \frac{Fe_2O_3 + CaO + MgO + K_2O + Na_2O}{SiO_2 + TiO_2 + Al_2O_3} \quad Eq. 2.11$$

However, there is not a single index which reliably determines the tendency of the ash for all combustion conditions.

Teixeira et al. (2012) conducted a study on using woody biomass as biofuel. In this study, it is stated that the slagging and fouling problems of this biomass can be prevented. Incineration of herbaceous and fruit biomass may cause slagging and fouling but proper co-firing and temperature control can eliminate these problems. In the study it is shown that the presence of Si and K leads to formation of sticky ashes which causes ash sintering and agglomeration. When the amounts of Si and K are high, the potassium silicate is formed and even at low temperatures, the formation of melt can occur. However, if Ca is also present in the ash, the fusion temperature of the ash increases because of the formation of potassium-calcium-silicates. But still, potassium-calcium-silicates can also contribute to agglomeration because of the hot spots in the combustion region. The potassium-calcium-silicates melts may adhere to ash particles and projected bed, the melt solidifies when these particles return to projected bed and by this way causes agglomeration. Another cause of agglomeration is contact of these particles with the surface of fuel particles (pellets), combustion temperature of which is higher than the temperature of the bed zone. When the K content is higher than Si in ash, it is more possible for silica particles to interact with the bed surfaces. K in this case may increase the stickiness of sand matrix by incorporating in their surfaces. Thus, covering layers are formed in their surface, which increases their diameter and stickiness, and finally may result in bridges built up between the particles.

The lower chlorine and higher sulphur contents, in other words; high sulphur to chlorine (S/Cl) ratio causes corrosion. In the study conducted by Beckmann and Ncube (2007), the corrosion caused by chlorine is investigated. It is stated that the chlorine bonding type (inorganic or organic) and its interaction with other elements such as alkalis, sulphur, heavy metals have the major importance in corrosion.

Mostly RDF with high plastic content includes chlorine with organic bound. In these types of RDF the inorganic bound chlorine content is 2% at most. The PVC plastic is decomposed in Helium gas, at 20K/min heating rate and it is shown that the chlorine is separated and forms HCl at 300 °C. As it is shown in Figure 2.12 below sulphur to chlorine ratio (S/Cl) of RDF is much smaller when compared to lignite and anthracite coal. So, RDF has much lower corrosion effects than these fuels.

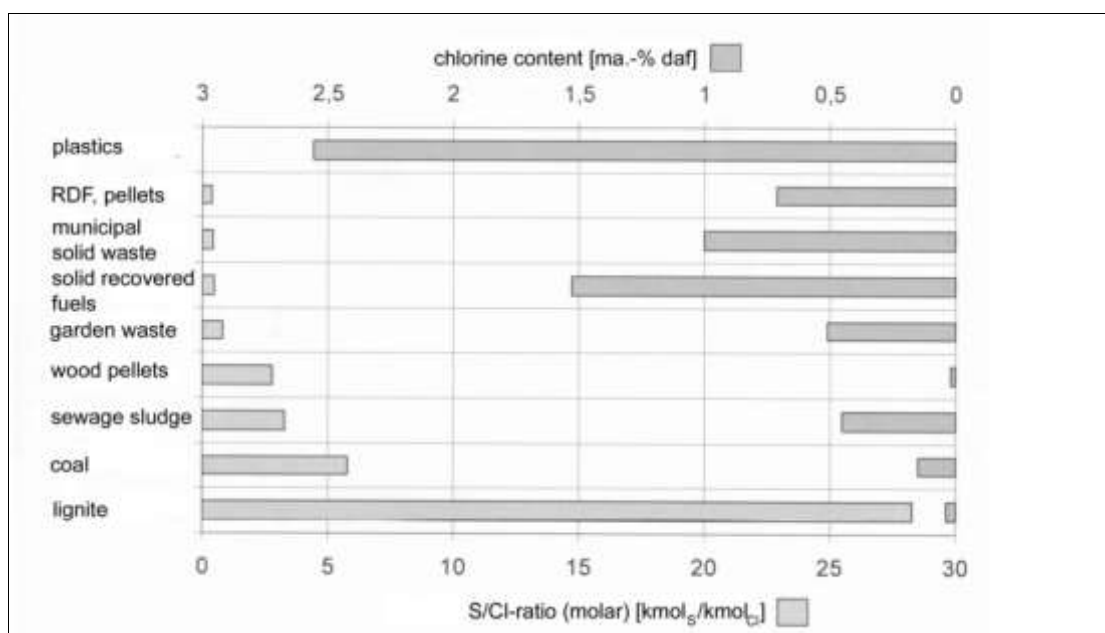


Fig 2.12 Chlorine content and molarity ratios of sulphur to chlorine for chosen fossil fuels, biomass fuels and RDF (Beckmann and Ncube, 2007)

In the research conducted by Seo et al. (2010), XRD technique is used for analyzing the ash components of the char products which are prepared in non-isothermal condition. The sulfur content of coal is given as 0.96% by the ultimate analysis. The sulfur in the coal is captured in the form of CaSO₃ by calcium. Quartz (SiO₂) is the main inorganic component of coal with the strongest peak while SiO₂, Al₂O₃, CaO, CaS and CaCO₃ are the other inorganic compounds of RDF with various peaks. In order to reduce the HCl emission from RDF combustion, the limestone (CaCO₃) is

added to RDF at the production stage. The limestone captures gases chlorine and sulfur. Addition of limestone provides a decrease in CaCO_3 intensity and an increase CaS and CaSO_3 intensities. These reactions happen during the coal/RDF blends pyrolysis. The surface area increase provides a large contact area with coal/RDF blends.

2.4. Studies on Thermal Analysis of RDF

In order to measure the mass loss of a sample or any reaction including mass change, Thermal Gravimetric Analysis (TG) and Differential Thermal Gravimetric Analysis curves are used (DTG). The rate of mass change is given by DTG as a function of temperature and/or time. DTG curve is useful for process which are overlapping and for some kinetic analysis methods. Individual stages of more complex TG curves are resolved by DTG curves. Some special terms about TG and DTG curves are given below (Brown, 2001).

Onset (initial) temperature, T_o : At this temperature, the thermo balance determined from DTG curve detects a change in mass of a sample for the first time.

Burn out (final) temperature, T_f : At this temperature, the mass change of a sample reaches its maximum.

Peak temperature, T_p : is the point at which the highest temperature from the baseline on DTG occurs.

Reaction interval: This defines the temperature interval at which the mass change occur.

Cozzani et al. (1995) conducted a study to present the characterization of the pyrolysis behaviors of different RDF samples under typical heating rates of conventional pyrolysis processes. The RDF weight loss curve presents two distinct weight loss steps which show cellulosic materials and plastic degradation respectively. The same qualitative behaviors are observed for different RDF samples

from different treatment plants and different MSW feedstock. It is stated that the applying conventional gasification processes to RDF may be problematic since the pyrolysis processes yields quite low char.

Marsh et al. (2007) examined the thermal characterization of RDF pellets made up by a range of Mechanical Biological Treatment plants in U.K. In this study, the following conclusions are made:

- According to devolatilisation tests, the char mass is 15% of the original pellet and half of this char amount is fixed carbon. Therefore, it can be concluded that, about 7.5% of pellet mass is carbon available for combustion.
- Devolatilisation process is faster at higher heating rates.
- For lower heating rates, two peaks are observed in the mass loss rate while for higher heating rates there is only one peak. This is opposite to the liquid fuel fractionation process. Therefore, it can be concluded that, if the heating rate is high, which means a higher devolatilisation rate, species which produce less off-gas are masked by a dominant species.
- Actual waste-to-energy process is closer to the process at which the heating rate is higher. Therefore, multiple species evolved in lower heating rates are evolved simultaneously in a process with higher heating rate, which is a more realistic scenario.

Seo et al. (2010) presented the TG and DTG curves for coal, RDF, and RDF-coal mixes. In pyrolysis of coal, the temperature range is wide and the decomposition rates are lower. Final mass of coal is larger (smaller weight loss) when compared to the one of RDF, since the decomposition of ash and fixed carbon is not achieved at high temperatures. Also, in RDF pyrolysis, two distinct peaks are observed. Decomposition of cellulosic and plastic components determines the RDF degradation. At lower temperatures (250–400°C), the cellulosic components are decomposed and at high temperatures (450–500°C), thermally stable plastic components are decomposed. When the RDF amount is increased in RDF-coal blends, the differential weight fraction at the first and second temperature peaks

(343°C and 478°C relatively) increases. At temperatures lower than 700°C, most of RDF and coal components are decomposed. The most of the weight loss occurs in first 30s, while decomposition of residual char and volatiles continues after 30s. When the RDF amount in RDF-coal mix is higher, the rate of decomposition increases, and also the residual char decreases because the RDF contains highly volatiles.

In the study conducted by Lin et al. (1999), the pyrolysis behaviors of the primary polymeric materials which are found in RDF are investigated. Thermogravimetry tests are done to obtain the derived kinetic parameters of the individual polymer paper, PS polystyrene, LDPE, HDPE, and PVC. In thermal degradations of newspaper, toilet paper, LDPE, HDPE, or PS a single stage process is obtained, while in thermal degradation of PVC there is a two stage process. There are two main weight loss stages; the first one is at about 600 K and the second stage is around 680–780 K. The first stage, FTIR spectroscopy detects high concentrations of gases HCl and CO which may be the result of PVC and cellulose materials degradation, respectively. The pyrolysis behavior observed at the first stage is in agreement with the TGA data for individual PVC, LDPE, and paper degradation. At the second stage the degradation of other plastics occurs.

Anouk Bosmans et al. (2014) utilized thermogravimetric analysis and a MATLAB optimization study to investigate the pyrolysis characteristics of RDF. The RDF samples used in this study are processed from excavated landfill waste. The size of the RDF samples is between 150 and 250 μm and they are heated to 800 °C with 10 °C min^{-1} heating rate. It is stated that if the RDF is processed by using household waste, the profiles found in the literature can be caught. Therefore, the kinetic parameters shown in this study provides a good approximation for the case in which RDF is processed from household waste.

RDF is being produced from MSW very recently in Turkey, and its usage as a fuel has not been adopted yet. In this scope, the current study focuses on the quality of

RDF produced at two plants in Turkey in terms of its composition and thermal properties. In the following section, the obtained results and interpretation of these results are presented.

CHAPTER 3

MATERIALS AND METHODS

In this study, combustion characteristics of two RDF, one coal and one petroleum coke samples are investigated. RDF samples are taken from two different material recovery facilities in Turkey; the coal and the petroleum coke samples are taken from a cement factory in Turkey. On these samples, proximate and ultimate analyses are conducted. Thermogravimetric analyses (TGA) are made to observe the combustion behavior of RDF, coal and petroleum coke samples. Also, elemental compositions of ash from RDF samples are determined by XRF analysis. RDF samples are co-combusted in a lab-scale reactor in mixtures with coal and petroleum coke at certain percentages on energy basis (3%, 5%, 10%, 20% and 30%) where co-combustion processes and efficiencies are investigated.

3.1. The Material Recovery Facilities Investigated

RDF samples from the two material recovery facilities (MRFs), MRF-A and MRF-B, are used in this study. From the MRFs, RDF samples were taken on February, 2014. The RDF samples were brought to Middle East Technical University, Department of Environmental Engineering laboratories for preparation and analysis. The samples were mixed well before the analysis to ensure their homogeneity.

The manufacturing process for both RDF-A and RDF-B is similar as both MRFs consist of material recovery units, composting systems and RDF unit for MSW.

Compost and recovery units are established for composting the organic fraction of the total waste and recycling the recyclable fraction of the waste and thus decreasing the amount of wastes landfilled.

Among the materials in wastes coming to the facilities, large wastes such as mattress, chair, textile waste, construction-renovation wastes automobile tires etc. are separated mechanically and sent to landfill area. After the large size wastes are separated, the remaining wastes are fed into sieves; the wastes below 80 mm, mainly organic wastes, are sent to composting unit, whereas the wastes above 80 mm are sent to recycling unit. In recycling unit, a fan separator is used to separate the light fraction of waste. Then, it is treated in pre-shredder followed by magnetic separator for recovery of magnetic fraction. Then, it is sent to ballistic separator to separate the low calorific value wastes. The rest of the waste material is sorting to remove the recyclable fractions (e.g. metal, glass). Also after the composting unit, the so-called coarse compost wastes with high calorific value are sent to RDF unit after separation of metals in it. The remaining wastes which are not valuable in recycling unit and composting unit are called as RDF. In other words, the non-recyclable wastes coming from these units' recycling bands such as plastic bags, textile wastes, nappies, paper wastes, wood pieces, plastics are converted into RDF product. The flow chart of the MRFs where the RDF sample is received is given in Figure 3.1.

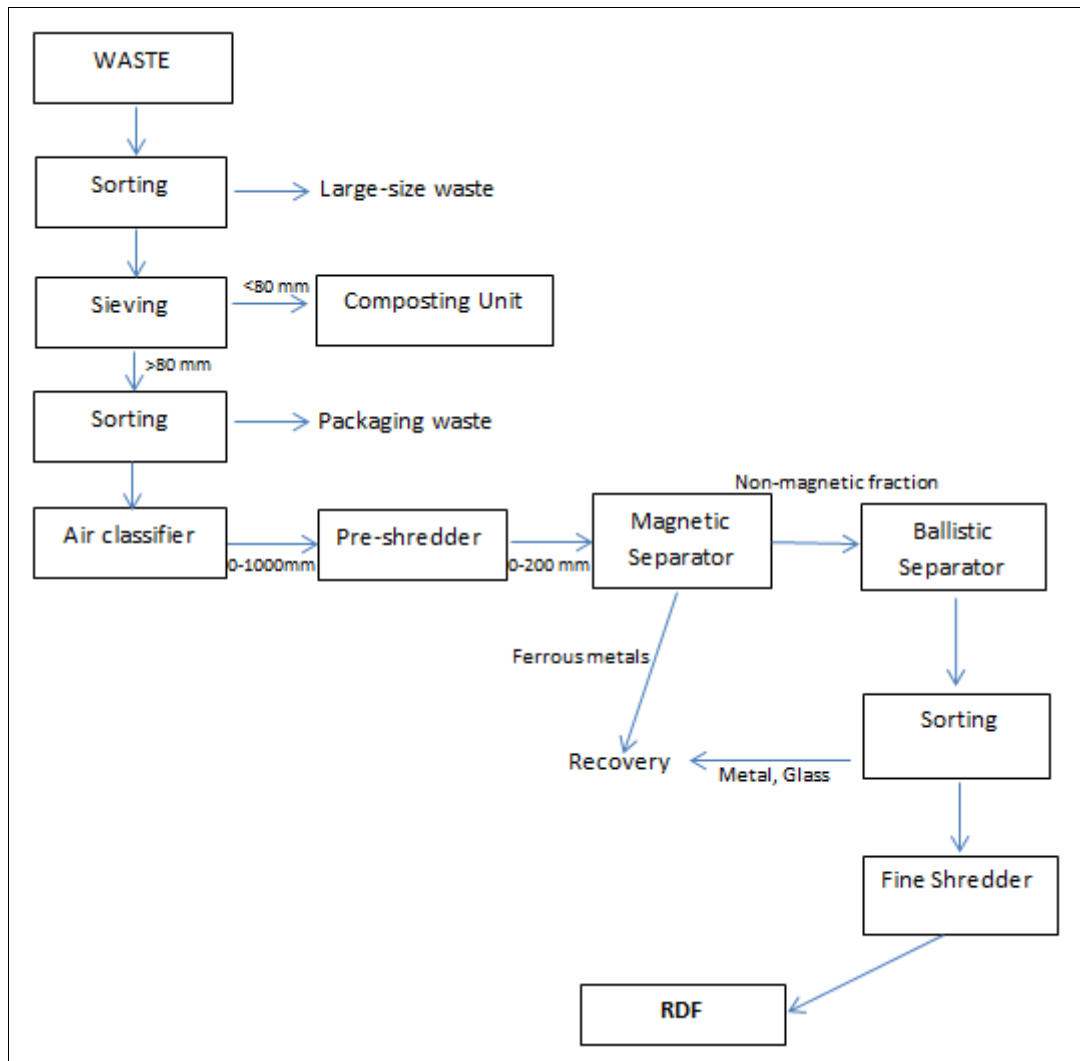


Fig 3.1 Flow diagram of the Material Recovery Facilities

The RDF samples in the form which they are received from these facilities are shown in Figure 3.2.



a) The picture of RDF-A



b) The picture of RDF-B

Figure 3.2 RDF Samples

3.2. Thermal Characterization of RDF Samples

On this stage, proximate, ultimate and XRF analyses are made on the RDF samples and their calorific values are also determined. All experiments were done with triplicate repeated measures.

3.2.1. Proximate Analysis

In proximate analysis, it is assumed that the fuel is composed of two types of materials; volatile and fixed carbon. In this analysis, first, the moisture of samples is determined by drying 1g of sample at 105°C for 2 hours and measuring the weight loss of the samples as percent of the initial weight of the sample. Then the weight loss of the RDF sample is measured after oxidation at 550°C and 750°C for 2 hours to decide its volatile matter and ash content, respectively. Then, the fixed carbon is calculated by subtracting the sum of percentages of volatile matter and ash content at dry basis from a hundred percent.

3.2.2. Ultimate Analysis

Carbon (C), oxygen (O), hydrogen (H), nitrogen (N) and sulfur (S) are the main chemical elements in a fuel. The chemical analysis is very important to calculate the

material balance accurately. Thus, carbon, hydrogen, nitrogen, sulfur and oxygen content of the samples are estimated by ultimate analysis conducted by Truspec Leco CHN-S analyzer in Middle East Technical University, Department of Environmental Engineering. There is an add-on for the device which has similar configuration with the main device in order to analyze sulfur content. Once the percentages of carbon, nitrogen, hydrogen, sulfur and ash are determined, the amount of oxygen is calculated by subtracting the total percentages of the mentioned elements from a hundred percent.

There are three phases during an analysis in the Truspec Leco CHN-S analyzer: purge, combust, and analyze. In the purge phase, the encapsulated sample which weights as about 1 gram is placed in the loading head, sealed and purged of any atmospheric gases that have entered during sample loading. During the combust phase, the sample is dropped into the 950°C furnace and flushed with oxygen for very rapid and complete combustion. The products of combustion are passed through a secondary furnace with 850°C for further oxidation and particulate removal. Then, the combustion gases are collected in a collection vessel. In the analyze phase, the homogeneous combustion gases in the vessel are purged through the CO₂ and H₂O infrared detectors and 3mL aliquot loop. Once the gases have equilibrated, carbon is measured as carbon dioxide by the CO₂ detector and hydrogen is measured as water vapor in the H₂O detector. The gases aliquot loop are transferred to the helium carrier flow, swept through hot copper to remove oxygen and change NO_x to N₂ and then flow through Lecosorb and Annhydron to remove carbon dioxide and water, respectively. A thermal conductivity cell is used to determine the nitrogen content. The final results are displayed in parts per million and are calculated on dry basis. The sulfur determination with the TruSpec Add-On Module is completely independent of the carbon, hydrogen and nitrogen determination. The sample weighting 0.350 gram is put into a combustion boat regulated at 1350°C with a pure oxygen environment. The materials in the sample go through an oxidative reduction process that causes sulfur-bearing compounds to break down and free the sulfur. The sulfur then oxidizes to form SO₂. From the combustion system, the gases flow

through the Anhydrone tube to remove moisture, then infrared detector is used to measure the concentration of the sulfur dioxide gas and the instrument converts that value to percentage on dry basis.

Before the RDF samples' analysis, three blank samples are analyzed to calculate blank area (area under the peak) which will be subtracted from every sample analyzed. After the blank is defined, a calibration is performed. At least three replicates of the same standard needs to be analyzed. The standards used in the study are EDTA for CHN analyzer, and coal for S analyzer. The blank samples are analyzed and subtracted from each of the standard samples. The adjusted area is plotted along the X-axis versus the known concentration along the Y-axis for each of the analyzed standard samples. The curve that best fits the plotted points is used as calibration curve.

Truspec Leco CHN-S analyzer is shown in Figure 3.3.



Figure 3.3 Truspec Leco CHN-S elemental analyzer

3.2.3. Calorific Values

Calorific values of RDF samples are determined by a bomb calorimeter, Leco AC500 model, in Middle East Technical University, Department of Environmental Engineering. The calibration of the device is done with using benzoic acid as a standard.

Figure 3.4 shows a picture of the bomb calorimeter. Known weight of the sample is placed in an empty vessel inside the bomb -a steel ball- where combustion takes place. Then, pressurized pure oxygen is injected into the bomb, and the bomb is placed in an adiabatic water bath, with wires leading from the bomb to a source of electrical current. The sample in the steel ball is combusted by a spark from the wires which in turn heats the water. By using an electronic thermometer measuring the change of temperature vs mass, the heat value of the sample is calculated. In this experiment, the calorimeter is standardized using benzoic acid pellets which have 6000 cal/g. heat value.



Figure 3.4 Leco AC 500 calorimeter

3.2.4. Micro X-Ray Fluorescence (XRF) Analysis

In the present study, XRF Analysis is done for the purpose of determining the inorganic content of RDF ash. The ash content of RDF samples is too small so there is almost no ash remaining in the combustion batch reactor used in the study. Thus, the ash used in the analysis is obtained from muffle furnace. XRF Analysis is done by the Institute of Earth Science, Ankara University.

SPECTRO X-LAB 2000 equipped with a 400 W Pd end window X-ray tube is used for the analysis. In the device, the excitation radiation is optimized using various polarization and secondary targets, the spectral background is reduced by up to an order of magnitude. A state-of-the-art high resolution Si (Li) semiconductor detector is selected for the device as detection system because of its excellent sensitivity for low and high energies at the same time. With this, it is possible to analyze wide range of elements (Na through U) with a high sensitivity.

The samples used in the study are fluxed with sodium tetraborate at 1100°C to achieve loss of organics on ignition. Then, the inorganic content remained is pressed into thick pellets of 32 mm diameter. USGS standards, GEOL, GBW 7109 and GBW-7309 Sediment are equally pressed into pellets in a similar way as the samples, and these are used for quality assurance. In XRF analysis, samples are irradiated by a high intensity x-ray beam which causes electrons to be dislodged from the inner-shell orbitals of atoms in the sample. Replacement of these electron vacancies with electrons from the outer electron shells causes the atoms to emit (fluoresce) x-rays that have a characteristic energy (or wavelength) for each element in the sample. The intensity of the characteristic fluorescent x-rays is proportional to the concentration of the element in the sample allowing for quantitative evaluation of the chemical composition of the sample. In the analysis conducted for this study; Na, Mg, Al, Si, P, S, Cl, K, Ca, Ti, V, Cr, Mn and Fe, which are the major inorganic elements in the sample, are determined. The measurements are done with three different targets and are read five times and the results are saved based on the average value. For each sample measurement takes about 600 seconds.

XRF analysis is important since slagging/fouling indices of RDF samples are calculated using the data gathered by the XRF analysis. The comparison of these values with the ones in the literature and a detailed discussion about these values are given in Chapter 4.1.2.

3.3. Thermogravimetric Analysis (TGA) of RDF Samples

Thermogravimetric analysis is carried out using the TGA instrument, Perkin Elmer Pyris STA 6000, which is able to provide a continuous measurement of sample weight as a function of time and temperature and also give DTG signal (rate of weight loss). TG Analyses of RDF samples were conducted by Middle East Technical University, Central Laboratory. The used TGA instrument's picture is shown Figure 3.5.



Figure 3.5 Perkin Elmer Pyris STA 6000 TG analyzer

Samples weighing about 3 mg were placed in a pottery crucible and temperature program is selected as an isothermal run in which RDF samples are held at 25 °C for 1 min. Then, the samples are heated with non-isothermal run from ambient to 950°C with the heating rate of 10°C/min, with a flow of 40 mL/min. Dry air is selected as the medium. The instrument's balance is calibrated using a certified weight. The experimental setup of this analysis is summarized in Table 3.1.

Table 3.1 Experimental Setup of TGA

Sample	Medium	Temperature Range of Isothermal Run (°C)	Duration of Isothermal Run (min)	Heating rate (°C/min)	Temperature Range of Non-Isothermal Run (°C)
RDF-A RDF-B	Dry Air (21% Oxygen - 79% Nitrogen)	25	1	10	25-950

At the end of this analysis, TGA and DTG curves for RDF-A and RDF-B samples are obtained.

3.4. Lab-Scale Combustion Experiments of RDF Sample - Coal Mixtures and RDF Sample - Petroleum coke Mixtures

A laboratory scale set up is established in order to evaluate the combustion characteristics of RDF samples which can act as an alternative fuel in combustion processes. In combustion experiments, pelletized RDF samples are burned with coal and petroleum coke in different mixtures in an electrically heated cylindrical quartz batch reactor with dimensions of 50 mm diameter and 1200 mm height. The pellets with 15 mm diameter and about 2 mm height are burned at the batch reactor where only one pellet is burned at a time at fixed temperature. More details about the sample preparation are given in Section 3.4.2.

The effect of the RDF addition to the main fuels which are coal and petroleum coke is investigated by analyzing the flue gases of combustion experiments. The experimental setup is given in Figure 3.6 and the Figure 3.7 shows the picture of the reactor.

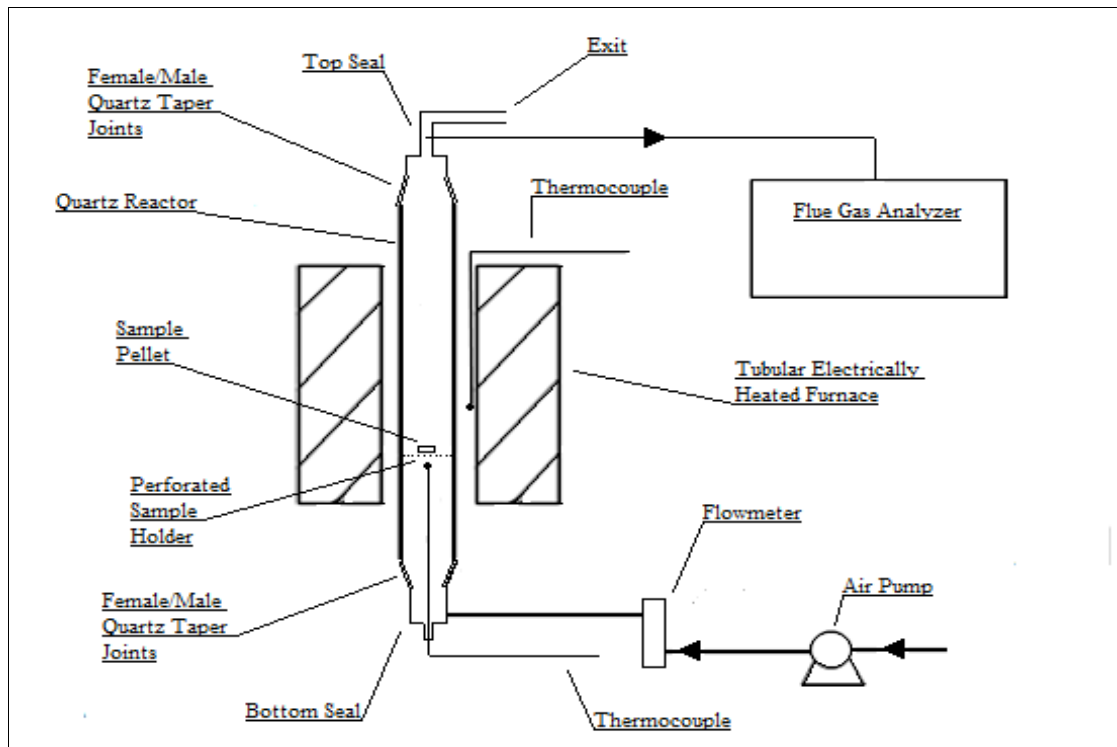


Figure 3.6 Lab scale combustion setup (Atak, 2013)



Figure 3.7 The picture of the reactor (located in the furnace) used in the study

Samples are burnt at 900°C because the previous work showed there was no difference between the combustion gases when combustion was conducted at 800°C, 850°C, 900°C (TUBITAK, KAMAG Project 108G188, Final Report). Higher temperatures are not preferred in order to protect the quartz reactor from extreme temperatures.

At the beginning of each experiment, the cylindrical quartz reactor is heated first by the tubular electric furnace. The temperature is set to 900°C at which the combustion occurs. The two thermocouples, which are located close to furnace wall and inside the quartz reactor (combustion zone), allow measuring the temperature of the furnace and the combustion zone. Then, air is introduced from the bottom of the reactor when the temperature of the combustion zone reaches to 900°C. The flow rate of air, which is 1000 cm³/min, is adjusted by a flow meter. Next, top seal of the reactor is opened in order to drop pelletized sample into the reactor and is closed rapidly. The pelletized sample instantly reaches the combustion zone of the reactor and combustion begins at once and the gas analyzer starts sampling the flue gas. During the test, the oxygen concentration measured by the flue gas analyzer is monitored and the test is ended when it reaches back to the atmospheric concentration (20.95%), which means the combustion process ended.

3.4.1. Flue Gas Analyzer

The combustion gases which are CO₂, CO, NO, NO₂ and SO₂ are monitored by Madur Photon flue gas analyzer continuously. The analyzer consists of two units which are conditioning unit and photon unit (analyzing unit). In the conditioning unit called as PDG-100, moisture in the flue gas is trapped and solid particles in the flue gas are filtered. Thus, the results of analysis are reported on dry basis. In the photon unit, the conditioned flue gas is analyzed. The Madur Photon flue gas analyzer is shown in Figure 3.8. The calibration of the device is done by the distributor company prior to the experiments.



Figure 3.8 Madur photon flue gas analyzer

The device measures the O₂ and CO₂ gases as volume percentage; other gases are measured in ppm. Also, the analyzer unit has unit conversion feature which converts the measured gases in ppm to mg/Nm³.

The detection limit of the device for CO gas is 5000 ppm and for all the other gases measured the limit is 1000 ppm. All gases apart from O₂ gas are detected by the nondispersive infrared sensor (NDIR) which is a simple spectroscopic device often used as gas detector. The NDIR is composed of an infrared source (lamp), a sample chamber or light tube, a wavelength filter and an infrared detector. The gas is pumped into the sample chamber and gas concentration is measured electro-optically by its absorption of a specific wavelength in the infrared (IR). The IR light is directed through the NDIR sample chamber towards the detector. The detector has an optical filter in front of it that eliminates all light with wavelength except the wavelength that the selected gas molecules can absorb. Other gas molecules do not absorb light at this wavelength, and do not affect the amount of light reaching the detector. The O₂ gas is detected by paramagnetic method. In the paramagnetic oxygen analysis, O₂ is attracted into a strong magnetic field; however, other gases are not. This paramagnetism is used to obtain fast, accurate oxygen measurements. A

focused magnetic field is created and the oxygen is attracted into the strongest part of the magnetic field. A current is formed proportional to the concentration of oxygen within the gas mixture and detected.

3.4.2. Sample Preparation

In order to observe the effects of RDF addition to main fuels during combustion, RDF-coal mixtures and RDF-petroleum coke mixtures are prepared by mixing RDF with conventional fuels at ratios of 3%, 5%, 10%, 20% and 30%. Each sample (pellet) combusted is formulated to keep the calorific value constant as 1000 calories. In this study, the RDF mixing ratio means the share of the energy input from the RDF in the total energy input from the fuel mixtures. Also, only RDF samples are combusted without any coal or petroleum coke addition to observe the efficiency of RDF combustion alone. The prepared samples are combusted in triplicate run. The experimental conditions are listed in Table 3.2.

Table 3.2 Percentages of RDF in mixtures

RDF Sample	Fuel Sample	Percentage of RDF in Mixtures by Energy Share	Temperature (°C)
A and B	Coal, Petroleum coke	0%, 3%, 5%, 10%, 15%, 30%, 100%	900 °C

*Ratio of RDF samples in fuel mixtures; 0% represents mixtures which contain no RDF sample; 20% indicates mixtures prepared by 20% RDF and 80% of coal or petroleum coke, 100% represents mixtures which contain only RDF.

The mass of RDF samples, coal and petroleum coke to get mixtures with 1000 cal/g heating value is determined by the following equation:

$$1000 \text{ calories} = M_1(g).LHV_{RDF \text{ Samples}}(cal/g) + M_2(g).LHV_{coal}(cal/g) \quad \text{Eq. 3.1}$$

$$1000 \text{ calories} = M_3(g).LHV_{RDF \text{ Samples}}\left(\frac{cal}{g}\right) + M_4(g).LHV_{petcoke}\left(\frac{cal}{g}\right) \quad \text{Eq. 3.2}$$

where;

M_1 = Mass of RDF sample added to mixtures shown in Table 3.4 (g)

M_2 = Mass of coal added to mixtures shown in Table 3.4 (g)

M_3 = Mass of petroleum coke added to mixtures shown in Table 3.4 (g)

LHV = Lower heating value on dried basis (cal/g)

The calorific values and the moisture contents of RDF samples, coal and petroleum coke are given in Table 3.3. The mass of each sample used for combustion experiments (total calories = 1000 cal each) are shown in Table 3.4.

To get the percentage contribution of RDF in total fuel shown in Table 3.2 based on M_1 , M_2 , and M_3 values are determined by the following relationships;

$$\text{Percentage of RDF (\%)} = \frac{M_1(g).LHV_{RDF}(cal/g)}{M_1(g).LHV_{RDF}(cal/g) + M_2(g).LHV_{coal}(cal/g)} 100 = \frac{M_1(g).LHV_{RDF}(cal/g)}{1000 \text{ calories}} 100 \quad \text{Eq. 3.3}$$

$$\text{Percentage of RDF (\%)} = \frac{M_1(g).LHV_{RDF}(cal/g)}{M_1(g).LHV_{RDF}(cal/g) + M_3(g).LHV_{petcoke}(cal/g)} 100 = \frac{M_1(g).LHV_{RDF}(cal/g)}{1000 \text{ calories}} 100 \quad \text{Eq. 3.4}$$

Table 3.3 Calorific value of RDF samples and coal and petroleum coke

Sample Name	LHV (cal/g)**	Moisture (%)*
RDF-A	5292.35±158.04	1.6± 0.02
RDF-B	4596.03±36.08	14.8±0.09
Coal	6128.43±66.75	4.3±0.03
Petroleum coke	8217.32±71.53	7.0±0.12

*% by weight
 **% on dry basis

Table 3.4 Mass of RDF samples, coal and petroleum coke used to obtain different fuel mixtures (each pellet has 1000 calories)

Sample Name	0% RDF	3% RDF	5% RDF	10% RDF	20% RDF	30% RDF	100% RDF
M1 RDF-A(g)	0	0.0058	0.0096	0.0192	0.0384	0.0576	0.1920
(g) RDF-B (g)	0	0.0077	0.0128	0.0256	0.0511	0.0767	0.2554
M2 Coal (g)	0.1706	0.1654	0.1620	0.1535	0.1364	0.1194	0
M3 Petroleum coke (g)	0.1302	0.1269	0.1243	0.1178	0.1047	0.0916	0

Last step of sample preparation is to pelletize the RDF sample-coal and RDF sample-petroleum coke mixtures for combustion experiments. The pelletization offers higher

density and therefore contains more energy per volume than unpelletised mixtures. In pelletization process, a hand sized pellet press is used. First, corresponding amounts of RDF samples, coal and petroleum coke whose masses are listed in Table 3.4 are mixed in separate holders in order to obtain RDF-coal mixtures and RDF-petroleum coke mixtures percentages of which are given in Table 3.2. Then, mixtures are poured into the mould of the pellet press and pressure is applied. Unfortunately, pelletizer used in this study is a hand sized and it is not possible to apply as much pressure as a controller. However, pressure applied in each pelletizing operation is kept the same. Consequently, pelletized RDF-coal and RDF-petroleum coke mixtures have 15 mm diameter and about 2 mm height. An example of the pellet used in this study is shown in Figure 3.9.



Figure 3.9 Example of a pellet

3.4.3. Combustion Experiments

Concentrations of O_2 , CO_2 , CO , NO , NO_2 and SO_2 from flue gas of the batch combustion experiments are measured by flue gas analyzer. The gases emission profile, an example of which is shown in Figure 3.10, is obtained from Madur analyzer. Then the amount of carbon, nitrogen and sulfur released through combustion experiment is calculated. Also, carbon, nitrogen and sulfur content of mixtures are already known by ultimate analysis. So, it is possible to make material

balance on carbon, nitrogen and sulfur for each experiment. Furthermore, the combustion efficiency for each experiment is calculated and analysis of variance (ANOVA) is performed by using the 16th version of STATGRAPHICS program to evaluate the results of the combustion efficiencies and see the differences between them. Each combustion experiment is made in triplicate to get more accurate results.

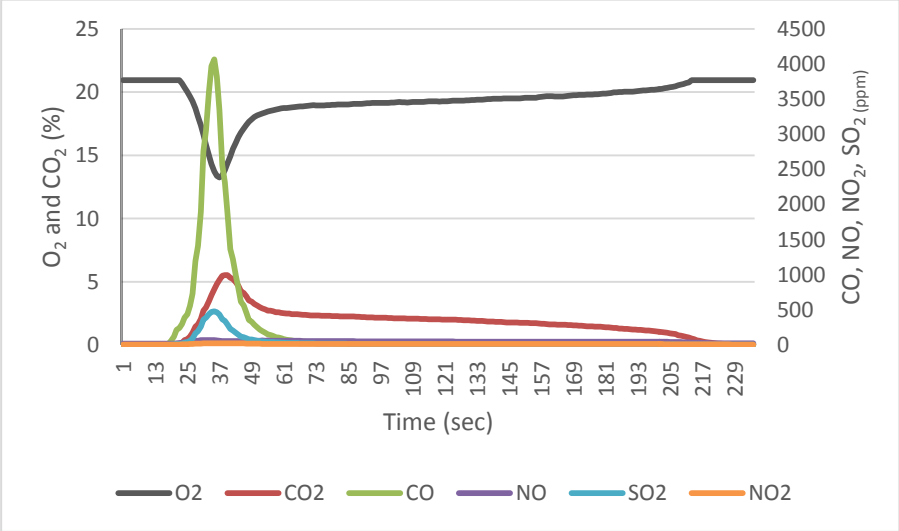


Figure 3.10 Emissions measured in a combustion experiments

By the observation of gases profiles, start and end time of each experiment is understood easily; each gases emission values returns to its original value when the combustion process ends. Also, the time passed in combustion process is seen from graph and the flow rate of dried air in and out of the reactor gases is known. Thus, to calculate mass of carbon, nitrogen and sulfur, an integration of the curve is done by the following equations;

Mass of carbon;

$$M_C = 1.25Q_{\text{analyzer}} \frac{12}{28} \int_{t_{\text{start}}}^{t_{\text{end}}} \text{Conc. of CO (ppm)} dt + Q_{\text{analyzer}} P_{\text{analyzer}} \frac{12}{T/R/100} \int_{t_{\text{start}}}^{t_{\text{end}}} \text{Conc. of CO}_2(\%) dt \quad \text{Eq. 3.5}$$

Mass of nitrogen;

$$M_N = 2.06Q_{\text{analyzer}} \frac{14}{46} \int_{t_{\text{start}}}^{t_{\text{end}}} \text{Conc. of NO}_2(\text{ppm}) dt + 1.34Q_{\text{analyzer}} \frac{14}{30} \int_{t_{\text{start}}}^{t_{\text{end}}} \text{Conc. of NO (ppm)} dt \quad \text{Eq. 3.6}$$

Mass of sulfur;

$$M_S = 2.86Q_{\text{analyzer}} \frac{32}{64} \int_{t_{\text{start}}}^{t_{\text{end}}} \text{Conc. of SO}_2(\text{ppm}) dt \quad \text{Eq. 3.7}$$

where;

Q_{analyzer} : volumetric flow rate of gas sampling by analyzer

P_{analyzer} : pressure of gas sampling by analyzer

t_{start} : time when experiment starts

t_{end} : time when experiment ends

R: ideal gas constant

T: temperature

The first terms which are the coefficients of 2.86; 2.06; 1.34; 1.25 are the conversion factors of gases from ppm to mg/Nm³ for SO₂, NO₂, NO and CO, respectively. The second term corresponds to the flow rate of flue gases measured by the analyzer.

Also, 32/64; 14/46; 14/30; 12/28 are the ratios of molecular weights of S, N and C to SO₂, NO₂, NO and CO, respectively. The gases concentration is measured with respect to time during the combustion. As seen from the formulas, an integration is taken to calculate the under the curve area which gives the total concentration of the corresponding pollutant gases along the combustion in ppm. The CO₂ gas is measured as volume percentage as mentioned before. So, gas law is also applied to calculate the CO₂ mass resulting of the combustion experiment.

CHAPTER 4

RESULTS AND DISCUSSION

In this section, results of proximate and ultimate analysis, XRF analysis, TG analysis of RDF samples, and also combustion experiments of RDF-coal mixtures and RDF-petroleum coke mixtures are given.

4.1. Thermal Characterization of RDF, Coal and Petroleum coke Samples

In the scope of thermal characterization, proximate and ultimate analyses were conducted on RDF, coal and petroleum coke samples. Also, elemental composition of ash from RDF sample is determined.

4.1.1. Proximate/Ulimate Analysis of RDF, Coal and Petroleum coke Samples

Combustion process is highly dependent on the moisture content, ash content and volatilization characteristics of the fuel. When these parameters are known quantitatively, it helps understanding the nature of the combustion process (Niessen, 2002)

Proximate analysis separates the products into four groups: (1) moisture, (2) volatile matter, consisting of gases and vapors, (3) fixed carbon, the nonvolatile fraction of sample, and (4) ash, the inorganic residue remaining after combustion.

In this sense, proximate analyses of RDF samples, besides coal and petroleum coke samples are made in triplicate. The results given in Table 4.1 are the average values of the results of these three separate analyses. Standard errors are also calculated and shown with the averaged results in the table.

Table 4.1 Proximate analysis of RDF samples, coal and petroleum coke

Sample	Moisture (%)[*]	Volatile Matter (%)^{**}	Fixed Carbon (%)^{**}	Ash (%)^{**}
RDF-A	1.6± 0.02	81.8±0.89	5.2±0.52	12.9±0.38
RDF-B	14.8±0.09	68.5± 0.52	16.6± 0.74	14.9± 0.64
Coal	4.3±0.03	29.3±0.11	53.5±0.12	17.2±0.22
Petroleum coke	7.0±0.12	12.1±0.17	87.4±0.31	0.7±0.01

*% by weight, as collected

**% by weight on dry basis

RDF samples are mainly composed of volatile matter (VM) and ash. Volatile matter contents of RDF samples used in this study are 81.5% and 68.5%; ash content of RDF samples are 12.9% and 14.9% , for RDF-A and RDF-B, respectively.

It can be seen in Table 4.1 that RDF-B has the higher ash content and lower volatile matter content than RDF-A. In addition, the moisture content of RDF-B higher than that of RDF-A, because the RDF-A sample is dried in its facility and then is send to our laboratory. Moreover, RDF-B probably has higher concentration of paper which absorbs ambient humidity. Also, paper and cartoon increases ash content, which clarifies the higher ash content of RDF-B. When the results of coal and petroleum coke are compared, it can be seen that petroleum coke has lower ash content and volatile matter than coal has, as expected.

Also, it should be emphasized that proximate analysis results of RDF samples are in accordance with the literature data. The values obtained in this study and the values gathered from the literature survey are given in Table 4.2 including the average values.

Table 4.2 Comparison of proximate analysis with literature data

	Moisture	Volatile Matter (%)*	Fixed Carbon (%)*	Ash (%)*
Literature ¹	1-12-48	46-74-90	1-10-21	3-13-27
RDF-A	2	82	5	13
RDF-B	15	68	17	15

¹Lower number indicates the minimum observed, upper number indicates the maximum and values in the middle correspond to averages
* % by weight on dry basis

The knowledge about the composition of the fuels is very important in the combustion experiments. The carbon, hydrogen, and oxygen content are important since these elements are the main fuel fraction of the waste. Nitrogen content is also required to be known because it determines the generation of NO_x formation. Sulfur is another important element, amount of which should be known since the presence of sulfur causes the generation of acid gases SO₂ and SO₃ which contribute to air pollution and corrosion (Niessen, 2002).

¹ (Abdul et al., 2011; Ahn et al., 2013; Astrup, Møller, & Fruergaard, 2009; Chang et al., 1998; Cozzani et al., 1995; Dunnu et al., 2010; Fernandez et al., 2003; Ferrer et al., 2005; Genon & Brizio, 2008; Pretz et al., 2003; Kers et al., 2010; Lin et al., 1999; Patumsawad & Cliffe, 2002; Piao et al., 1999; Ryu et al., 2006; Saxena & Rao, 1993; Scala & Chirone, 2004; Seo et al., 2010; Vainikka et al., 2013; Wagland et al., 2011; Wang et al., 2014; Wang et al., 2002)

In this context, an ultimate analysis which gives the elemental composition of RDF, coal and petroleum coke samples are conducted and calorific values of the samples are determined and the results are given in Table 4.3.

Table 4.3 Ultimate analysis and calorific values of RDF samples, coal and petroleum coke

Sample	Carbon (%)[*]	Hydroge n (%)[*]	Nitroge n (%)[*]	Sulfur (%)[*]	Oxygen (%)[*]	Calorific Value (cal/g)^{**}
RDF-A	44.14±1.09	5.63±0.37	0.97±0.31	-	36.26±1.20	5292.35±158.04
RDF-B	56.47±0.53	8.96±0.25	1.50±0.08	0.45±0.02	17.73±0.17	4596.03±36.08
Coal	63.80±0.15	3.65±0.02	1.88±0.04	0.55±0.02	12.94±0.06	6128.43±66.75
Petroleu m coke	68.12±0.21	3.63±0.05	1.94±0.06	4.73±0.09	20.51±0.11	8217.32±71.53

*% by weight on dry basis

** Lower heating value on dry basis (cal/g)

The results of ultimate analysis of RDF samples are in agreement with the literature data. The values obtained in this study and the values gathered from the literature survey including minimum, maximum and average values are given in Table 4.4.

Table 4.4 Comparison of ultimate analysis with literature data

	C (%)*	H(%)*	O(%)*	N(%)*	S(%)*	Calorific Value (cal/g)**
Literatur e ²	24- 47-70	1-6-11	11-30-44	0.04-0.9-4	0.06-0.2-1.6	2095-4525- 5900
RDF-A	44	6	36	1	n.d.	5292
RDF-B	56	9	18	1.5	0.4	4596

²Lower number indicates the minimum observed, upper number indicates the maximum and values in the middle correspond to averages * % by weight on dry basis

* % by weight on dry basis

** Lower heating value on dry basis (cal/g)

n.d.: not detected

Ultimate analysis of the samples reveals that organic fraction of RDF contains predominantly carbon and oxygen. Nitrogen and hydrogen percentages in the samples are not higher than 9%. However, the content of hydrogen is higher in RDF samples than the one in coal and in petroleum coke samples as seen in Table 4.3. The higher hydrogen content may occur because of the organic matters in the waste.

² (Abdul et al., 2011; Ahn et al., 2013; Astrup et al., 2009; Chang et al., 1998; Cozzani et al., 1995; Dunnu et al., 2010; Fernandez et al., 2003; Ferrer et al., 2005; Genon & Brizio, 2008; Pretz et al., 2003; Kers et al., 2010; Lin et al., 1999; Patumsawad & Cliffe, 2002; Piao et al., 1999; Ryu et al., 2006; Saxena & Rao, 1993; Scala & Chirone, 2004; Seo et al., 2010; Vainikka et al., 2013; Wagland et al., 2011; Wang et al., 2014; Wang et al., 2002)

Sulfur has the lowest percentage among all elements; in RDF-B the sulfur content is 0.45% and sulfur is not detected in RDF-A. Calorific values of samples are 5292 and 4596 cal/g on dry basis, for RDF-A and RDF-B, respectively.

The carbon contents of RDF, coal and petroleum coke samples are very close to each other. This is because of the removal of inert material such as glass, stones, metals etc. from input waste before production of RDF. Also, as it is stated in Beckmann et al. (2012), the calorific value of the RDF increases by separating the inert material and moisture, which enriches the organic substances.

Calorific value of RDF-A is quite higher than RDF-B. This may be associated with the higher amount of organic substances and particularly the plastics. In addition, the calorific values of RDF samples are very close to that of the coal and petroleum coke used in this study. The coal used in this study is considered to be high in calorific value in reference to URL 6 and URL 7. Comparison of calorific values of different fuel types is given in Figure 4.1.

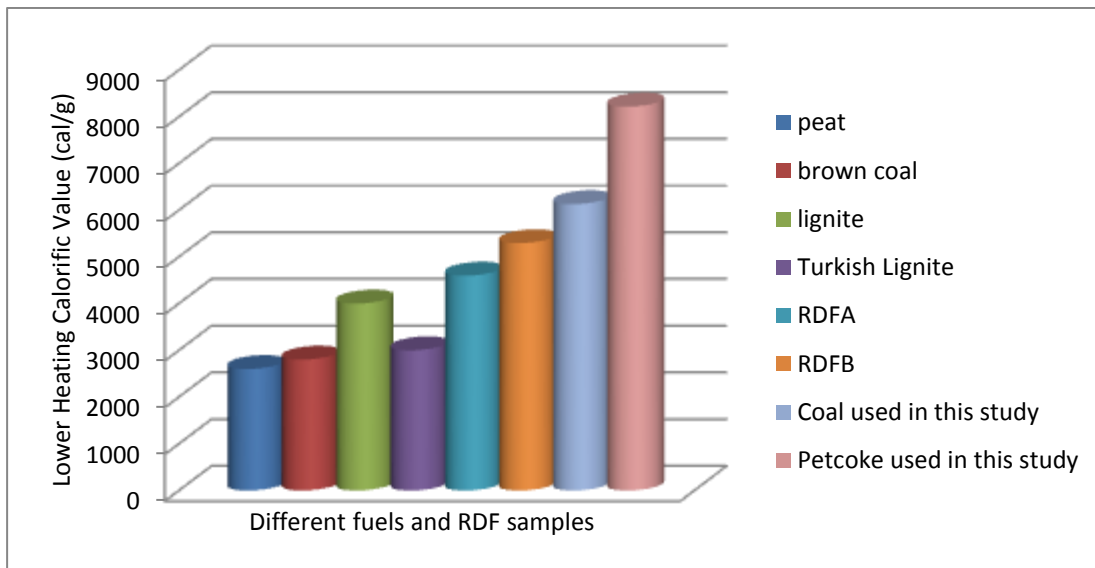


Figure 4.1 Comparison of calorific values of different fuel types

The calorific value of petroleum coke is higher than that of the coal. Due to the lower VM content and higher C content, petroleum coke has the higher calorific value. In addition, the C/H ratio of the petroleum coke is higher; while, C/O ratio of the petroleum coke is smaller than the coal, as in the primary fuels. However, as stated in Beckmann et al. 2012, when the C content of RDF increases, the volatile matter remains constant, or increases slightly. Also, when the calorific value increases, the C/H ratio does not change and the C/O ratio increases. So, it can be said that the RDF and fossil fuels illustrates different characteristics.

The comparison of volatile matter and C-content of different fuels and different RDF samples given in the literature are presented in Figure 4.2. Also, C/H and C/O ratio with calorific values of different biomass fuels and different Solid Recovered Fuel (SRF) are given Figure 4.3.

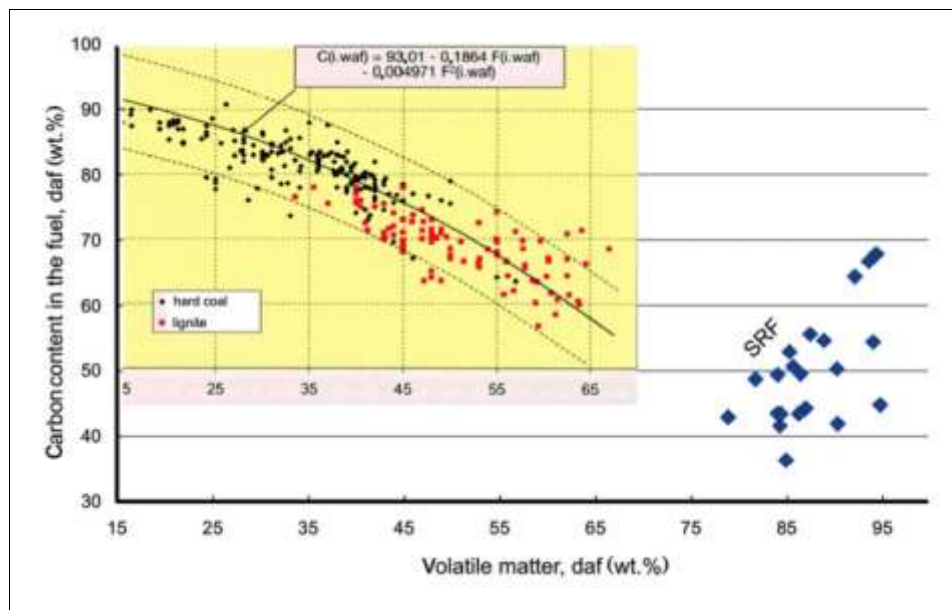


Figure 4.2 Comparison of volatile matter and C-content of the fuel of different coals and different SRF (Beckmann et al., 2012).

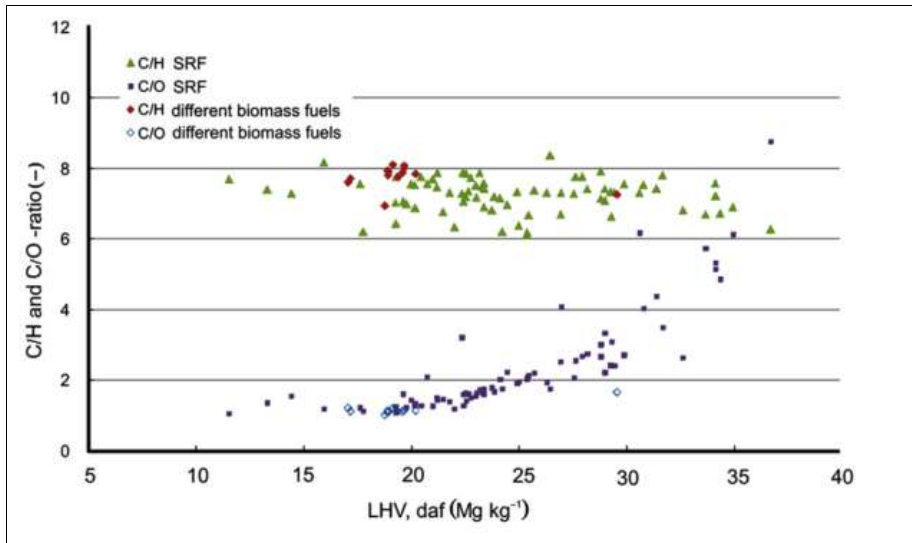


Figure 4.3. C/H and C/O – ratio of different biomass fuels and of SRF (Beckmann et al., 2012).

However, in this study the behavior of RDF samples are found to be very similar to the fossil fuels as the volatile matter content decreases with an increase in the C content and the C/H ratio increases and the C/O ratio decreases as the calorific value increases. Since this study used only two RDF samples, the results may not be enough to express any trend and comment on. Besides, the data for RDF in literature are also so limited currently.

The European Committee for standardization (CEN) has proposed a draft standard (CEN TC 343) of quality categories according to the calorific value, chlorine content, and mercury content as mentioned in Section 2.3. The criteria used for defining the characteristics of SRF are shown in Table 4.5. It should be noted that desirability decreases with higher rated classes.

Table 4.5 SRF classification according to CEN standardization

Classification property	Unit	Class 1	Class 2	Class 3	Class 4	Class 5
Biomass content (as received)	% (mean)	≥90	≥80	≥60	≥50	<50
Net calorific value (as received)	MJ/kg (mean)	≥25	≥20	≥15	≥10	≥6.5
Moisture content	% wt/wt (mean)	≤10	≤15	≤20	≤30	<40
Chlorine Content (dry)	% wt/wt (mean)	≤0.2	≤0.6	≤0.8	-	-
Ash content (dry)	% wt/wt (mean)	≤10	≤20	≤30	≤40	<50
Bulk density (as received)	kg/m ³ (mean)	>650	≥450	≥350	≥250	≥100
Mercury (Hg) (as received)	Mg/MJ (Median)	≤0.02	≤0.03	≤0.06	-	-
Cadmium (Cd) (as received)	Mg/MJ (Median)	≤0.1	≤0.3	≤1.0	≤5.0	≤7.5
Sum of heavy metals (HM) (as received)	Mg/MJ (Median)	≤15	≤30	≤50	≤100	≤190

According to the proposed standard, the RDF-A is in the second category of calorific value (22.14MJ/kg), in the first category of moisture content (1.6%) and in the first category concerning its chlorine content (0.29%). The proposed chlorine content of RDF samples is shown in the following section. In addition, RDF-B is in the third category of calorific value (19.2 MJ/kg), in the second category of moisture content (14.8%) and in the second category concerning its chlorine content (0.32%).

4.1.2. Determination of Ash Composition of RDF Samples by XRF Analysis

Slagging and fouling are the two types of deposit formation during combustion. Slagging refers to the deposition of ash in the high temperature heat-resistant sections of reactors and it occurs because of the formation of low melting temperature ashes. Besides, the alkali metals reduce the melting point of ash. Fouling occurs due to the deposit of ash particles in the convective heat transfer zones of the reactor where temperature is relatively colder and the gases cool down (Teixeira et al., 2012).

There is a wide range of elements which contributes to slagging and fouling in combustion experiments. XRF analysis is done to determine the inorganic elements, which forms the ash content of RDF samples. Using the result of this analysis, fouling and slagging indices of RDF samples are calculated. Results of XRF analysis are presented as element oxides and on dry basis in Table 4.6.

Table 4.6 Inorganic element contents of RDF samples (% by wt.)

	RDF-A	RDF-B
Na ₂ O	0.20	0.06
MgO	0.13	0.12
Al ₂ O ₃	0.43	0.42
SiO ₂	1.21	1.54
P ₂ O ₅	0.14	0.11
SO ₃	0.20	0.24
Cl	0.29	0.32
K ₂ O	0.27	0.44
CaO	3.36	2.72
TiO ₂	0.15	0.13
V ₂ O ₅	-	-
Cr ₂ O ₃	-	0.01
MnO	0.01	0.01
Fe ₂ O ₃	0.08	0.23

It can be seen in Table 4.6 that Si and Ca are the most abundant inorganic elements in RDF samples tested in this study. The Cl content of RDF samples is also high, which may originate from the presence of chlorine in PVC (polyvinyl chloride) plastic and waste paper as well as the salt in food wastes in RDF content. Moreover, Fe, K, Al and S are other inorganic elements that are found in high concentrations.

Slagging and fouling indices are calculated for the RDF samples by using the formula given in section 2.2.3, Table 2.6. Particularly “Base to acid ratio” (B/A), and

“sulfur ratio” (R_s) are used as slagging indices; “total alkalis” (TA), and “fouling index” (F_u) are used as fouling indices, as they are used in Teixeira et al. (2012).

B/A considers that the alkali and alkali-earth oxides have the same role in the melting formation relatively to Al_2O_3 , SiO_2 , and TiO_2 content, i.e., the basic compounds, B, are assumed to decrease the melting temperature, while the acidic ones, A, increase it.

The sulfur ratio, R_s , is related to slagging potential of sample. The slagging potential is found to be low when $R_s < 0.6$, medium when $R_s = 0.6-2.0$, high when $R_s = 2.0-2.6$, and extremely high for $R_s > 2.6$

The fouling index, F_u , which is based on Base-to-Acid ratio, according to Eq. 4.4, gives more relevance to the alkaline elements which are the main agents of fouling. The fouling potential is found to be low when $F_u \leq 0.6$, medium for $0.6 < F_u \leq 1.6$, high for $1.6 < F_u \leq 40$.

However, it is worth to note that contrary to coal ashes, major elements included in RDF ashes are not from geological origin. They are mostly derived from refined products which are used in the production of RDF. Therefore, the fouling and slagging propensity of RDF ashes may not be predicted very accurately since the indices used are applicable to coal ashes (Dunnu et al., 2010).

An example calculation of slagging and fouling indices for RDF-A is illustrated below:

<p>Base to Acid Ratio (B/A)</p> $= \frac{\text{Fe}_2\text{O}_3 + \text{CaO} + \text{MgO} + \text{K}_2\text{O} + \text{Na}_2\text{O} + \text{P}_2\text{O}_5}{\text{Al}_2\text{O}_3 + \text{SiO}_2 + \text{TiO}_2}$ $= \frac{0.08 + 3.36 + 0.13 + 0.27 + 0.20 + 0.14}{0.43 + 1.21 + 0.15} = 2.3$	<i>Eq. 4.1</i>
<p>Sulfur Ratio (R_s) = $\left(\frac{B}{A}\right) \times S = 2.3 \times 0.20 = 0.46$</p>	<i>Eq. 4.2</i>
<p>Total Alkalis (TA) = $\text{Na}_2\text{O} + \text{K}_2\text{O} = 0.20 + 0.27 = 0.47$</p>	<i>Eq. 4.3</i>
<p>Fu = $(B/A) \times (\text{Na}_2\text{O} + \text{K}_2\text{O}) = 2.3 \times 0.47 = 1.08$</p>	<i>Eq. 4.4</i>

The calculations are also made for RDF-B using the inorganic element contents of it. The slagging and fouling calculations results along with the reference levels for low, medium and high slagging and fouling indices are listed in Table 4.7.

Table 4.7 Slagging and fouling indices of RDF samples

Slagging-Fouling Indices of RDF Samples				Limit Values (Pronobis, 2005; Vamvuka et al.,2009)		
		RDF-A	RDF-B	Low	Medium	High
Slagging	B/A	2.3	1.8	<0.5	0.5<B/A<1	>1
Index	R_s	0.5	0.3	<0.6	0.6< R_s <2	>2
Fouling	TA	0.5	0.5	<0.3	0.3<TA<0.4	>0.4
index	Fu	1.1	0.9	≤0.6	-	0.6<Fu≤40

Table 4.7 shows that the RDF samples have moderate to high slagging and fouling tendency when compared to limit values. Base to acid ratio (B/A) of both RDF samples are higher than “high” class. Sulfur ratios of both RDF bottom samples are low propensity. Fouling tendency of RDF samples is high when compared to limit value because of the high content of volatile inorganic components Na_2O , K_2O as shown in ash composition table.

Moreover, the relation between alkalis (K + Na) and Cl is investigated in order to understand if slagging aspects dominate over the corrosion potential. Results in Table 4.6 reveal that ratio is bigger than 1 for both RDF samples suggesting that there is an excess of alkalis available for reaction with other compounds like Si, potentiating slagging, and also that the majority of chlorine in these fuels is likely to be found as alkali chlorides and this causes the low contents of chlorine found in the RDF samples.

When the ash composition of the fuels is evaluated, it is obvious that the RDF samples have some fouling and slagging potential. Therefore, it can be said that using large proportions of RDF in the combustion as a secondary fuel could be restrained. In other words, a caution is required in deciding co-combustion rate due to high possibility of slagging and fouling occurrences.

4.2. Co-combustion of RDF–Coal and RDF–Petroleum coke Mixtures

In this part of the experiments, the effect of RDF addition on the efficiency of coal combustion and petroleum coke combustion is investigated. Only RDF samples are combusted in the batch reactor first in order to determine its combustion characteristics. RDF-coal mixtures and RDF-petroleum coke mixtures with varying fractions are then combusted in the reactor. Thus, both RDF samples are added at 3%, 5%, 10%, 20% and 30% fractions to coal and petroleum coke. The pellets are prepared using these RDF-coal and RDF-petroleum coke mixtures in such a way that each pellet has 1000 cal/g calorific value. At this point, it is worth to note that two

different main fuels -coal and petroleum coke - are used for the purpose of observing effects of main fuel value to the co-combustion efficiency.

The main reason to select the upper limit fraction 30% is the results of previous studies and the results of the single RDF sample combustion experiment in this study that have very low combustion efficiency. According to Chyang et al. (2010), pollutant emissions concentration is increasing with the co-firing ratio of RDF/(RDF+coal). Another study conducted by Piao et al. (1999) shows that 12 kg/h of RDF feed rate is too high feed for its test unit, which is bubbling type fluidized-bed combustor, and the CO level is higher than 500 ppm. However, 10 kg/h of RDF is a proper feed rate and the CO level is kept under 150 ppm. The other study affecting the choice of the 30% fraction as upper limit for this study conducted by Wan et al. (2008) shows that when the RDF co-firing ratio is increased to 30%, all emission of pollutants mainly NO_x increases and the properties of bottom and fly ash get worse. The other co-combustion of RDF and coal study conducted by Fernandez et al. (2003), RDF mixing ratio is selected as 17–19% of the total load on a thermal basis. Kara et al. (2012) investigates the possibility of using RDF as an alternative fuel in cement production. As a result of this study, it is confirmed that clinker quality conforms to the standards when RDF is used as supplementary fuel together with petroleum coke with the ratio of 15%. Genon and Brizio (2008) reveal the statistics showing that different countries have different substitution rate of RDF co-incinerated in the cement industry in Europe. The RDF fraction used in some European countries are 26% in Austria, 24% in France, 23% in Denmark, 1.5% in Italy, 13% in Sweden, 5-10% in Luxembourg, and 1.2% in Estonia. Also, in the studies conducted by (Norton and Levine, 1989; Manninen et al., 1997; Marton and Alwast, 2012), the RDF co-firing ratio has shared a 5-40% heating value in some boiler.

Figure 4.4 is given as an example showing the result of a batch combustion experiment run in triplicate. Graphical representations of all results of triplicate combustion experiments are given in Appendix A.

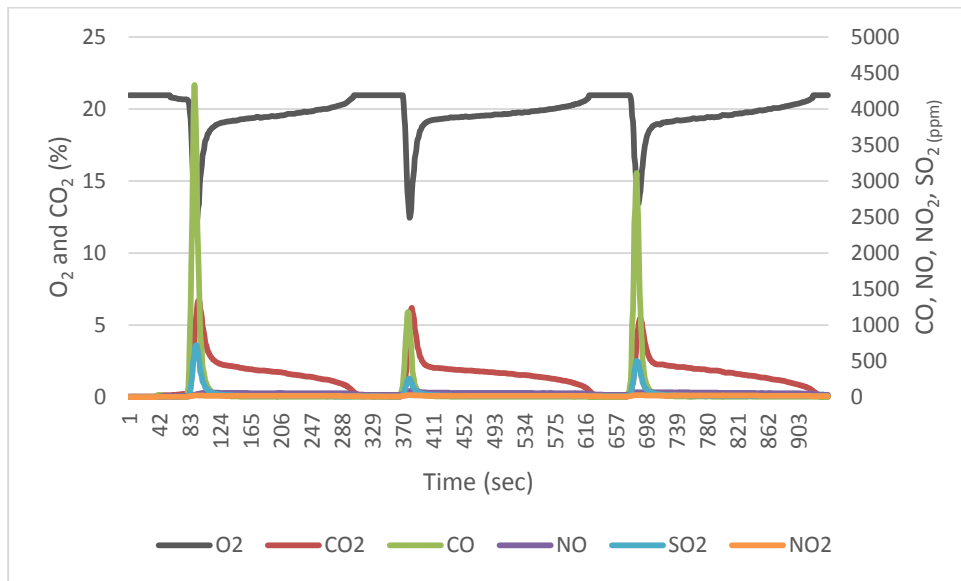


Figure 4.4 Results of co-combustion of coal with 3% RDF-B

In these graphical representations, change in O₂ and CO₂ concentrations in the flue gas with respect to time is shown on the left hand side of the graphs. The flue gas analyzer measures these two gases in volume percentage basis. CO, NO, NO₂ and SO₂ concentrations which are measured as ppm are shown on the right hand side of the graph. Measurements of flue gas composition are performed with two seconds period; therefore, the profiles of gases products are plotted with respect to time.

From the graphs given in Figure 4.4 and Appendix A, it can be seen that as soon as pellets are dropped into the reactor, sharp decrease in oxygen concentration and increase in carbon monoxide and carbon dioxide concentration are observed in the flue gases. On the average, oxygen level drops to around 10% immediately, carbon dioxide rises to around 5-10%. Concentration of carbon monoxide depends on the RDF percentages in mixtures; it can change between 1000 ppm and 5000 ppm when RDF percentage is 3-5%; on the other hand, it could increase up to 6000 ppm when RDF percentage is higher. The carbon monoxide concentration can get to even higher values that they cannot be measured when the mixtures with 20%-30% RDF content or sole RDF is burned. From the graphs, it can also be seen that the carbon

monoxide formation is lower in RDF-petroleum coke mixtures than the one in RDF-coal mixtures. Because the combustion characteristics of petroleum coke, which have higher calorific value and carbon content and lower volatile matter content than coal, is better.

The increase of carbon monoxide and carbon dioxide formation and decrease of oxygen emission in the combustion experiments last 30-40 seconds, then formation of carbon monoxide ends and levels of carbon dioxide and oxygen in the flue gas gradually reach to atmospheric values.

The increase of the carbon monoxide formation with increasing RDF fraction is a result of the high volatile content in RDF samples. The fix carbon/volatile matter ratios of RDF samples are quite small (see Table 4.1); therefore, as it is stated in Kobayashi et al. (2005), the volatile matter burns quickly as soon as the pellet is dropped to the reactor and the combustion process starts. The burning of volatile matter creates an unstable medium. Char in the fuel (RDF, coal, and petroleum coke) starts to burn in a more stable medium which is present after the fuel is totally oxidized.

Moreover, another reason for the high carbon monoxide concentrations occur at the beginning of the experiments may be the temperature difference between the reactor and the fuel (pellet). The pellet is at room temperature when it is thrown to the reactor. Incomplete combustion occurs until the pellet is heated up to the reactor temperature, which results in high carbon monoxide emission.

The fracture strength of the pellet has an indirect effect on CO emission. The more brittle pellets are fractured into small particles when they are placed into the reactor because of the dropping and therefore they burn faster. This fast burning increases the emission of volatiles and thus causes an unstable medium, which causes an increase in carbon monoxide concentration (Kobayashi et al., 2005).

In the current study, all pellets are produced by applying the same pressure on it, therefore the fracture strength of the samples are almost the same and there is no

significant CO emission difference caused by fragility between the burning of different pellets.

Then, mass balance on carbon is applied in order to calculate the efficiency of the combustion processes. The efficiencies of the combustion in the tests are determined by calculating the amount of carbon which transforms into carbon dioxide.

First step of creating a mass balance is to determine the amount of carbon introduced into the reactor in each set of experiment. By using, the amount of coal, petroleum coke and RDF used in the experiments (see Table 3.4), carbon contents in each sample are calculated and are shown in Table 4.8.

Table 4.8 Amount of carbon (g) introduced into the reactor by different mixtures

	0%*	3%*	5%*	10%*	20%*	30%*	100%*
RDF _A – Coal(g)	0.1041	0.1035	0.1031	0.1020	0.1000	0.0979	0.0649
RDF _A – Petroleum coke (g)	0.0829	0.0829	0.0829	0.0829	0.0830	0.0831	0.0649
RDF _B – Coal (g)	0.1041	0.1047	0.1050	0.1060	0.1079	0.1097	0.0759
RDF _B – Petroleum coke (g)	0.0829	0.0841	0.0849	0.0869	0.0909	0.0949	0.0759

*Ratio of RDF samples in fuel mixtures; 0% represents mixtures which contain no RDF sample; 20% indicates mixtures prepared by 20% RDF and 80% of coal/petroleum coke, 100% represents mixtures which contain only RDF.

Then, the amount of carbon which has been transformed into carbon monoxide and carbon dioxide is calculated according to the procedure given in Section 3.4.3.

An example of this calculation is presented below for 3% RDF_B-Coal mixture emissions of which are illustrated in Figure 4.4.

The formula given in Equation 3.5 is used to determine the mass of carbon transformed into carbon dioxide and carbon monoxide and then combustion efficiency is calculated.

By using the equation, the amount of carbon in the form of oxides is calculated. The first term in the equation is the amount of CO and the second term is the amount of CO₂. Summation of the two gives the mass of carbon in the flue gases. Since combustion experiments are carried in triplicate tests, the calculations are done three times and the results are averaged.

For the RDF_B - coal mixture with 3% fraction, detailed calculations for the carbon content detected in the flue gas are shown below:

$$M_{carbon} = \frac{(M_{carbon\ from\ CO_2})_{experiment1} + (M_{carbon\ from\ CO_2})_{experiment2} + (M_{carbon\ from\ CO_2})_{experiment3}}{3} + \frac{(M_{carbon\ from\ CO})_{experiment1} + (M_{carbon\ from\ CO})_{experiment2} + (M_{carbon\ from\ CO})_{experiment3}}{3} \quad Eq. 4.5$$

$$M_{carbon} = \frac{0.1004 + 0.0996 + 0.1021}{3} + \frac{0.0011 + 0.0003 + 0.0008}{3}$$

$$M_{carbon} = 0.1015 \text{ g}$$

Similar calculations are conducted for the other mixtures and the results are given in Table 4.9.

Table 4.9 Amount of carbon released as CO and CO₂ by combustion experiments

	0%	3%	5%	10%	20%	30%	100%
RDF _A – Coal(g)	0.0911	0.0925	0.0933	0.1070	0.0944	0.0916	0.0834
RDF _A – Petroleum coke (g)	0.0917	0.0956	0.0951	0.1043	0.0996	0.0900	0.0834
RDF _B – Coal(g)	0.0911	0.1015	0.0890	0.0991	0.0876	0.0983	0.1229
RDF _B – Petroleum coke (g)	0.0917	0.0970	0.1025	0.1033	0.1047	0.0991	0.1229

*Ratio of RDF samples in fuel mixtures; 0% represents mixtures which contain no RDF sample; 20% indicates mixtures prepared by 20% RDF and 80% of coal/petroleum coke, 100% represents mixtures which contain only RDF.

Now, the percentage of carbon that is captured as carbon monoxide and carbon dioxide can be calculated for all experiments. The carbon measured by the ultimate analysis is used for the calculation of the amount of carbon in the feed. This calculation allows us to check the degree of control that we have on the system as well as the accuracy of our analysis during the experiments. As it can be seen in Table 4.10, carbon balance holds within $\pm 20\%$ deviation, where in most cases the deviation is less than 10%. Especially when the RDF alone is combusted, the deviation increases considerably. This is possibly because of the high volatile content of RDF. The high volatile matter content causes the temperature decrease in combustion zone which can be one of the reasons of incomplete combustion and so the deviation. Also some amount of carbon is captured by the ash and this can be the other reason for the deviation. Moreover, there may be some experimental errors which affect the results.

Table 4.10 Percentage of carbon captured as CO and CO₂ in combustion experiments (%)

	0%	3%	5%	10%	20%	30%	100%
RDF _A – Coal(g)	87.5%	89.3%	90.6%	104.8%	94.4%	93.6%	77.8%
RDF _A – Petroleum coke (g)	110.6%	115.3%	114.7%	120.8%	120.0%	108.4%	77.8%
RDF _B –Coal(g)	87.5%	97.0%	84.7%	93.5%	81.2%	89.6%	61.8%
RDF _B – Petroleum coke (g)	110.6%	115.3%	120.8%	118.9%	115.2%	104.4%	61.8%

*Ratio of RDF samples in fuel mixtures; 0% represents mixtures which contain no RDF sample; 20% indicates mixtures prepared by 20% RDF and 80% of coal/petroleum coke, 100% represents mixtures which contain only RDF.

The carbon monoxide in the flue gas is the indicator of incomplete combustion, which can be taken as the indicator of inefficiency of combustion. In this scope, the combustion efficiency is defined as the ratio of the amount of carbon leaving the reactor as carbon dioxide to the total amount of carbon leaving the reactor.

Therefore, combustion efficiency is defined with the following equation (Patumsawad and Cliffe, 2002):

$$\text{Combustion efficiency}(\%) = \frac{\text{Carbon showing as carbon dioxide in flue gas}}{\text{Carbon showing as carbon monoxide+carbon dioxide in flue gas}} \times 100 \text{ Eq. 4.6}$$

For the sample 3% RDF_A- coal mixture, the above calculation will have the following form:

$$\text{Combustion efficiency}(\%) = \frac{0.0915}{0.0925} \times 100 = 99.0$$

In this study, the results of carbon combustion efficiency for all experiments are shown in Figure 4.5 and 4.6.

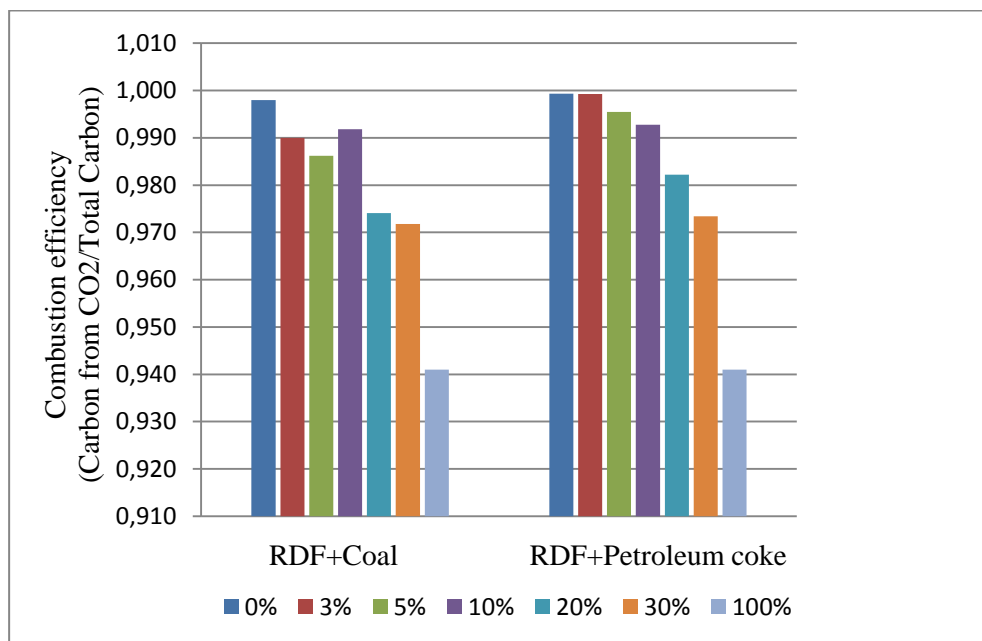


Figure 4.5 Combustion Efficiency of RDF-A

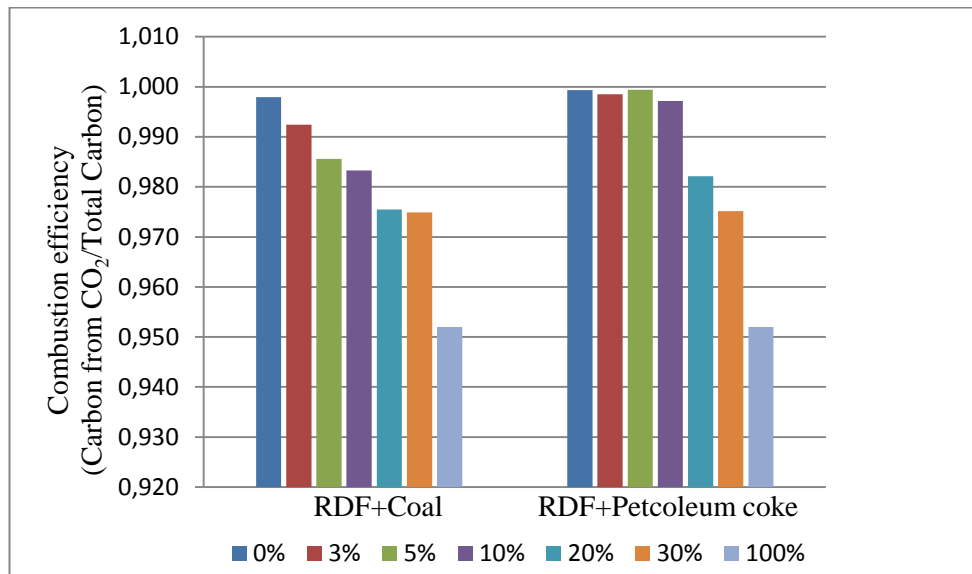


Figure 4.6 Combustion Efficiency of RDF-B

As it can be seen from Figure 4.5 and Figure 4.6, the increasing RDF fraction causes the decrease of combustion efficiency. However, ANOVA tests are performed to interpret the efficiency results statistically.

The RDF sample's combustion efficiencies are selected as dependent variable and the RDF fractions are chosen as an independent factor for the ANOVA test. Also, it should not be forgotten that the combustion experiments for each RDF fraction is performed in triplicate. F-tests and multiple range tests are performed in the ANOVA test to compare the mean values of the combustion efficiencies of RDF samples for the 7 different levels (0%, 3%, 5%, 10%, 20%, 30, and 100%) of RDF fractions.

Since the P values of the F-test, which check whether there are any significant differences amongst the means or not, for the all combustion experiments (RDF-A and Coal, RDF-A and Petroleum coke , RDF-B and Coal and RDF-B and Petroleum coke) are found as less than 0.05 (it is found as 0.0000 for each experiments), it can be said that there is a statistically significant difference between the mean of RDF combustion efficiencies from one level of RDF fractions to another at the 95.0% confidence level.

The box and whisker plots of combustion efficiencies for different RDF fractions are given in Figure 4.7, Figure 4.8, Figure 4.9 and Figure 4.10 for each combustion experiments. These box and whisker plots show the differences in combustion efficiencies. For each RDF fraction, the red point seen in the figure represents the average of three values of co-combustion efficiencies which are gathered by the triplicate run of the experiments. The width of the blue region shows the standard deviation of the co-combustion efficiencies observed in the triplicated experiments. The wider blue region represents a higher deviation.

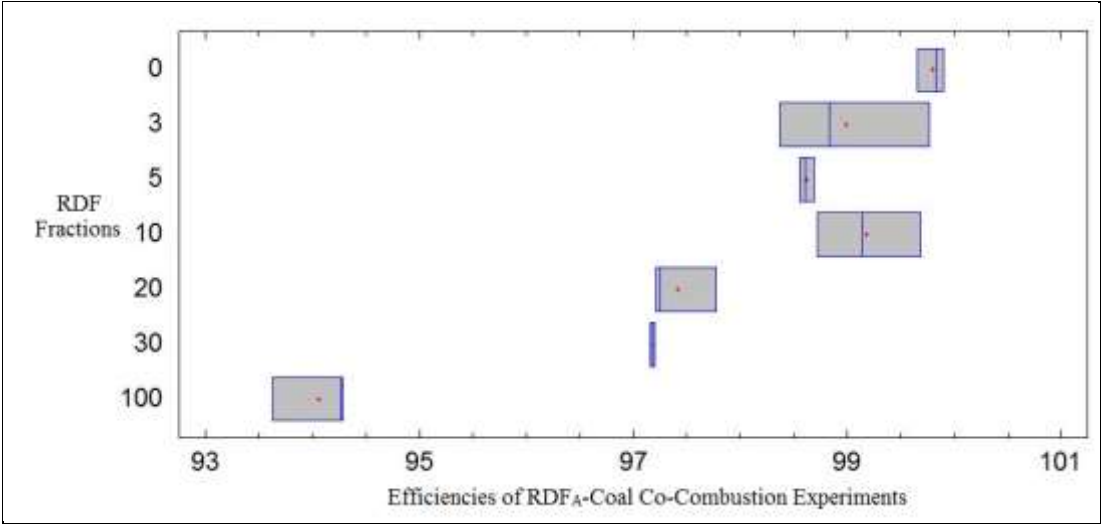


Figure 4.7 Box and whisker plot for RDF_A-Coal co-combustion experiment

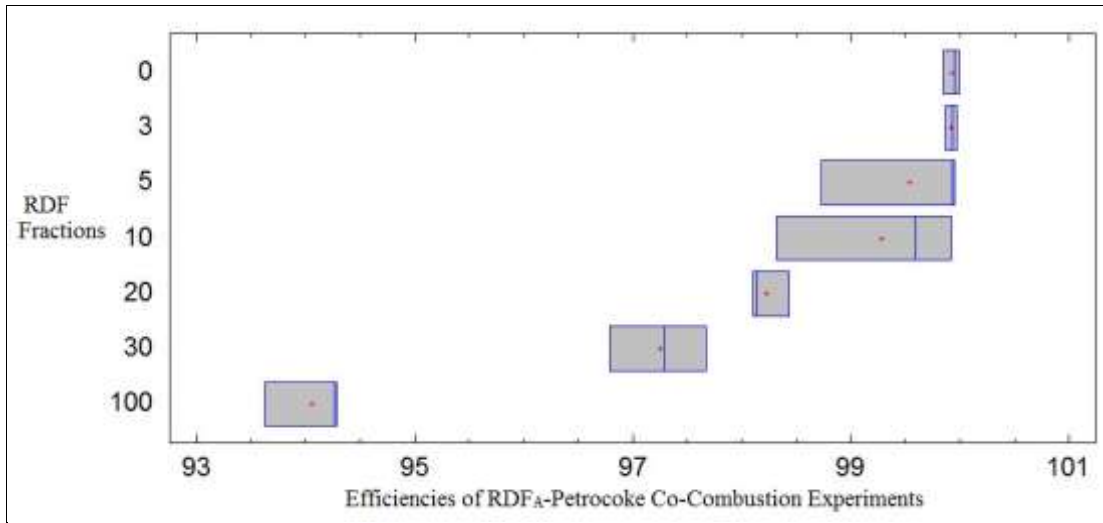


Figure 4.8 Box and whisker plot for RDF_A-Petroleum coke co-combustion experiment

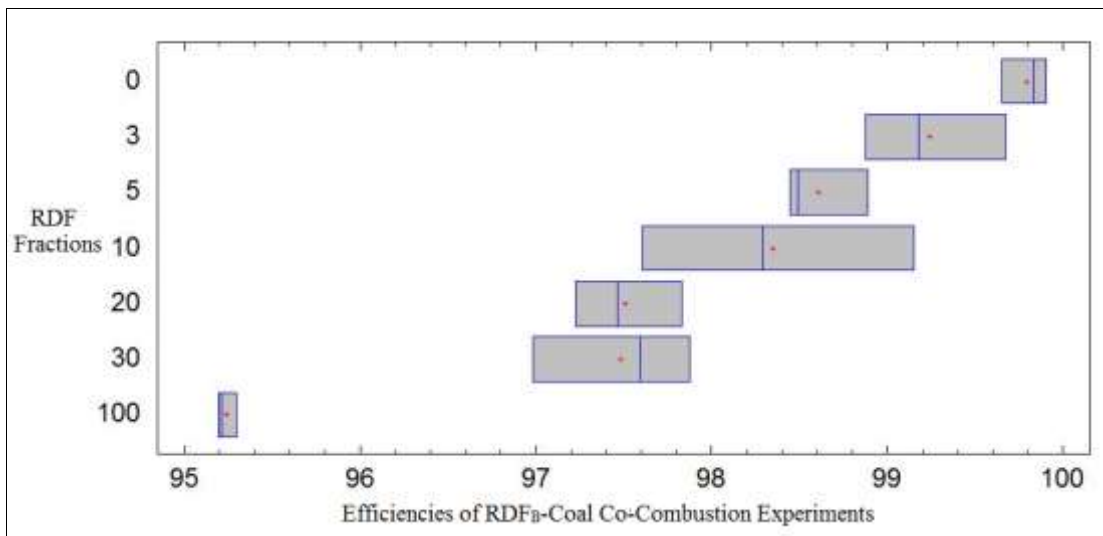


Figure 4.9 Box and whisker plot for RDF_B-Coal co-combustion experiment

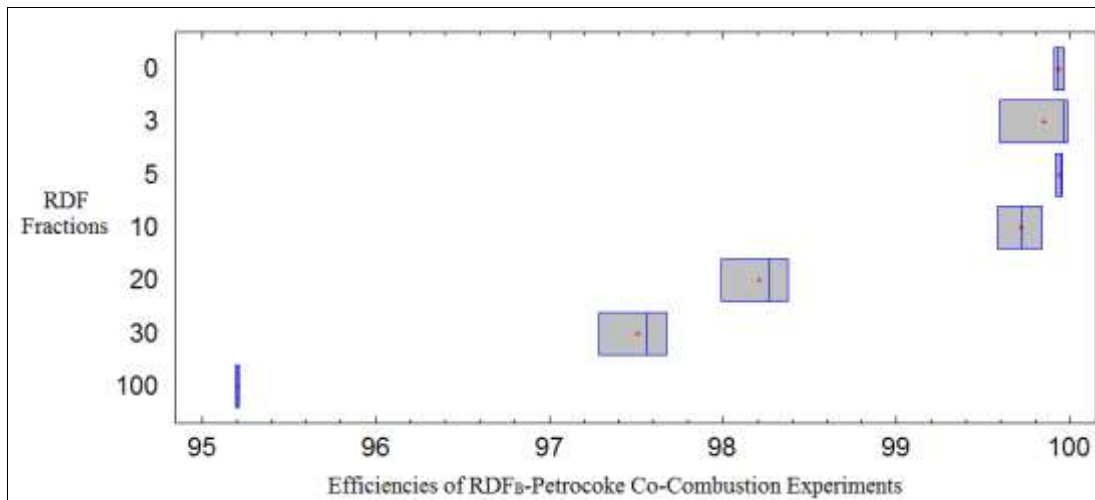


Figure 4.10 Box and whisker plot for RDF_B-Petroleum coke co-combustion experiment

As seen from figures, the combustion efficiencies decrease with the increasing RDF fraction. As expected, the minimum efficiencies are observed at the combustion of pure RDF without any coal or petroleum coke fraction.

Also, the multiple range tests results of which are given Table 4.11, Table 4.12, Table 4.13 and Table 4.14 for each combustion experiments are performed to determine which means are significantly different from the others.

Table 4.11 Multiple range test for RDF_A-Coal co-combustion experiments' efficiency results

	<i>Count</i>	<i>Mean</i>	<i>Homogeneous Groups</i>
RDF _A -Coal (100%)	3	94.0598	X
RDF _A -Coal (30%)	3	97.1808	X
RDF _A -Coal (20%)	3	97.4123	X
RDF _A -Coal (5%)	3	98.6169	X
RDF _A -Coal (3%)	3	98.9901	X
RDF _A -Coal (10%)	3	99.1816	XX
RDF _A -Coal (0%)	3	99.795	X

Table 4.12 Multiple range test for RDF_A-Petroleum coke co-combustion experiments' efficiency results

	<i>Count</i>	<i>Mean</i>	<i>Homogeneous Groups</i>
RDF _A -Petroleum coke (100%)	3	94.0598	x
RDF _A -Petroleum coke (30%)	3	97.2511	x
RDF _A -Petroleum coke (20%)	3	98.2228	x
RDF _A -Petroleum coke (10%)	3	99.2804	x
RDF _A -Petroleum coke (5%)	3	99.5373	x
RDF _A -Petroleum coke (3%)	3	99.9232	x
RDF _A -Petroleum coke (0%)	3	99.9344	x

Table 4.13 Multiple range test for RDF_B-Coal co-combustion experiments' efficiency results

	<i>Count</i>	<i>Mean</i>	<i>Homogeneous Groups</i>
RDF _B -Coal (100%)	3	95.2361	x
RDF _B -Coal (30%)	3	97.4858	x
RDF _B -Coal (20%)	3	97.508	x
RDF _B -Coal (10%)	3	98.3511	x
RDF _B -Coal (5%)	3	98.607	xx
RDF _B -Coal (3%)	3	99.2428	xx
RDF _B -Coal (0%)	3	99.795	x

Table 4.14 Multiple range test for RDF_B-Petroleum coke co-combustion experiments' efficiency results

	<i>Count</i>	<i>Mean</i>	<i>Homogeneous Groups</i>
RDF _B -Petroleum coke (100%)	3	95.2361	x
RDF _B -Petroleum coke (30%)	3	97.5082	x
RDF _B -Petroleum coke (20%)	3	98.2116	x
RDF _B -Petroleum coke (10%)	3	99.7136	x
RDF _B -Petroleum coke (3%)	3	99.85	x
RDF _B -Petroleum coke (0%)	3	99.9344	x
RDF _B -Petroleum coke (5%)	3	99.9402	x

It is concluded from the multiple range tests results that there are no statistically significant differences between pure coal/petroleum coke combustion and co-

combustion of coal/petroleum coke with the addition of 3%, 5% and 10% RDF. However, the test results show that the significant decreases are observed as the RDF fraction increases from 10% to 20% in both coal and petroleum coke mixtures. Furthermore, the combustion efficiency is also decreased when the RDF ratio is increased from 20% to 30%. Also, the minimum efficiencies are observed at only RDF samples combustion without any coal and petroleum coke addition. Furthermore, for the co-combustion experiments with coal, it is seen that there is no efficiency differences between the 20% and 30% mixing ratio. Also, the general combustion efficiencies of petroleum coke–RDF mixtures are higher than coal–RDF mixtures combustion efficiencies because of more valuable fuel features of petroleum coke. It is concluded that the combustion efficiencies decreases significantly if the RDF sample fraction in the mixtures are more than 10%.

The reason of the decreases in combustion efficiency is the more carbon monoxide formation which is the indication of incomplete combustion with the replacement of coal and petroleum coke with RDF.

In the study done by Suksankraisorn et al. (2004), it is stated that the efficiency decrease due to the RDF addition is mainly associated with the temperature decrease in bed zone. The temperature decrease is caused by the increase of the moisture. Also it is stated that the other reason for the efficiency decrease is the high volatile content of RDF. Furthermore, since most fixed carbon generally burns in the bed while the volatile gas burns in the freeboard, there is less chance for fuel C conversion to CO₂ as the RDF fraction increases because of the reduced fixed carbon, while there is more chance for the volatiles to escape combustion because of the increased concentration.

The combustion efficiency of 10% RDF fraction-coal mixtures is found as higher than 5% RDF-coal fraction mixtures, which contradicts the expectations. This result is probably caused by an experimental error. Nevertheless, both cases imply that addition of this RDF to coal in amount more than 10% decreases the combustion efficiency.

According to Patumsawad and Cliffe (2002), loss of carbon in the elutriated solids and loss of carbon as CO due to incomplete combustion are the factors that affects the combustion efficiency. They stated that losses due to CO are negligible, thus the carbon losses due to the amount of elutriated solids are important. Both fine particles in the feed and/or size reduction by attrition in the bed cause the formation of elutriated solids. Thus, high amount of fine particles in fuel affects the combustion efficiency negatively. However, the elutriated solid can burn in the freeboard region, depending on the temperature, residence time and burnout time in this zone. In the study conducted by Patumsawad and Cliffe (2002), fine particles were defined as the particle that was smaller than 1.4 mm. The particle size of RDF samples used in this study is about 0.5 mm. Thus, loss of carbon in the elutriated solids may one of the reasons of the incomplete combustion for the study.

Hernandez-Atonal et al. (2007) suggested that keeping the hot gases in the reactor for a long period of time increases the combustion efficiency. Increasing the residence time increases the amount of oxidized carbon and thus prevents incomplete combustion in the system. However, this technique is not implemented in the current study.

In conclusion, given a combustion system which is optimized for coal and petroleum coke, co-combustion of RDF with coal and petroleum coke reduces the combustion efficiency when RDF fraction increases in the mixtures. The point at which the combustion efficiency drops dramatically depends on many factors as stated above studies such as the content of RDF, experimental setup, fracture strength of pellet, residence time and temperature of the reactor. Furthermore, it should be noted that another experimental setups in lab-scale or full scale may yield different combustion efficiencies than the ones obtained in the current study.

Mass balances on nitrogen and sulfur are also calculated in this study. Example calculation procedures for sulfur and nitrogen, for 3% RDF-B-coal mixture are demonstrated below:

For sulfur determination:

$$M_{Sulfur} = \frac{(M_{sulfur\ from\ SO_2})_{experiment1} + (M_{sulfur\ from\ SO_2})_{experiment2} + (M_{sulfur\ from\ SO_2})_{experiment3}}{3} \text{ Eq. 4.7}$$

$$M_{Sulfur} = \frac{0.000852 + 0.000468 + 0.000711}{3} = 0.000677$$

For nitrogen determination:

$$M_{Nitrogen} = \frac{(M_{Nitrogen\ from\ Nox})_{experiment1} + (M_{Nitrogen\ from\ Nox})_{experiment2} + (M_{Nitrogen\ from\ Nox})_{experiment3}}{3} \text{ Eq. 4.8}$$

$$M_{nitrogen} = \frac{0.000753 + 0.000917 + 0.000912}{3} = 0.000861$$

By using the amount of coal, petroleum coke and RDF used in the experiments (see Table 3.4) and results of ultimate analysis, sulfur and nitrogen contents in each sample are calculated. These values are compared with the nitrogen and sulfur amount in the emissions calculated as above. The results of mass balances of nitrogen and sulfur are listed in Table 4.11 and Table 4.12, respectively.

Table 4.15 Percentage of nitrogen converted to NO_x in combustion experiments (%)

	3%*	5%*	10%*	20%*	30%*	100%*
RDF _A – Coal	18.6%	18.6%	21.2%	18.6%	16.9%	17.1%
RDF _A – Petroleum coke	26.7%	25.4%	24.6%	21.9%	24.4%	17.1%
RDF _B – Coal	28.0%	19.7%	25.0%	16.7%	16.5%	6.5%
RDF _B – Petroleum coke	28.9%	27.5%	23.4%	21.7%	21.9%	6.5%

*Ratio of RDF samples in fuel mixtures; 0% represents mixtures which contain no RDF sample; 20% indicates mixtures prepared by 20% RDF and 80% of coal/petroleum coke, 100% represents mixtures which contain only RDF.

Table 4.16 Percentage of sulfur converted to SO₂ in combustion experiments (%)

	3%*	5%*	10%*	20%*	30%*	100%*
RDF _A – Coal	67.0%	66.2%	65.7%	101.7%	122.6%	–
RDF _A – Petroleum coke	52.1%	75.3%	78.3%	81.9%	72.8%	–
RDF _B – Coal	75.0%	66.4%	68.3%	68.4%	78.6%	143.5%
RDF _B – Petroleum coke	55.8%	69.6%	75.0%	89.9%	80.0%	143.5%

* Ratio of RDF samples in fuel mixtures; 0% represents mixtures which contain no RDF sample; 20% indicates mixtures prepared by 20% RDF and 80% of coal/petroleum coke, 100% represents mixtures which contain only RDF.

– Represents the ratio cannot be calculated for RDF-A; because no S content can be detected in it.

It can be seen in Table 4.11 that amount of emitted nitrogen is fairly low when compared to the amount of nitrogen introduced in experiments and nitrogen balance do not hold for the experiments. Thus, there is no profile which represents the effect of RDF addition on nitrogen oxides formation, i.e nitrogen oxide concentrations appear to be constant almost in all cases. However, it can be said that the sulfur mass balance holds more successfully than nitrogen mass balance as seen in Table 4.12

and it is observed that the SO₂ emission slightly decreases with increasing RDF fraction due to lower sulfur content in the RDF than in the coal and petroleum coke. Also, SO₂ emission is higher in petroleum coke mixtures than coal mixtures since the sulfur content of petroleum coke is higher than coal.

While the amount of coal and petroleum coke in the mixtures increase, the deviation in the calculated sulfur mass balance increases too. Because when the amount of coal and petroleum coke in the mixtures increases, the amount of ash involving high S content also increases; nevertheless, the S amount in the ash is not involved our mass balance calculation. On the contrary, while the RDF amount in the mixtures increases, the sulfur mass balance holds more successfully due to the less ash formation. However, for the single RDF combustion experiment, the result of mass balance does not make sense. Actually, because of a lot less ash formation in this combustion, almost all the S content entered the reactor is emitted. It is apparent that there are some experimental errors such as wrong measurements by the analyzer or some operational errors.

Kobyashi et al. (2005) stated that NO_x mass balance in these types of combustion experiments is controlled very low because the NO_x formation mechanisms are very complicated and also the NO_x emissions are affected by shape, size and strength of the RDF pellets. Thus, it is said that further studies are needed to solve the NO_x balance problems.

One reason of the inaccurate mass balance obtained in this study may be the amount of nitrogen introduced to the system is very small; about 0.15 gr pellets are burned in the current study, when the nitrogen contents of RDF, coal, and petroleum coke are considered, the NO_x emissions are expected to be very low. In addition, the NO_x may condense in the moisture trap section in gas analyzer (PGD-100) and therefore the NO_x may not be accurately measured by the gas analyzer. Also, reactions may occur between nitrogen oxides and unburned hydrocarbons. Being influenced by such factors mentioned above, the experimental setup used in the current study is not successful to observe the effect of RDF addition on NO_x formation in co-combustion.

4.3. Thermogravimetric Analysis (TGA) of RDF

The thermal behaviors of the samples are generally characterized by TGA method. In the current study, the RDF, coal, and petroleum coke sample weights are measured as a function of time and temperature by TGA. The rate of weight losses of these samples are also measured by Differential Thermogravimetric (DTG) signal. Using a constant heating rate, $10\text{C}^{\circ}/\text{min}$, in dry atmosphere, the samples are heated from 25C° to 950C° . TGA and DTG profiles evaluated in the combustion tests of RDF-A, RDF-B, coal and petroleum coke samples are represented in Figure 4.11., Figure 4.12, Figure 4.13 and Figure 4.14 respectively.

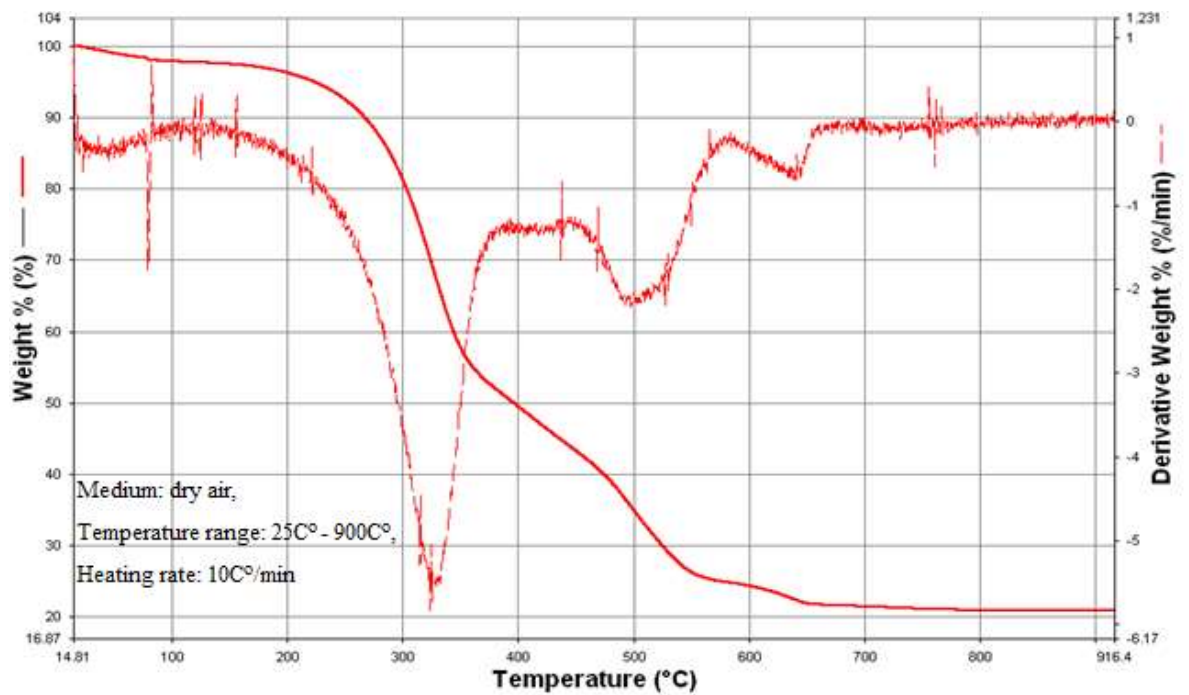


Figure 4.11 TGA and DTG profiles of RDF-A

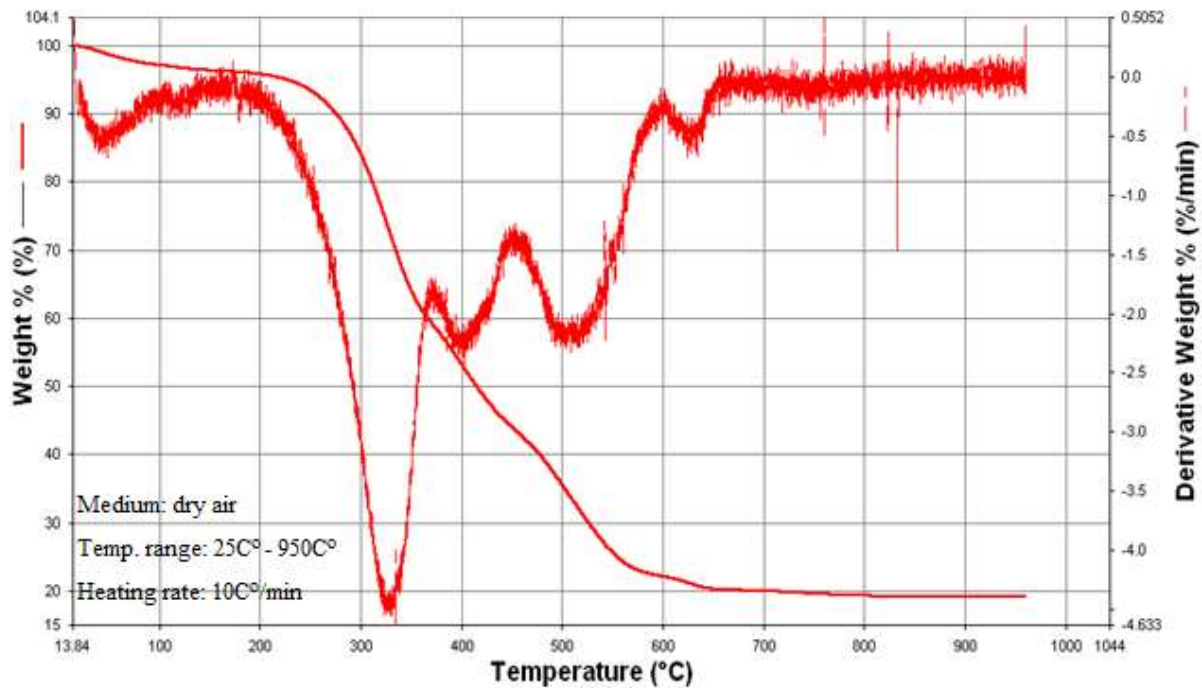


Figure 4.12 TGA and DTG profiles of RDF-B

The above two figures show the TG and DTG curves for the two RDF samples used in this study. As seen from the figures, the DTG curves of both RDF samples in figures have shoulders/peaks which are caused by the huge mass loss observed in three different regions. In the first region (0°C-120°C), the moisture of RDF sample is volatilized. When the moisture loss region ends, the second region, extending up to the 600°C, is observed where the volatile matter in the RDF sample is oxidized. Following this region, after the volatile matter of RDF is decomposed; it is thought that char combustion takes place in the third region.

The first mass loss observed at the beginning the of the experiment, from ambient temperature to about 120°C, is due to the loss of moisture and very light volatile matter content of the fuel. Here the difference between the RDF-A and RDF-B in terms of moisture reflects upon the TGA profiles. The RDF-A has less moisture, which yields a smaller peak at around 100°C compared to RDF-B.

During the combustion process, the main decomposition of RDF samples takes place in between temperatures 200°C - 600°C. The rate of weight loss is maximum at around 320°C for RDF-A and at around 330°C for RDF-B in the dry air environment. Unlike the moisture loss region, more than one peak is observed in this region. In the RDF-B curves, three exothermic peaks are observed at 330, 400, and 510 °C; while, in RDF-A curves, there are two peaks at 320°C and 500°C. At these peak points the mass loss is significant. As mentioned in Piao et al. 2000, the presence of the shoulders shows that there are different volatile matter fractions in RDF samples; the decomposition of cellulosic materials creates the first peak, and the proceeding peak may be formed because of plastics' degradation. In addition, when the temperature and the speed of combustion of the volatile matters included in RDF are closer to each other, less peaks are formed, which may be the case we have in RDF-A.

For both RDF samples, a last peak occurs at about 650°C. This last peak is due to the char combustion. Also the reactions between char and volatiles, which are coming from previous phases of the process, may be another cause of this last peak.

The combustion process in the experiments is complete at around 700°C and the mass loss of RDF-A and RDF-B are found as 79.1%, 80.9%, respectively, which means 20% of char is remained at the end of the process.

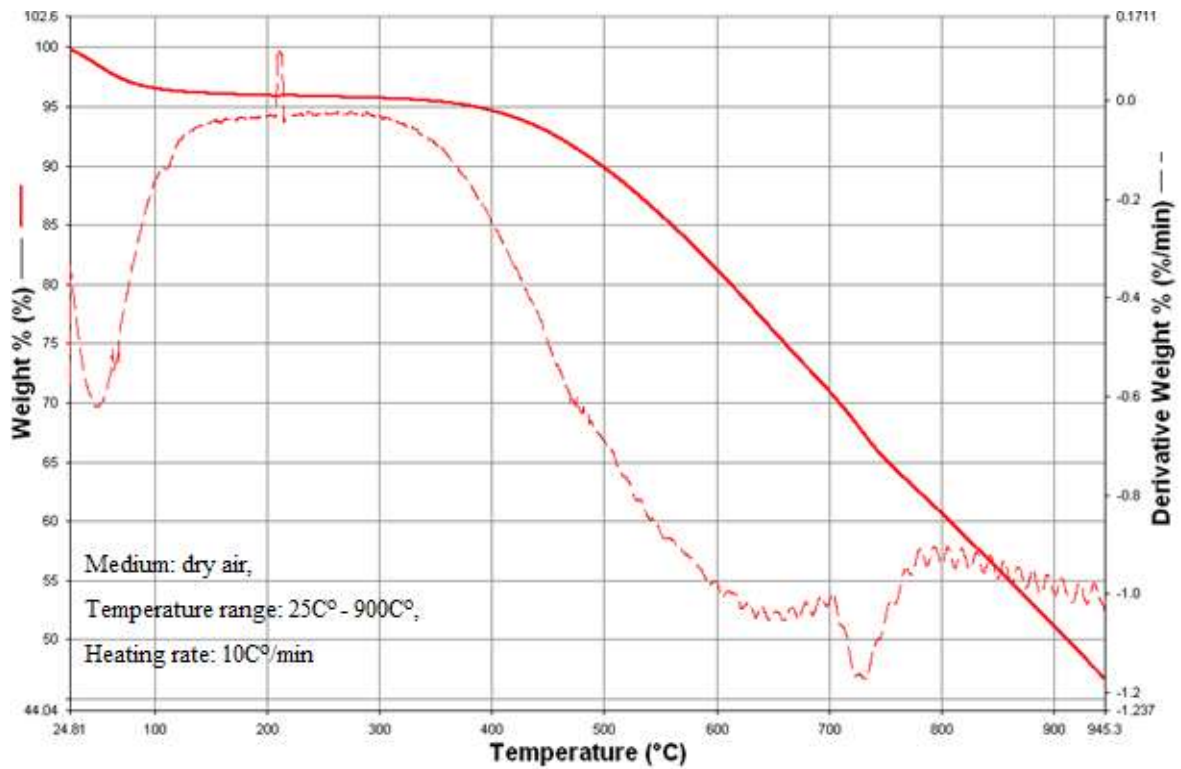


Figure 4.13 TGA and DTG profiles of coal

The Figure 4.13 presents the TG and DTG curves observed for coal sample. The first peak observed at the beginning of the experiment is due to dehydration and drying processes. These processes continue up to 130°C.

Unlike the RDF combustion, the main decomposition of coal samples takes place at higher temperatures (between 700°C-800°C). The highest mass loss, which is corresponded by the peak at 720°C, is mainly due to the volatile matters and char decomposition. At the end of the process the degraded mass is 53.3% of the original mass.

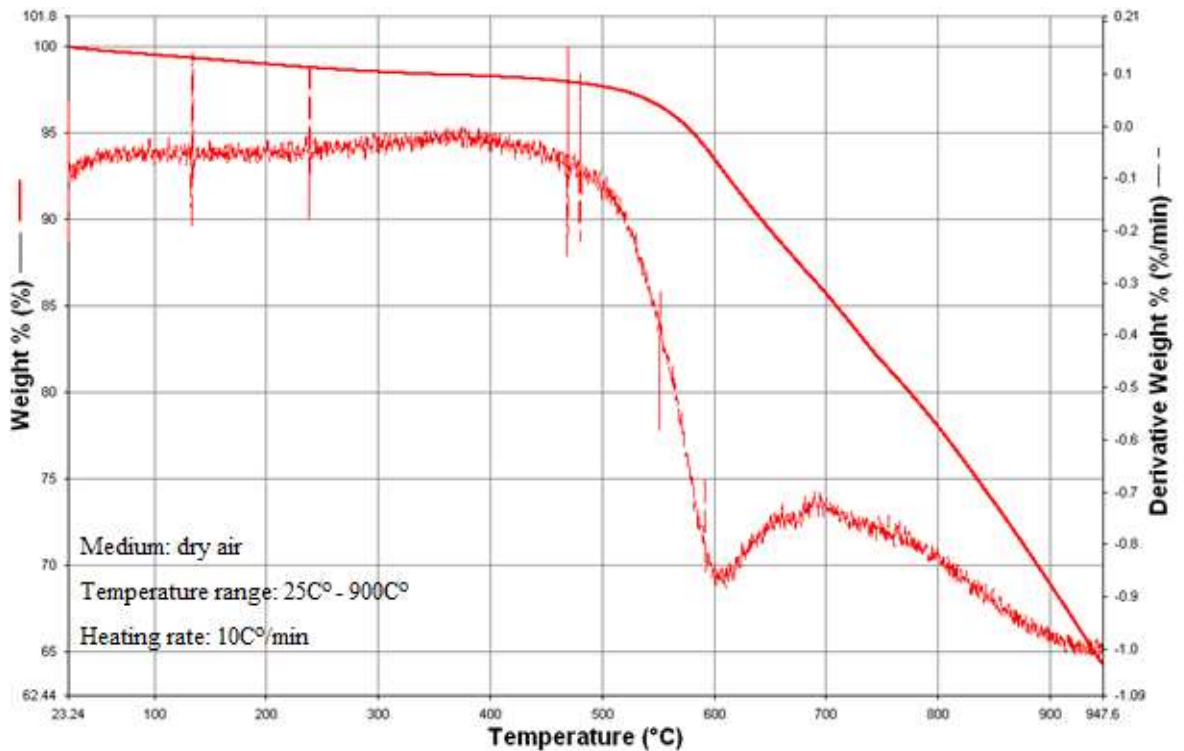


Figure 4.14 TGA and DTG profiles of petroleum coke

TG and DTG curves of petroleum coke sample are presented in Figure 4.14. The typical DTG curve characteristics for petroleum coke mentioned in Magdziarz and Werle 2014 are observed in the current study; there is only one peak between the temperatures 500°C and 700°C due to the decomposition of all organic matter, loss of volatiles and char. The total weight loss in the combustion process is 35.8% and the maximum weight loss occurs at around 610°C .

The initial decomposition temperature of petroleum coke is the highest when compared to coal and RDF samples. Therefore, having the highest ignition and burnout temperatures, petroleum coke is the hardest fuel to ignite and burnout totally among the samples burnt in the current study.

As mentioned before, according to proximate and ultimate analyses, RDF samples contain less than 16% fixed carbon while coal and petroleum coke contain 53% and

87% fixed carbon, respectively. However, the RDF samples contain around 70% to 80% volatile matter, which is much higher than volatile matter content of coal and petroleum coke. In coal and petroleum coke combustion, the constituents of the fuel decomposes in solid-phase at the char combustion; however, in RDF combustion, the decomposition occurs at early stages of the combustion in gas phase due to the low fixed-carbon and high volatile matter content of RDF.

The temperature at which the 50% weight loss is achieved is about 400 °C for both RDF samples while it is 720 °C and 610°C for coal and petroleum coke, respectively. The reason for this can be the decomposition of the complex organic structure of RDF. Due to the same reason, as mentioned before, DTG curves of RDF samples have several peaks at low-medium temperature region, while coal and petroleum coke DTG curves only have one or two peaks. These different combustion characteristics of RDF, coal and petroleum coke, which are obtained in the current study, are in agreement with the ones stated in Kobyashi et al. (2005).

Also, it can be stated that the combustion mechanisms of volatile matters in RDF samples are complicated than that of char. Moreover, as seen from the curves, the temperature interval of char combustion is narrower, about 100 °C, when compared to volatile matter. Therefore, char combustion characteristics is not a criteria for RDF combustibility. However, volatile matter combustion is the most crucial parameter and should be investigated since the combustion duration, speed and mass loss of volatile matters affect the RDF combustibility.

However, it should be considered that TG and DTG studies for RDF combustion are totally complicated because RDF has a great number of components and parallel reactions of these components that occur at the same time.

CHAPTER 5

CONCLUSIONS

Results of this study have shown that calorific values of RDF samples on dry basis are close to that of coal and a little lower compared to petroleum coke used in this study.

Although the calorific values of RDF samples are sufficient, the use of sole RDF samples in combustion processes is limited due to its combustion characteristics. While the RDF sample fraction in the fuel mixtures is increased (more than 10%), the combustion characteristics of the fuel mixtures changes from char combustion to volatile combustion. In addition, CO emission increases and so the combustion efficiency decreases significantly when the RDF fraction in the mixture is higher than 10%. However, the co-combustion of RDF with the ratios of 3%, 5%, and 10% does not decrease the combustion efficiency significantly. Also, the minimum efficiency is observed at the combustion of pure RDF without any coal or petroleum coke fraction. Also, the general combustion efficiencies of petroleum coke–RDF blends are higher than those of coal–RDF mixtures because of higher quality fuel features of the petroleum coke.

RDF addition to the fuel blends decreases the SO₂ emission due to the lower sulfur content in the RDF samples than in the coal and petroleum coke samples, but it does not change NO emission appreciably. Also, SO₂ emission is found higher in petroleum coke blends than coal blends since the sulfur content of petroleum coke is higher than the coal. Also, the general combustion efficiencies of petroleum coke – RDF blends are higher than coal – RDF blends combustion efficiencies because of more valuable fuel features of the petroleum coke.

Slagging and fouling intensity of RDF samples determined in this study indicates that the use of RDF samples in co-combustion processes needs to be kept in certain

amounts. Presence of alkaline elements in the RDF samples causes the high base to acid ratios, which are 1.8 and 2.3 for RDF-A and RDF-B respectively. It should be noted that the values higher than 1 corresponds to high tendency of slagging. Also, sulfur and phosphorus content of RDF samples' ash are high, which makes nearly all of slagging and fouling indices higher than the limit values.

TGA results showed that the combustion mechanisms of volatile matters in RDF samples are complicated than that of char. The mass loss of RDF-A and RDF-B are found as 79.1%, 80.9%, respectively, which means about 20% of char is remained at the end of the process. In coal and petroleum coke combustion, the constituents of the fuel decomposes in solid-phase at the char combustion; however, in RDF combustion, the decomposition occurs at early stages of the combustion in gas phase due to the low fixed-carbon and high volatile matter content of RDF. Therefore, char combustion characteristics is not a criteria for RDF combustibility. However, volatile matter combustion is the most crucial parameter and should be investigated since the combustion duration, speed and mass loss of volatile matters affect the RDF combustibility.

CHAPTER 6

FUTURE STUDIES AND RECOMMENDATIONS

- This study investigates the co-combustion of RDF-coal and RDF-petroleum coke in prefixed conditions. Studies to minimize the CO emissions and increase the co-combustion efficiency of those mixtures could be conducted. In this context, different reactor types and experimental conditions such as mass and condition of samples (pellets or loose material), temperature and flow diagram of reactor can be studied.
- Experimental parameters in TGA analysis can be changed to obtain data with better quality. The composition and the flow rate of air, set of heating rates, temperature intervals can be sequentially changed.
- Pilot plants in many sectors like cement factories or coal thermal power plants can be selected and their realistic maximum potential utilization of RDF can be investigated.

REFERENCES

- Abd Kadir, S. A. S., Yin, C.Y., Rosli Sulaiman, M., Chen, X., & El Harbawi, M. (2013). Incineration of municipal solid waste in Malaysia: Salient issues, policies and waste-to-energy initiatives. *Renewable and Sustainable Energy Reviews*, 24, 181–186. doi:10.1016/j.rser.2013.03.041
- Abdul, a., Anwar, J. M., & Wan Alwi, R.. (2011). Combustion studies of refused-derived fuel (RDF) in fluidized bed (FB) system a method. *2011 IEEE Conference on Clean Energy and Technology (CET)*, (5), 11–14. doi:10.1109/CET.2011.6041450
- Abfallwirtschafts, B., Berlin, E., & Glorius, T. (2012). Production and use of solid recovered fuels - developments and prospects. Berlin, Thomas Glorius final.
- Ahn, S. Y., Eom, S. Y., Rhie, Y. H., Sung, Y. M., Moon, C. E., Choi, G. M., & Kim, D. J. (2013). Application of refuse fuels in a direct carbon fuel cell system. *Energy*, 51, 447–456. doi:10.1016/j.energy.2012.12.025
- Alter, H. (1983). Material recovery from municipal waste. Unit operation in practice. *Pollution Engineering Technology*, (24).
- Arena, U. (2012). Process and technological aspects of municipal solid waste gasification. A review. *Waste Management (New York, N.Y.)*, 32(4), 625–39. doi:10.1016/j.wasman.2011.09.025
- Astrup, T., Møller, J., & Fruergaard, T. (2009). Incineration and co-combustion of waste: accounting of greenhouse gases and global warming contributions. *Waste Management & Research : The Journal of the International Solid Wastes and Public Cleansing Association, ISWA*, 27(8), 789–99. doi:10.1177/0734242X09343774
- Atak, O. (2013). Combustion characteristics and thermal utilization of sewage sludge and coal mixtures. Master thesis, Middle East Technical University, Ankara, Turkey.
- Beckmann, M., & Ncube, S. (2007). Characterisation of Refuse Derived Fuels (RDF) in reference to the Fuel Technical Properties. 26th Annual International Conference on Incineration and Thermal Treatment Technologies, IT3; Phoenix, AZ; United States.
- Beckmann, M., Pohl, M., Bernhardt, D., & Gebauer, K. (2012). Criteria for solid recovered fuels as a substitute for fossil fuels-a review. *Waste Management &*

Research : The Journal of the International Solid Wastes and Public Cleansing Association, ISWA, 30(4), 354–69. doi:10.1177/0734242X12441237

- Blumenthal K. (2012). Statistics in focus – generation and treatment of municipal waste. European Commission Statistics EUROSTAT. Available at: <http://ec.europa.eu>
- Bosmans, A., De Dobbelaere, C., & Helsen, L. (2014). Pyrolysis characteristics of excavated waste material processed into refuse derived fuel. *Fuel, 122*, 198–205. doi:10.1016/j.fuel.2014.01.019
- Bosmans, A., Vanderreydt, I., Geysen, D., & Helsen, L. (2013). The crucial role of Waste-to-Energy technologies in enhanced landfill mining: a technology review. *Journal of Cleaner Production, 55*, 10–23. doi:10.1016/j.jclepro.2012.05.032
- Brown M.E. (2001). Introduction to Thermal Analysis. *Kluwer Aca. Pub.*,(4-6), 19-88.
- Caputo, A. C., & Pelagagge, P. M. (2002). RDF production plants: I Design and costs. *Applied Thermal Engineering, 22(4)*, 423–437. doi:10.1016/S1359-4311(01)00100-4
- CEMBUREAU (The European Cement Association). (2009). Sustainable Cement Production: Co-processing of Alternative Fuels and Raw Materials in the European Cement Industry. Available at: <http://www.cembureau.be/sustainable-cement-production-co-processing-alternative-fuels-and-raw-materials-cement-industry>
- Cesi Ricerca Report. (2007). Quality management, organisation, validation of standards, developments and inquiries for SRF. 1005047 EC EUROPEAN COMMISSION – QUOVADIS EIE/04/031/S07.3859708001001.
- Chang, Y.-H., Chen, W. C., & Chang, N.-B. (1998). Comparative evaluation of RDF and MSW incineration. *Journal of Hazardous Materials, 58(1-3)*, 33–45. doi:10.1016/S0304-3894(97)00118-0
- Chyang, C.S., Han, Y.L., Wu, L.W., Wan, H.P., Lee, H.T., & Chang, Y.H. (2010). An investigation on pollutant emissions from co-firing of RDF and coal. *Waste Management (New York, N.Y.), 30(7)*, 1334–40. doi:10.1016/j.wasman.2009.11.018
- Cozzani, V., Petarca, L., & Tognotti, L. (1995). Devolatilization and pyrolysis of refuse derived fuels: characterization and kinetic modelling by a

thermogravimetric and calorimetric approach. *Fuel*, 74(6), 903–912.
doi:10.1016/0016-2361(94)00018-M

Crujeira, T., Lopes, H., Abelha, P., Sargaço, C., Gonçalves, R., Freire, M., Gulyurtlu, I. (2010). Study of Toxic Metals during Combustion of RDF in a Fluidized Bed Pilot. *Environmental Engineering Science*, 22(2), 241-250.

Dong, C., Jin, B., Zhong, Z., & Lan, J. (2002). Tests on co-firing of municipal solid waste and coal in a circulating fluidized bed. *Energy Conversion and Management*, 43(16), 2189–2199. doi:10.1016/S0196-8904(01)00157-1

Dong, T. T. T., & Lee, B.K. (2009). Analysis of potential RDF resources from solid waste and their energy values in the largest industrial city of Korea. *Waste Management (New York, N.Y.)*, 29(5), 1725–31.
doi:10.1016/j.wasman.2008.11.022

Dunnu, G., Maier, J., & Scheffknecht, G. (2010). Ash fusibility and compositional data of solid recovered fuels. *Fuel*, 89(7), 1534–1540.
doi:10.1016/j.fuel.2009.09.008

Ekmann, J., Winslow, J., Smouse, S., & Ramezan, M. (1998). International survey of cofiring coal with biomass and other wastes. *Fuel Processing Technology*, 54(1-3), 171–188. doi:10.1016/S0378-3820(97)00068-4

Engblom, M., Kilpinen, P., Klingstedt, F., Eränen, K., & Kumar, R.K. (2005). NO_x and N₂O emission formation tendency from multi fuel CFB-boilers: a further development of the predictor. In: Proceedings of FBC2005 18th International Conference on Fluidized Bed Combustion, Toronto, May, pp. 725–741.

Fernandez, A., Wendt, J. O. L., Wolski, N., Hein, K. R. G., Wang, S., & Witten, M. L. (2003). Inhalation health effects of fine particles from the co-combustion of coal and refuse derived fuel. *Chemosphere*, 51(10), 1129–37.
doi:10.1016/S0045-6535(02)00720-8

Ferrer, E., Aho, M., Silvennoinen, J., & Nurminen, R.V. (2005). Fluidized bed combustion of refuse-derived fuel in presence of protective coal ash. *Fuel Processing Technology*, 87(1), 33–44. doi:10.1016/j.fuproc.2005.04.004

Gani, A., & Naruse, I. (2005). NO and N₂O formation/decomposition characteristics during co-combustion of coal with biomass. In: Proceedings of FBC2005 18th International Conference on Fluidized Bed Combustion, Toronto, May, pp. 219– 223.

- Gendebien, A., Leavens, A., Blackmore, K., Godley, A., Lewin, K., Whiting, K. J., et al. (2003). Refuse Derived Fuel, Current Practice and Perspectives Final Report. European Commission.
- Genon, G., & Brizio, E. (2008). Perspectives and limits for cement kilns as a destination for RDF. *Waste Management (New York, N.Y.)*, 28(11), 2375–85. doi:10.1016/j.wasman.2007.10.022
- Hämäläinen, J.P., Aho, M.J., & Tummavuori, J.L. (1994). Formation of nitrogen oxides from fuel-N through HCN and NH₃: a model-compound study. *Fuel* 73, 1894– 1898.
- Hatanaka, T., Kitajima, A., & Takeuchi, M. (2005). Role of Chlorine in Combustion Field in Formation of Polychlorinated Dibenzo- p -dioxins and Dibenzofurans during Waste Incineration. *Environmental Science & Technology*, 39(24), 9452–9456. doi:10.1021/es050707r
- Hernandez-Atonal, F. D., Ryu, C., Sharifi, V. N., & Swithenbank, J. (2007). Combustion of refuse-derived fuel in a fluidised bed. *Chemical Engineering Science*, 62(1-2), 627–635. doi:10.1016/j.ces.2006.09.025
- Hoorweg, D., & Tata, P.B. (2012). What a waste: a global review of solid waste management. The World Bank: Urban Development Series Knowledge Papers.
- Ibbetson, C. & Wengenroth, K. (2007). Optimisation of Fuels from MBT processes. In Proceedings of International Symposium of Mechanical Biological Treatment: 372-384. Germany: Wasteconsult International.
- Jenkins, B. ., Baxter, L. ., & Miles, T. . (1998). Combustion properties of biomass. *Fuel Processing Technology*, 54(1-3), 17–46. doi:10.1016/S0378-3820(97)00059-3
- Kalyani, K. A., & Pandey, K. K. (2014). Waste to energy status in India: A short review. *Renewable and Sustainable Energy Reviews*, 31, 113–120. doi:10.1016/j.rser.2013.11.020
- Kara, M. (2012). Environmental and economic advantages associated with the use of RDF in cement kilns. *Resources, Conservation and Recycling*, 68, 21–28. doi:10.1016/j.resconrec.2012.06.011
- Kers, J., Kulu, P., Aruniit, a, Laurmaa, V., Križan, P., Šooš, L., & Kask, Ü. (2010). Determination of physical, mechanical and burning characteristics of polymeric waste material briquettes. *Estonian Journal of Engineering*, 16(4), 307. doi:10.3176/eng.2010.4.06

- Kobyashi, N., Itaya, Y., Piao, G., Mori, S., Kondo, M., Hamai, M., & Yamaguchi, M. (2005). The behavior of flue gas from RDF combustion in a fluidized bed. *Powder Technology*, *151*(1-3), 87–95. doi:10.1016/j.powtec.2004.11.038
- Lin, K.S., Wang, H. P., Liu, S.H., Chang, N.B., Huang, Y.J., & Wang, H.C. (1999). Pyrolysis kinetics of refuse-derived fuel. *Fuel Processing Technology*, *60*(2), 103–110. doi:10.1016/S0378-3820(99)00043-0
- Liu, G.Q., Itaya, Y., Yamazaki, R., Mori, S., Yamaguchi, M., & Kondoh, M. (2001). Fundamental study of the behavior of chlorine during the combustion of single RDF. *Waste Management*, *21*(5), 427–433. doi:10.1016/S0956-053X(00)00134-3
- Liu, D.C., Zhang, C.L., Mi, T., Shen, B.X., Feng, B. (2002). Reduction of N₂O and NO emissions by co-combustion of coal and biomass. *Journal of the Institute of Energy* *75*, 81–84.
- Lockwood, F. C., & Ou, J. J. (1993). Review: Burning refuse-derived fuel in a rotary cement kiln. *Proceedings of the Institution of Mechanical Engineers, Part A: Journal of Power and Energy*, *207*(1), 65–70. Retrieved from <http://www.scopus.com/inward/record.url?eid=2-s2.0-0027211596&partnerID=tZOtx3y1>
- Magdziarz, A., & Werle, S. (2014). Analysis of the combustion and pyrolysis of dried sewage sludge by TGA and MS. *Waste Management (New York, N.Y.)*, *34*(1), 174–9. doi:10.1016/j.wasman.2013.10.033
- Manninen, H., Peltola, K., & Ruuskanen, J. (1997). Co-combustion of refusederived and packaging-derived fuels (RDF and PDF) with conventional fuels. *Waste Management*, *15*, 137–147.
- Marsh, R., Griffiths, A. J., Williams, K. P., & Wilcox, S. J. (2007). Physical and thermal properties of extruded refuse derived fuel. *Fuel Processing Technology*, *88*(7), 701–706. doi:10.1016/j.fuproc.2007.01.015
- Marton, C., & Alwast, H. (2002). Report: Operational experiences and legal aspects of co-combustion in Germany. *Waste Management*, *20*, 476–483.
- Milios, L. (2013). Municipal waste management in Turkey. European Environment Agency, ETC/SCP.
- Miller, B.B., Kandiyoti, R., & Dugwell, D.R. (2002). Trace element emissions from co-combustion of secondary fuels with coal: a comparison of bench-scale experimental data with predictions of a thermodynamic equilibrium model. *Energy Fuels*, *16*(4), 956-963.

- MoEU, 2014. Information received during the writing of thesis. E-mail of 1 September 2014 from Hasan Önel, Turkish Ministry of Environment and Urbanisation.
- MoEU2, 2014. Information received during the writing of thesis. E-mail of 3 September 2014 from Sabriye Ayhan, Turkish Ministry of Environment and Urbanisation.
- Nemet, A., Varbanov, P., Klemes, J.J. (2011). Waste-to-energy technologies performance evaluation techniques. *Chemical Engineering Transactions*, 24.
- Niessen, W. R. (2002). Combustion and Incineration Processes. USA: Marcel Dekker, Inc.
- Norton, G. A. & Levine, A. D. (1989). Co-combustion of refuse-derived fuel and coal. *Environ. Sci. Technol.*, 23, 774–783.
- European Environment Agency (EEA) Report. (2013). Managing municipal solid waste - a review of achievements in 32 European countries. Luxembourg: Publications Office of the European Union.
- Park, S.W., & Jang, C.H. (2011). Characteristics of carbonized sludge for co-combustion in pulverized coal power plants. *Waste Management (New York, N.Y.)*, 31(3), 523–9. doi:10.1016/j.wasman.2010.10.009
- Patumsawad, S., & Cliffe, K. R. (2002). Experimental study on fluidised bed combustion of high moisture municipal solid waste. *Energy Conversion and Management*, 43(17), 2329–2340. doi:10.1016/S0196-8904(01)00179-0
- Pettersson, A., Zevenhoven, M., Steenari, B.-M., & Åmand, L.E. (2008). Application of chemical fractionation methods for characterisation of biofuels, waste derived fuels and CFB co-combustion fly ashes. *Fuel*, 87(15-16), 3183–3193. doi:10.1016/j.fuel.2008.05.030
- Piao, G., Aono, S., Kondoh, M., & Yamazaki, R. (2000). Combustion test of refuse derived fuel in a fluidized bed. *Waste Management*, 20(5-6), 443–447.
- Piao, G., Aono, S., Mori, S., Deguchi, S., & Fujima, Y. (1999). Combustion of refuse derived fuel in a fluidized bed. *Waste Management*, 18(6-8), 509–512.
- Pretz, T., Khoury, A., Uepping, R., & Glorius, T., Tubergen, J.V. (2003). BREF waste treatment-solid recovered fuels. IAR RWTH and European Recovered Fuel Organisation (Erfo). Aachen; 2003.

- Prognos; Final Report. (2008, October). Resource savings and CO2 reduction potential in waste management in Europe and the possible contribution to the CO2 reduction target in 2020.
- Pronobis, M. (2005). Evaluation of the influence of biomass co-combustion on boiler furnace slagging by means of fusibility correlations. *Biomass and Bioenergy*, 28(4), 375–383. doi:10.1016/j.biombioe.2004.11.003
- Ryu, C., Yang, Y. Bin, Khor, A., Yates, N. E., Sharifi, V. N., & Swithenbank, J. (2006). Effect of fuel properties on biomass combustion: Part I. Experiments—fuel type, equivalence ratio and particle size. *Fuel*, 85(7-8), 1039–1046. doi:10.1016/j.fuel.2005.09.019
- Saxena, S. C., & Rao, N. S. (1993). Fluidized-Bed Incineration of Refuse-Derived Fuel Pellets. *Energy and Fuels*, 7, 273–278.
- Scala, F., & Chirone, R. (2004). Fluidized bed combustion of alternative solid fuels. *Experimental Thermal and Fluid Science*, 28(7), 691–699. doi:10.1016/j.expthermflusci.2003.12.005
- Seo, M. W., Kim, S. D., Lee, S. H., & Lee, J. G. (2010). Pyrolysis characteristics of coal and RDF blends in non-isothermal and isothermal conditions. *Journal of Analytical and Applied Pyrolysis*, 88(2), 160–167. doi:10.1016/j.jaap.2010.03.010
- Suksankraisorn, K., Patumsawad, S., Vallikul, P., Fungtammasan, B., & Accary, A. (2004). Co-combustion of municipal solid waste and Thai lignite in a fluidized bed. *Energy Conversion and Management*, 45(6), 947–962. doi:10.1016/S0196-8904(03)00187-0
- Tarelho, L. A. C., Matos, M. A. A., & Pereira, F. J. M. A. (2004). Axial Concentration Profiles and NO Flue Gas in a Pilot-Scale Bubbling Fluidized Bed Coal Combustor. *Energy & Fuels*, 18(6), 1615–1624. doi:10.1021/ef049940l
- Tchobanoglous, G., & Kreith, F. (2002). Handbook of Solid Waste Management. U.S.A: McGraw Hill Professional.
- Tchobanoglous, G., Theisen, H., & Vigil, S. (1993). Integrated Solid Waste Management: Engineering Principles and Management Issues. U.S.A: McGraw Hill Professional.
- Teixeira, P., Lopes, H., Gulyurtlu, I., Lapa, N., & Abelha, P. (2012). Evaluation of slagging and fouling tendency during biomass co-firing with coal in a fluidized bed. *Biomass and Bioenergy*, 39, 192–203. doi:10.1016/j.biombioe.2012.01.010

TUBITAK-KAMAG 108G167 Project: Management of Domestic/Urban Wastewater Sludges in Turkey, 2012.

URL 1: EPA. (2014). Municipal solid waste. [online]
<http://www.epa.gov/waste/nonhaz/municipal/>. Last accessed date: 13.06.2014

URL 2: TÜİK. (2014). Bertaraf yöntemlerine göre belediye atık miktarları. Turkish Statistical Institute. [online]
<http://www.tuik.gov.tr/UstMenu.do?metod=temelist>. Last accessed date: 02.07.2014

URL 3: EPA. (2014). Non-Hazardous Waste Management Hierarchy. [online]
<http://www.epa.gov/waste/nonhaz/municipal/hierarchy.htm>. Last accessed date: 22.06.2014

URL 4: European Recovered Fuel Organisation. CEN TC 343 - "Solid recovered fuel" [online] <http://erfo.info/CEN-TC-343.26.0.html>. Last accessed date: 11.07.2014

URL 5: (2009). FOE, Briefing - Pyrolysis, gasification and plasma. Friends of the Earth. [online]
http://www.foe.co.uk/resource/briefings/gasification_pyrolysis.pdf. Last accessed date: 08.06.2014

URL 6: (2014, June). EUROCOAL. Turkey. [online]
<http://www.euracoal.be/pages/layout1sp.php?idpage=475>. Last accessed date: 05.07.2014

URL 7: (2012) Coal Marketing International Ltd. Coal Basics. [online]
<http://www.coalmarketinginfo.com/coal-basics/>. Last accessed date: 19.06.2014

U.S. EPA. (2012). Municipal Solid Waste Generation , Recycling , and Disposal in the United States : Facts and Figures for 2012, 1–14.

Vainikka, P., Lindberg, D., Moilanen, A., Ollila, H., Tiainen, M., Silvennoinen, J., & Hupa, M. (2013). Trace elements found in the fuel and in-furnace fine particles collected from 80MW BFB combusting solid recovered fuel. *Fuel Processing Technology*, 105, 202–211. doi:10.1016/j.fuproc.2011.06.023

Vamvuka, D., Salpigidou, N., Kastanaki, E., & Sfakiotakis, S. (2009). Possibility of using paper sludge in co-firing applications. *Fuel*, 88(4), 637–643. doi:10.1016/j.fuel.2008.09.029

Wagland, S. T., Kilgallon, P., Coveney, R., Garg, A., Smith, R., Longhurst, P. J., Simms, N. (2011). Comparison of coal/solid recovered fuel (SRF) with

coal/refuse derived fuel (RDF) in a fluidized bed reactor. *Waste Management (New York, N.Y.)*, 31(6), 1176–83. doi:10.1016/j.wasman.2011.01.001

Wan, H.-P., Chang, Y.-H., Chien, W.-C., Lee, H.-T., & Huang, C. C. (2008). Emissions during co-firing of RDF-5 with bituminous coal, paper sludge and waste tires in a commercial circulating fluidized bed co-generation boiler. *Fuel*, 87(6), 761–767. doi:10.1016/j.fuel.2007.06.004

Wang, G., Silva, R. B., Azevedo, J. L. T., Martins-Dias, S., & Costa, M. (2014). Evaluation of the combustion behaviour and ash characteristics of biomass waste derived fuels, pine and coal in a drop tube furnace. *Energy & Fuels*, 117, 809–824. doi:10.1016/j.fuel.2013.09.080

Wang, Z., Huang, H., Li, H., Wu, C., & Chen, Y. (2002). Pyrolysis and Combustion of Refuse-Derived Fuels in a Spouting - Moving Bed Reactor. *Energy & Fuels*, (9), 136–142.

Wei, X., Wang, Y., Liu, D., Sheng, H., & Tian, W. (2009). Release of Sulfur and Chlorine during Cofiring RDF and Coal in an Internally Circulating Fluidized Bed. *Energy&Fuels*, 23, 1390–1397.

Wilson, B., Ph, D., Williams, N., Liss, B., & Wilson, B. (2013). A Comparative Assessment of Commercial Technologies for Conversion of Solid Waste to Energy. EnviroPower Renewable, Inc.

APPENDIX A

EMISSIONS OBTAINED IN CO-COMBUSTION EXPERIMENTS

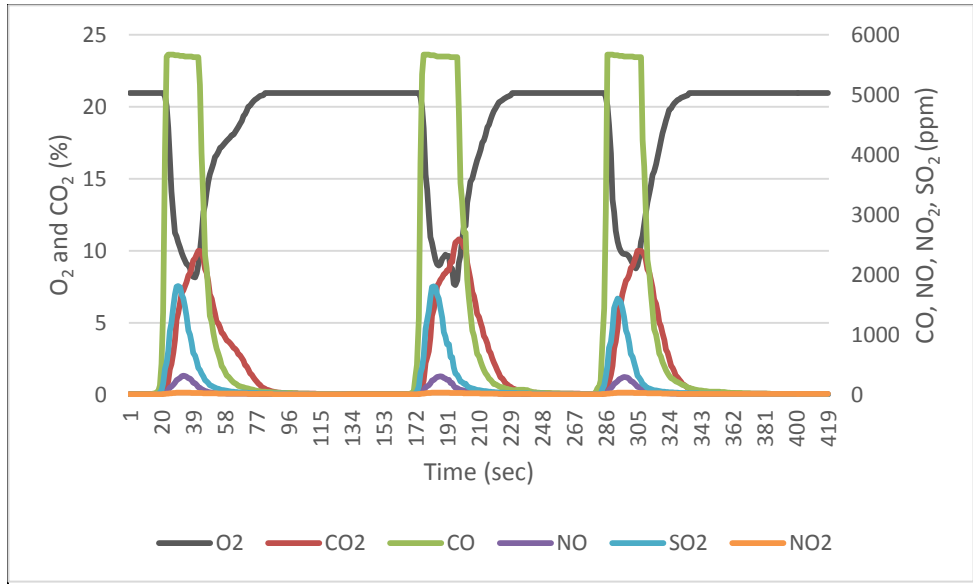


Figure A-1 Results of combustion of RDF_A

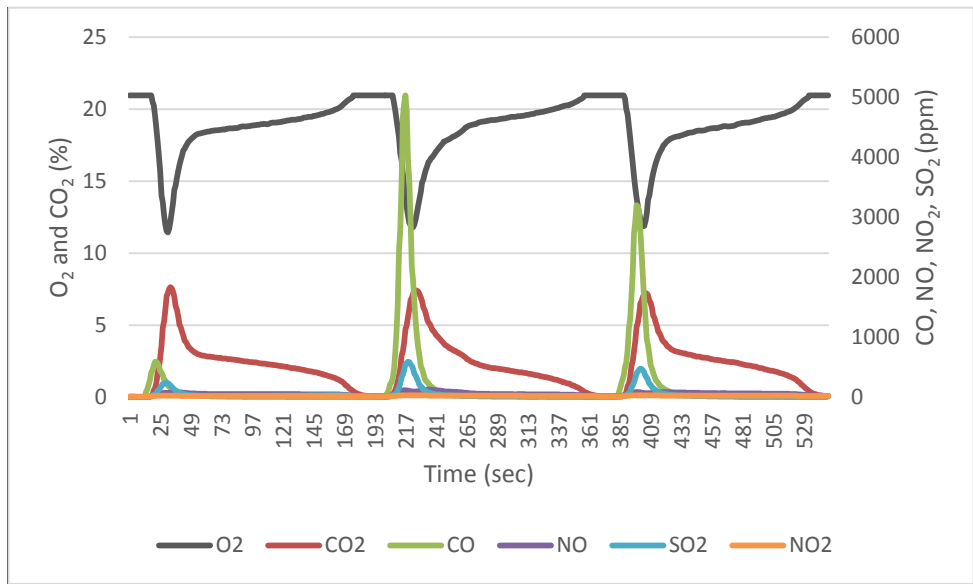


Figure A-2 Results of co-combustion of coal with 3% RDF_A

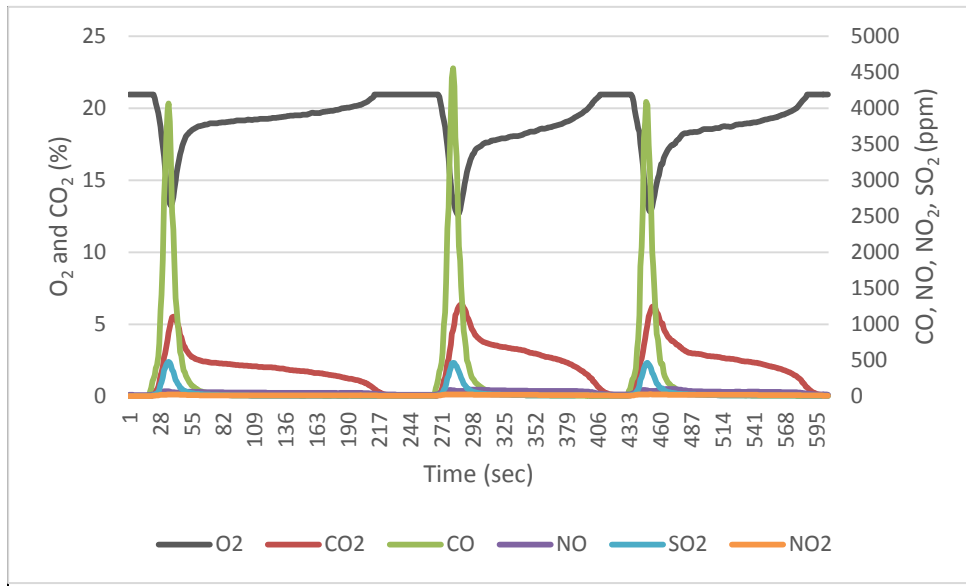


Figure A-3 Results of co-combustion of coal with 5% RDF_A

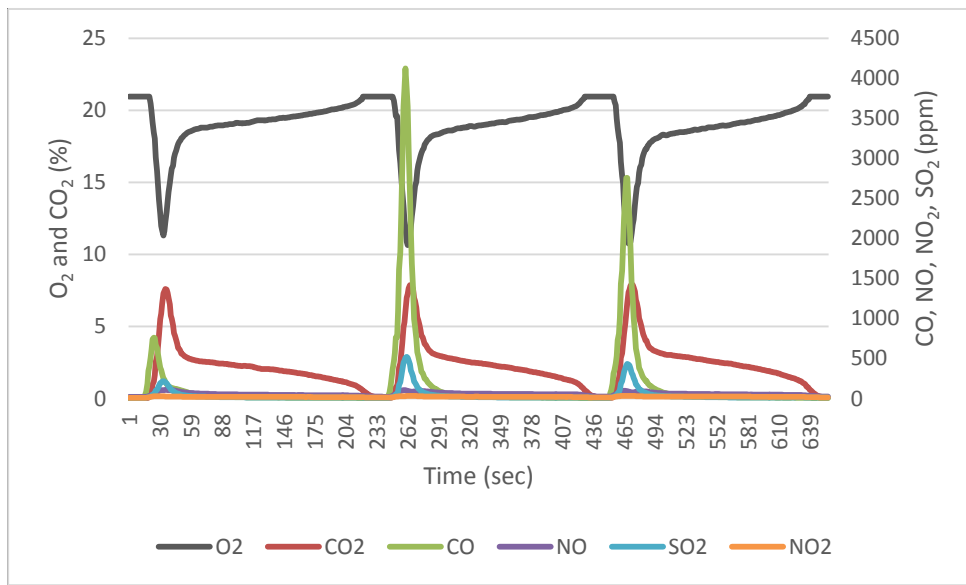


Figure A-4 Results of co-combustion of coal with 10% RDF_A

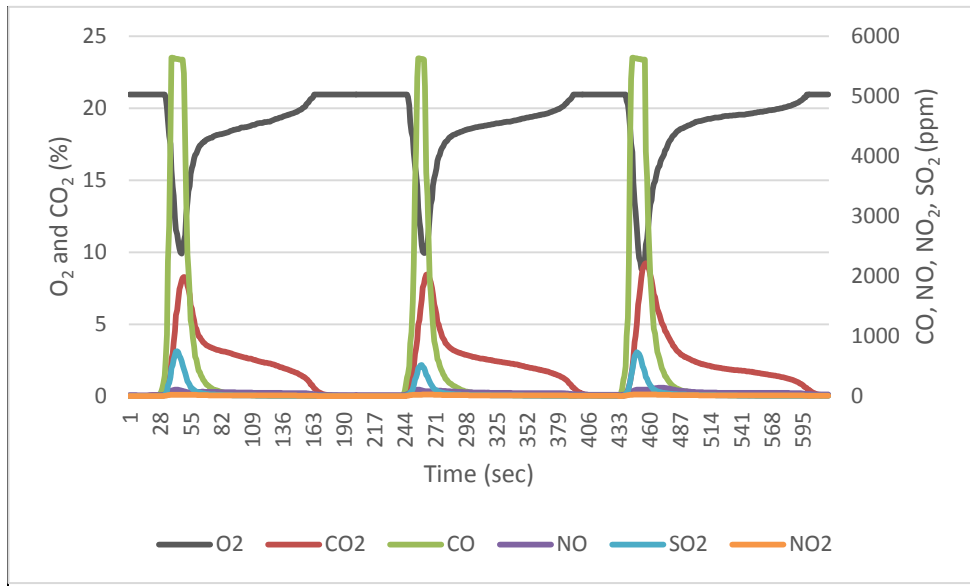


Figure A-5 Results of co-combustion of coal with 20% RDF_A

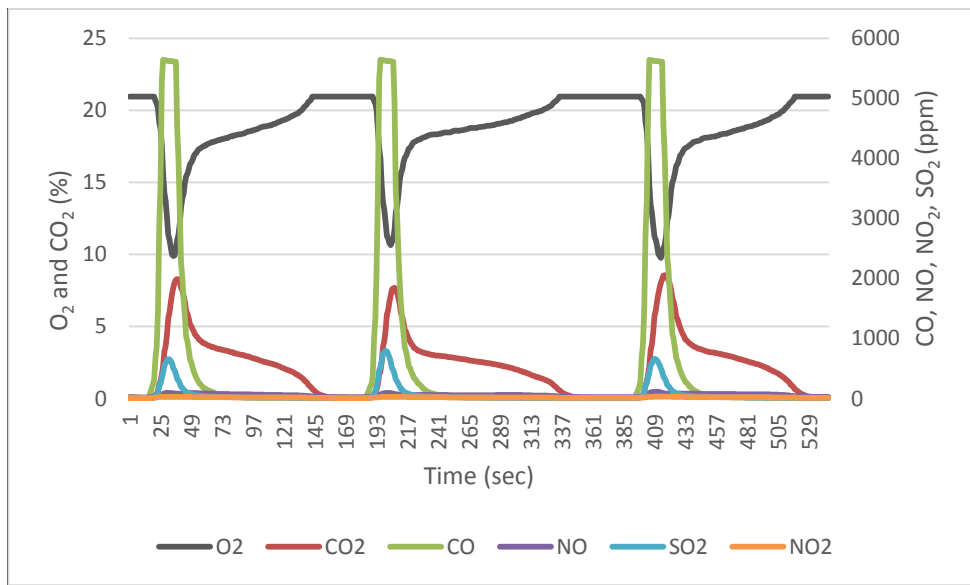


Figure A-6 Results of co-combustion of coal with 30% RDF_A

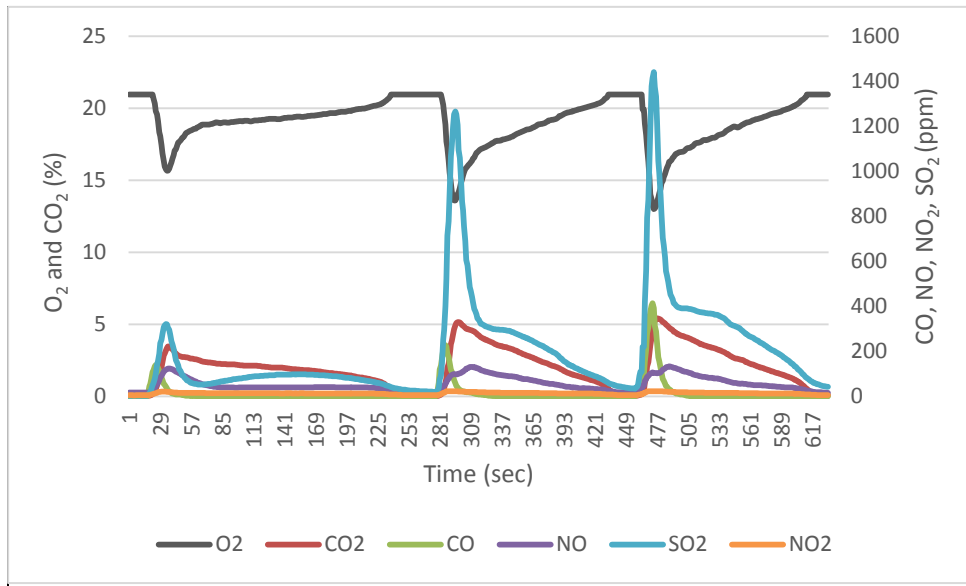


Figure A-7 Results of co-combustion of petroleum coke with 3% RDF_A

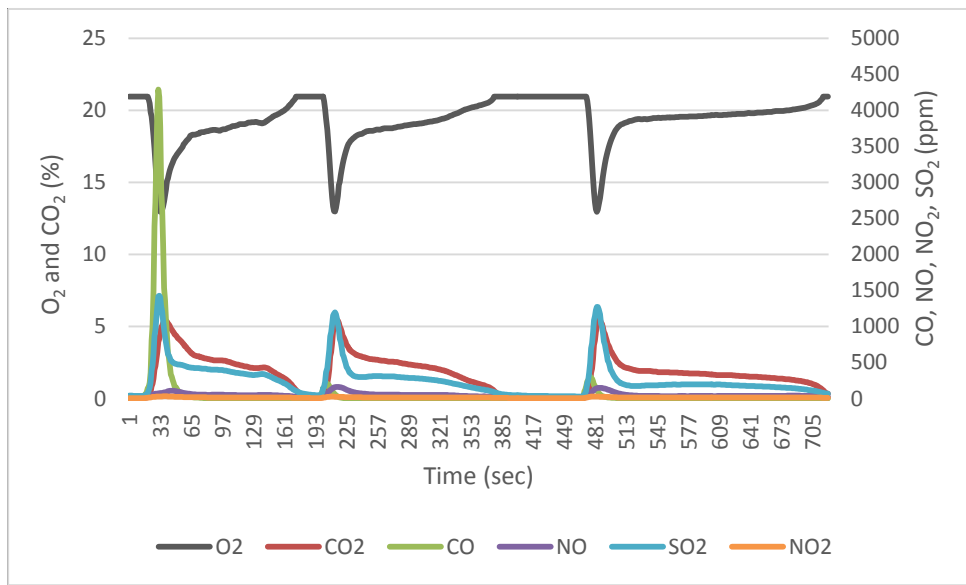


Figure A-8 Results of co-combustion of petroleum coke with 5% RDF_A

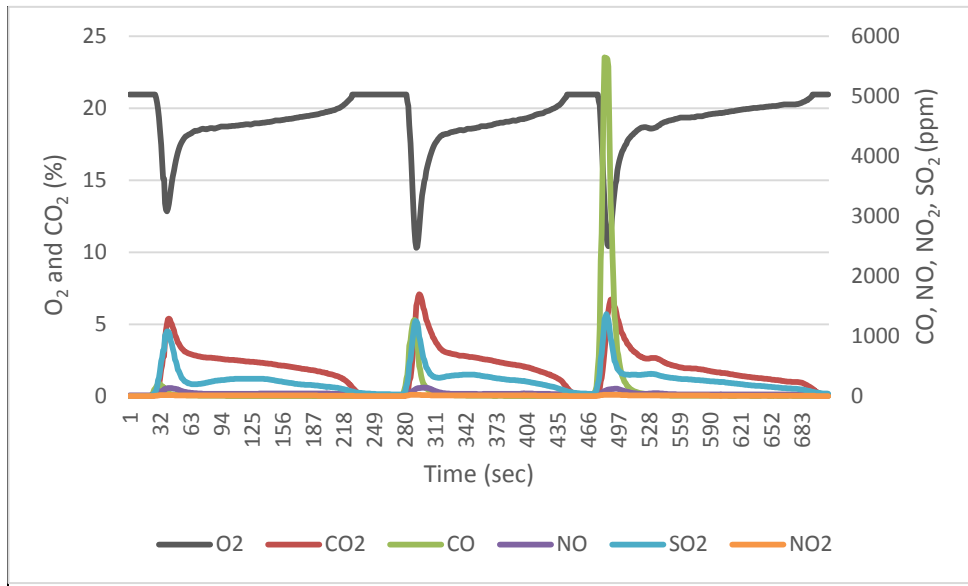


Figure A-9 Results of co-combustion of petroleum coke with 10% RDF_A

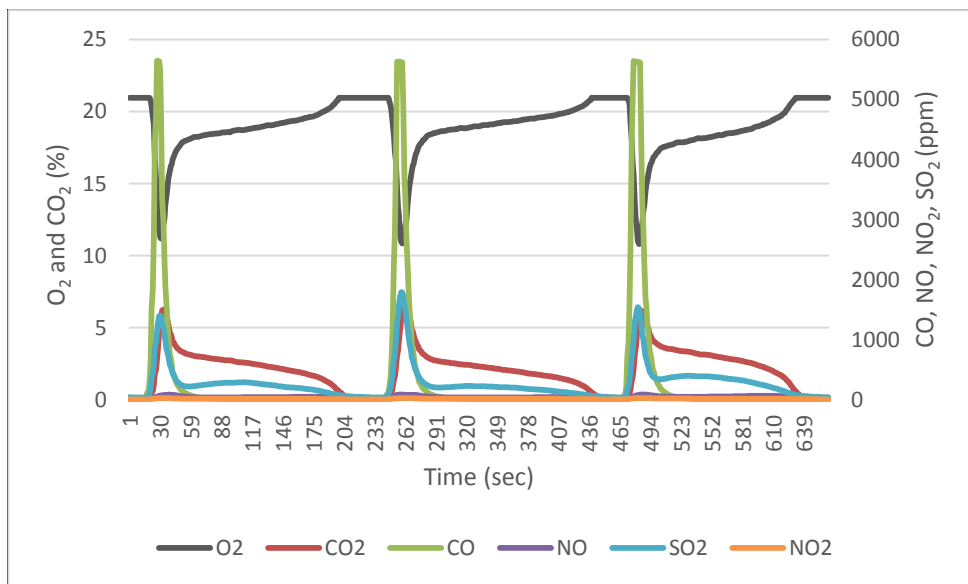


Figure A-10 Results of co-combustion of petroleum coke with 20% RDF_A

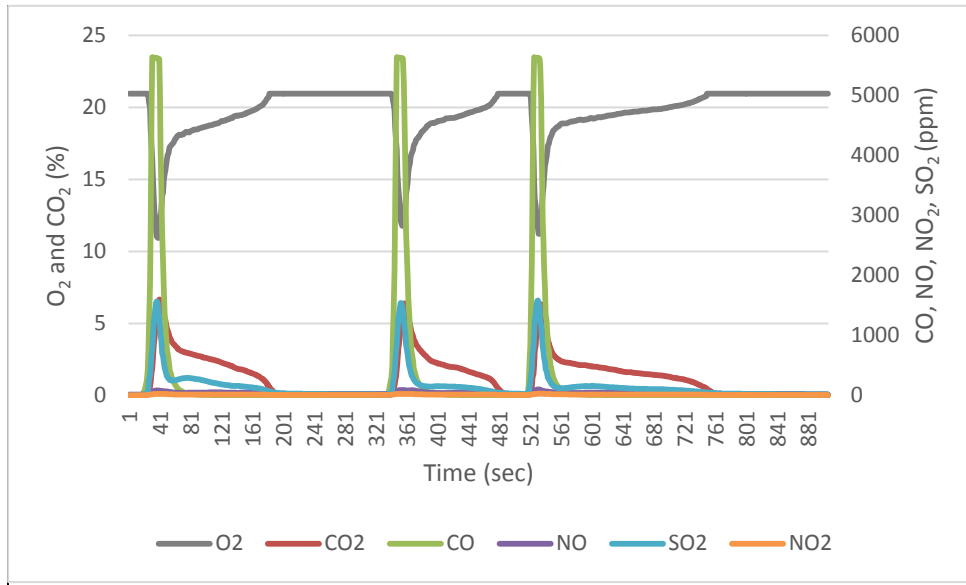


Figure A-11 Results of co-combustion of petroleum coke with 30% RDF_A

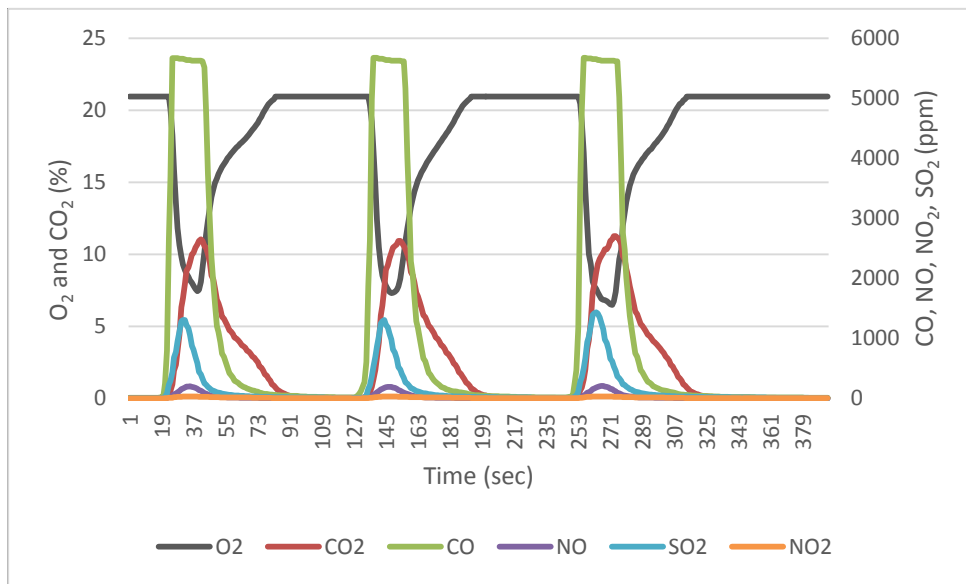


Figure A-12 Results of combustion of RDF_B

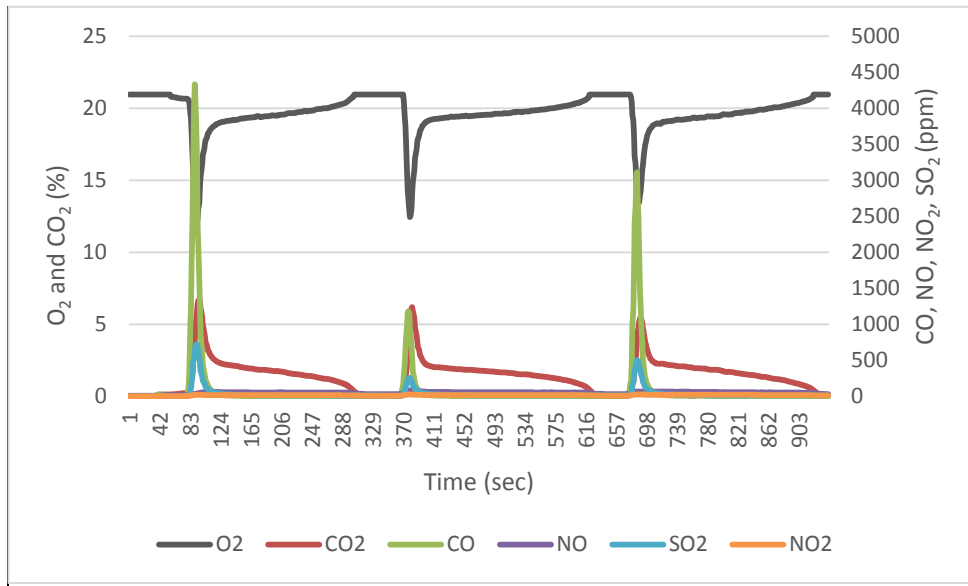


Figure A-13 Results of co-combustion of coal with 3% RDF_B

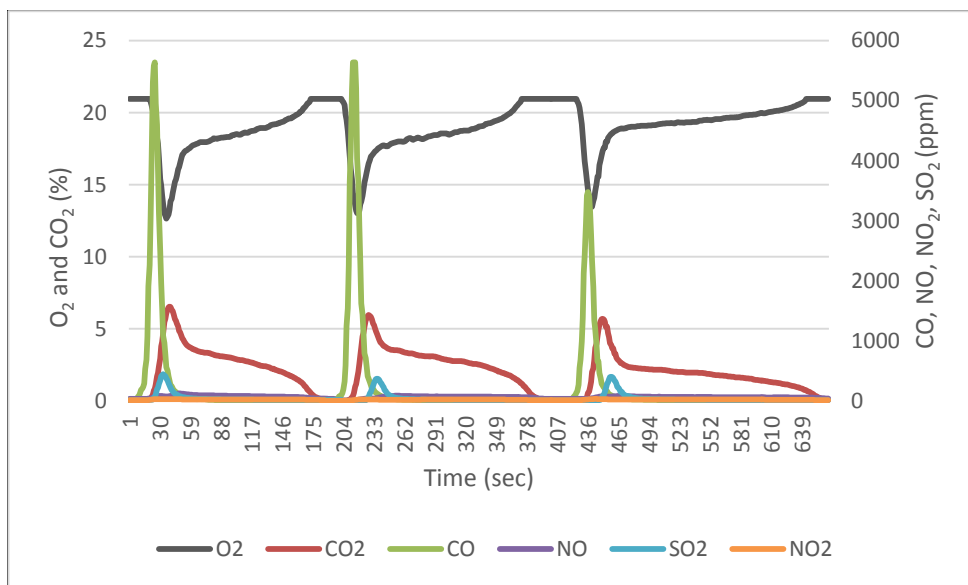


Figure A-14 Results of co-combustion of coal with 5% RDF_B

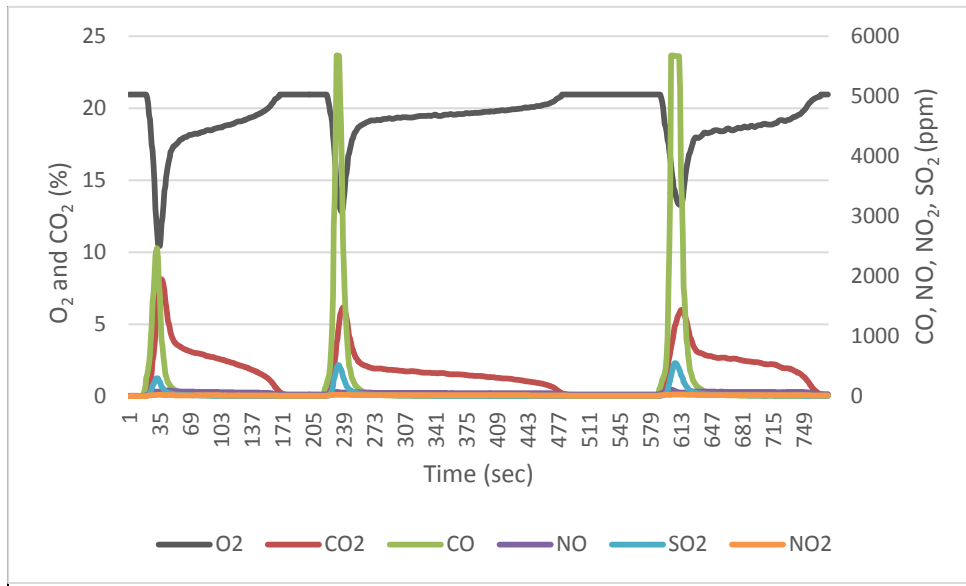


Figure A-15 Results of co-combustion of coal with 10% RDF_B

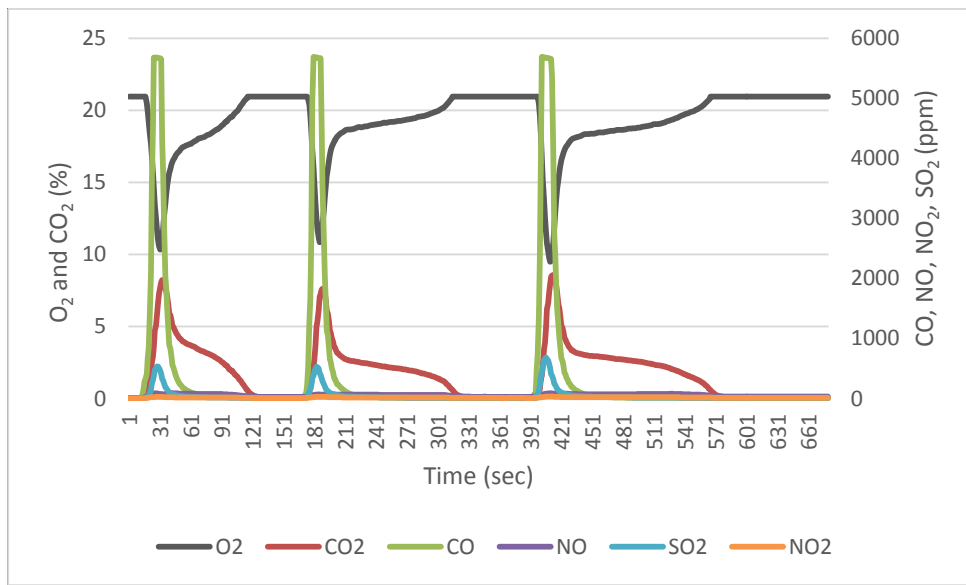


Figure A-16 Results of co-combustion of coal with 20% RDF_B

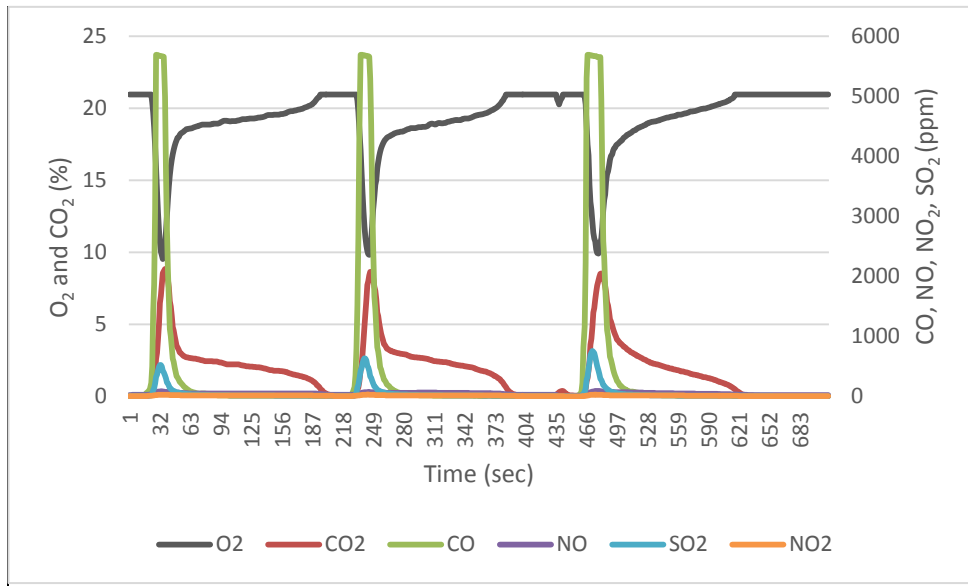


Figure A-17 Results of co-combustion of coal with 30% RDF_B

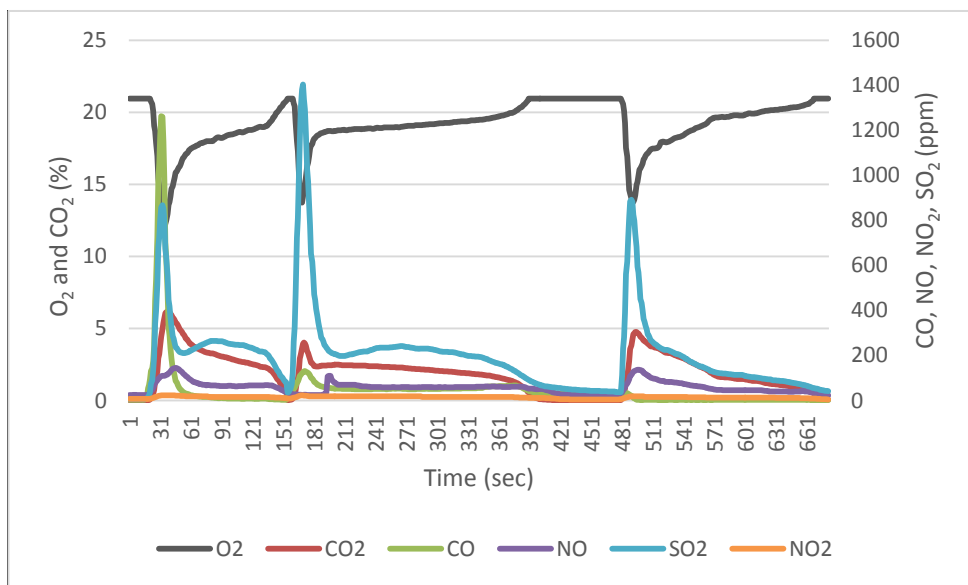


Figure A-18 Results of co-combustion of petroleum coke with 3% RDF_B

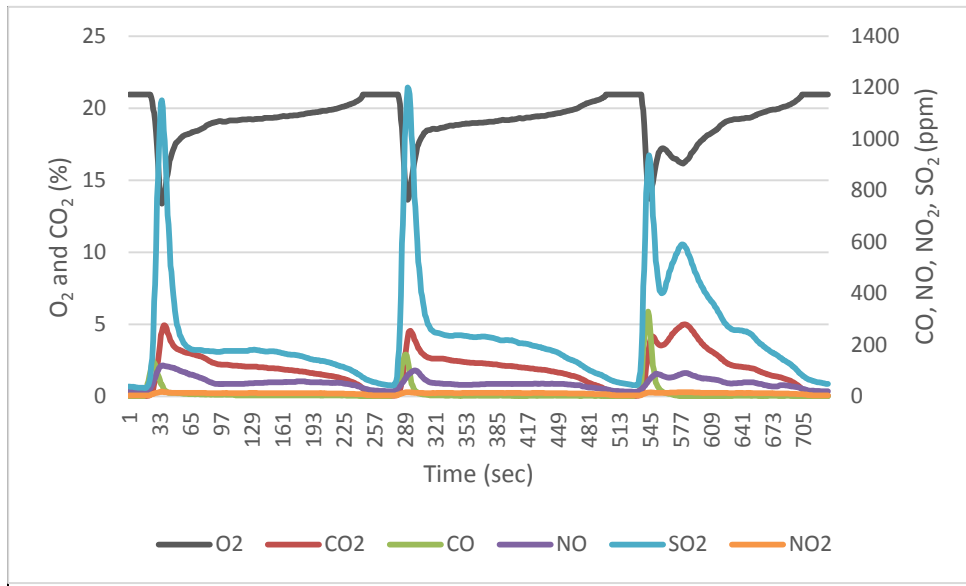


Figure A-19 Results of co-combustion of petroleum coke with 5% RDF_B

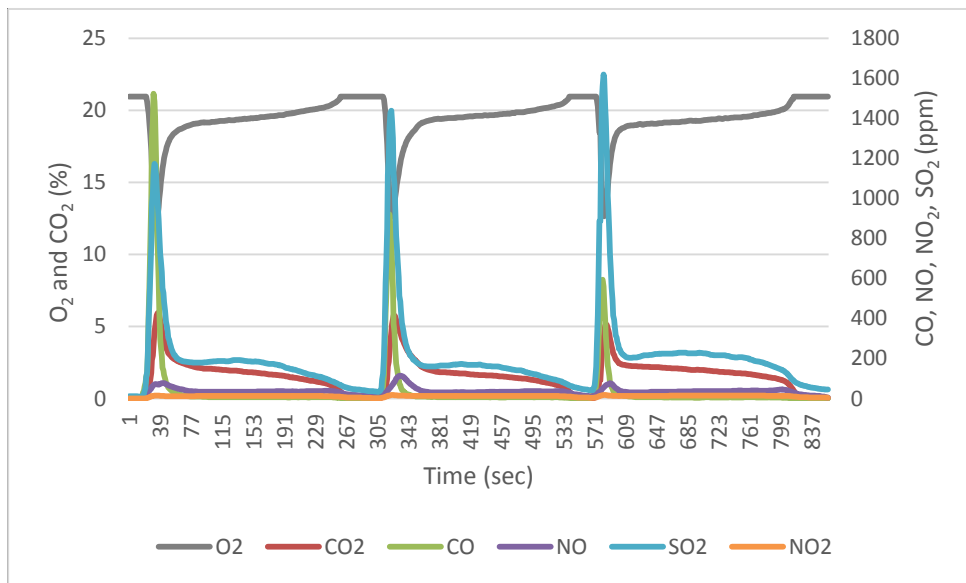


Figure A-20 Results of co-combustion of petroleum coke with 10% RDF

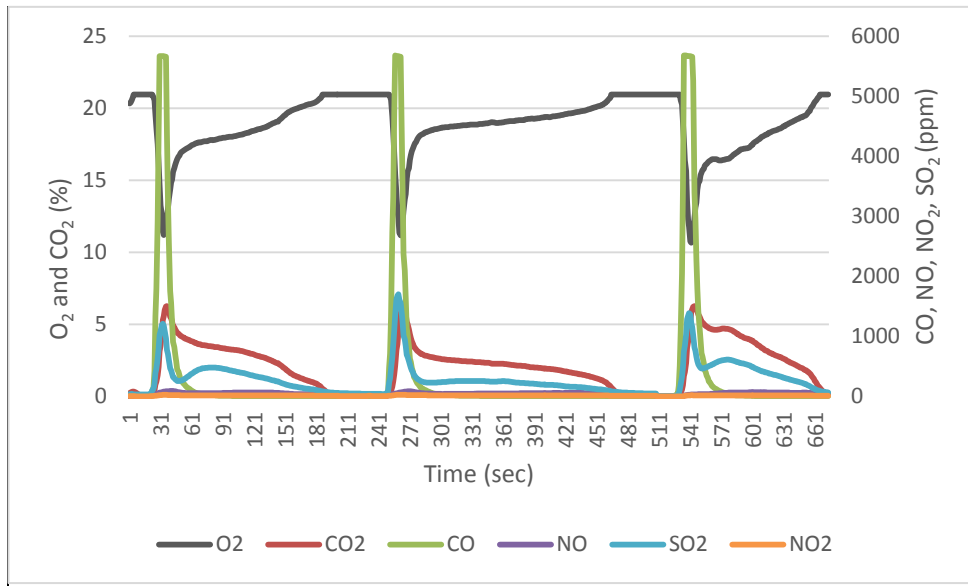


Figure A-21 Results of co-combustion of petroleum coke with 20% RDF_B

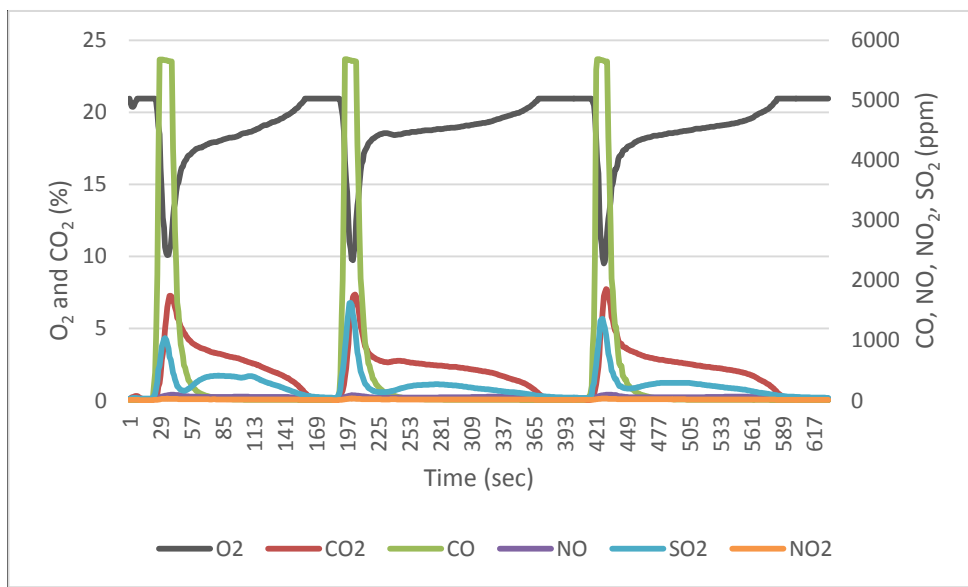


Figure A-22 Results of co-combustion of petroleum coke with 30% RDF_B